Investigation and Characterization of Antibacterial Proteins from the Eastern Subterranean Termites *Reticulitermes flavipes* in Response to Multidrug Resistant Bacteria

by

Yuan Zeng

A dissertation submitted to the Graduate Faculty of
Auburn University
in partial fulfillment of the
requirements for the Degree of
Doctor of Philosophy

Auburn, Alabama
May 6th, 2017

Keywords: termite, antibacterial, multidrug-resistant pathogens, proteiomic

Copyright 2017 by Yuan Zeng

Approved by

Xing Ping Hu, Chair, Professor of Entomology and Plant Pathology
Nannan Liu, Professor of Entomology and Plant Pathology
Arthur Appel, Professor of Entomology and Plant Pathology

Abstract

Immune system of insects has been of great interest for discovering novel compounds against microbes. Subterranean termites (Blattodea: Isoptera: Rhinotermitidae), especially the *Reticulitermes* species, have a wide distribution in the U.S. These termites have developed disease resistance mechanisms that facilitated their survival and propagation as they nest and forage in soil. However, an improved understanding of the mechanisms governing antimicrobial production and the spectrum of antibiotic properties are necessary and would be helpful to develop novel strategies for discovering new antimicrobials against bacterial pathogens including multidrug resistant bacteria (MDR) as well as exploring new approaches to control termites.

To assess the presence of antibacterial proteins in *R. flavipes,* termite colonies were collected on the Auburn University, and maintained in Urban Entomology Laboratory. First, the presence of antibacterial activities of the cell free whole body crude extract as well as five size-fractionated solutions of unsterilized *R. flavipes* workers were investigated against a common soil bacterium *Bacillus subtilis* using the inhibition zone assay. The activity against *B. subtilis* was observed in both crude extract and all size fractions. Next, the spectrum of antibacterial activity of the extract and the origin of antimicrobials were investigated against a panel of bacteria including three MDR and four non-MDR human pathogens. The crude extract of naïve (control) termites showed a broad activity against the non-MDR bacteria but it was ineffective against the three MDR pathogens *Pseudomonas aeruginosa*, methicillin-resistant *Staphylococcus aureus* (MRSA), and *Acinetobacter baumannii*. Interestingly, feeding termites with either heat-

killed *P. aeruginosa* or MRSA dramatically induced activities against MDR, and maintain or slightly increased activities against most of the non-MDRs. Further investigation demonstrated that hemolymph, not the hind-gut, was the primary source of antibiotic activities.

In the effort to discover new therapeutic approaches against two common multidrug resistant opportunistic bacterial pathogens, *P. aeruginosa* and MRSA, the alterations in hemolymph protein profiles of *P. aeruginosa* and MRSA induced termites were investigated, aiming to identify proteins with antimicrobial activities. The protein profiles were determined through two proteomic approaches via two-dimensional gel electrophoretic analyses and liquid-chromatography-MS/MS analysis. Two-dimensional gel electrophoretic analyses indicated that 38 and 65 proteins of the 493 hemolymph protein spots were differentially expressed at least 2.5-fold in *P. aeruginosa* and MRSA-fed termites, respectively. Mass spectrometry (MS) analysis indicated a total of 578 proteins, and 80 and 36 proteins were differentially expressed at least 2.5-fold in response to *P. aeruginosa* and MRSA-challenge, respectively. Many of these differentially expressed hemolymph proteins (actins, tublins, transferrin, dehydrogenases, peroxiredoxin, catalase and etc.) were known to be involved in immune-related processes including iron metabolism, antioxidant-related response**,** general stress response, and immune effectors. This research provided the first evidence of constitutive and inducible activities expressed by *R. flavipes* against human bacterial pathogens, and alternations of termite hemolymph proteins in response to bacterial challenges. These findings suggest an exploration of humoral as well as cellular immunity in *R. flavipes* upon being fed with multidrug-resistant bacteria.

Acknowledgments

I would like to express my special appreciation and thanks to Dr. Xing Ping Hu, my major advisor, for providing the opportunity for me to work on this project and guidance to this project. I would like to thank Dr. Sang-Jin Suh, my previous co-advisor, for his valuable advices and his expertise on microbiology, as well as the kindness for giving me the freedom to explore on my own of doing research. I would like to thank my committee members: Dr. Arthur Appel and Dr. Nannan Liu, for their encouragement and thought-provoking questions. Without their generous support, this dissertation would never be accomplished. I would also to express my gratitude to the dissertation university outside reader, Dr. Lori Eckhardt, for reviewing my dissertation and my major advisor of Master of Probability and Statistics, Dr. Guanqun Cao, for advice on proteomic data analysis.

Sincere and special thanks to Drs. Xiaoqiang Yu, Xue Zhong, Huiyu Yi, and Xiangli Dang in University of Missouri, Kansas City, as well as Dr. Divya Prakash, a former doctorate student in Department of Chemistry and Biochemistry of Auburn University for their generous technical assistance and support.

A special thank goes to the late Dr. James Barbaree in the Department of Biological Sciences for providing Methicillin-resistant *Staphylococcus aerues* (MRSA), and to Dr. Alan Wilson in the School of Fisheries, Aquaculture and Aquatic Sciences, Dr. Aaron Rashotte in the Department of Biological Sciences, and Dr. Evert Duin in the Department of Chemistry and Biochemistry for allowing access to their equipments.

I am also grateful to the following former and current fellow labmates from Dr. Hu and Dr. Suh's labs: Dr. Znar Barway, Mr. Hao Wu, Mr. Julian Golec, Dr. Xiangli Dong, Dr. Liu Yang, Miss Yuexun Tian, Mr. Meng Chen, Dr. Jinxiang Luo, Dr. Suihan Wu, Dr. Zhou Tong, Dr. Bingyu Li, Miss Shiqi Gao, Mr. Anwar Kalalah, Mr. Huachen Gan, and Miss Subarna Barua for the stimulating discussions, for the help of doing experiments, and for all the fun we have had in the past five years. In addition, Dr. Wen Shi, Miss Shiqi Gao, Dr. Ting Li and many friends have helped me stay sane through these difficult years. Their support and concern helped me overcome setbacks and stay focused on my goal. I greatly value their friendship and deeply appreciate their belief in me.

Finally, I would like to thank my beloved parents, Mr. Daqing Zeng and Mrs. Xingqun Liu, as well as my 93-year-old Grandma, Mrs. Yourong Li for supporting me throughout all my studies in Auburn University. Words cannot express how grateful I am to my family for all their sacrifices and endless love.

Table of Contents

List of Tables

List of Figures

Chapter One

Introduction and Review of Literature

The global success of insects and their wide range of habitats on earth indicate their remarkable ability to adapt environments and confront various pathogens during their life stages. These abilities are known as insect immunocompetence (IC). According to the different characteristics of insect IC, several mechanisms have been documented, such as biochemical and physiological mechanisms (immunological reactions), behavioral resistance, as well as acquired protection from their symbionts (Wilson-Rich et al. 2009; Chouvenc et al. 2013; Mattoso et al. 2012; Wang and Henderson 2013; Rosengaus et al. 2014). Some insects with behavioral resistance may treat their nest materials with antimicrobial substances such as pieces of solidified resin and propolis produced by the metapleural gland or venom glad (Simone et al. 2009; Kuhn-Nentwig 2003; Turillazzi et al. 2004), others may take advantage of grooming and corpse management to reduce horizontal transmission of disease. However, the most important and significant mechanisms of insect IC are the mechanisms of their innate immune responses. Insects can distinguish and recognize non-self and pathogenic microorganisms (pathogen-associated molecular patterns (PAMPs)) which can lead an efficient innate immune response to eliminate pathogens (Koropatnick et al. 2004, Moreno-García et al. 2014). Although the study of insect innate immune responses has grown to considerable prominence over the past several decades and has made rapid progress in unraveling the mechanisms of insect immunity, it is very important to deeply understand these mechanisms to combat pathogens in terms of biological

control of pests and insect vectors, and to identify molecules produced by insect immune reactions for developing potential therapeutic approaches on human and animal health.

1.1 General Introduction of Insect Innate Immunity

The insect defense processes can be divided into two main stages: recognition and response. Recognition is carried out by proteins such as Gram-negative binding proteins (GNBPs) and peptidoglycan recognition proteins (PGRPs) that recognize peptidoglycan and Gram-negative bacteria, thioester bond-containing proteins (TEPs), and scavenger receptor type lectins (SCRTLs). After a foreign element (fungi, bacteria, parasites, viruses, as well as tissue damages) is recognized, a signal is transmitted to the cell nucleus for activation of target genes. These signal transduction pathways include the Toll pathway, the Immune deficiency (IMD) pathway, c-Jun N-terminal protein kinases (JNK) pathway, and the Janus kinase/signal transducer and activator of transcription (JAK/STAT) pathway (Hoffmann 2003; Brennan and Anderson 2004; Ferrandon et al. 2007; Lemaitre and Hoffmann 2007).

1.1.1 An overview of insect signal transduction pathways

1.1.1.1 The Toll pathway

The Toll pathway regulates the response to gram-positive bacterial, fungal and viral infestation. The toll receptor is activated when the proteolytically cleaved ligand Spätzle binds to the receptor. After activation, the signal is transduced to an inducible trans-activator of the NF-kB-Rel family, and Cactus in the cytoplasm (Geisler et al. 1992). Dissociation of Cactus is triggered by phosphorylation from three Death domain-containing proteins (MyD88, Tube, and Pell). Dorsal mediates Toll signaling during dorsoventral axis formation, and Dorsal-related immunity factor (DIF) mediates Toll signaling during fungal or Gram-positive bacterial infections (Ip et al. 1993; Rutschmann et al. 2000). The two Rel proteins are then translocated into the nucleus of immune cells where they activate the target AMPs.

1.1.1.2 The IMD pathway

In contrast to the Toll pathway, the IMD pathway usually interacts with Gram-negative bacteria and is activated by the diaminopimelate (DAP)-type peptidoglycan and a transmembrane receptor PGRP-LC. After the activation of PGRP-LC, the death-domain (DD) adaptor protein IMD binds to FADD (Fas-associated protein with death-domain), which interacts with the caspase DREDD (Death-related ced-3/Nedd2-like protein). When relish is phosphorylated by the *Drosophila* IKK (inhibitor of NF-B (IB)-kinase) complex, DREDD might cleave the complex, and Relish domain is translocated into intracellular of nucleus to participate in immune gene regulation. The IMD pathway is used to regulate the expression of the antibacterial peptides diptericin, attacin, drosocin, cecropin and defensin during an infection.

1.1.1.3 The JNK and JAK/STAT pathways

Compared to the Toll and Imd pathways, the knowledge to JNK and JAK/STAT pathways is limited. The JNK pathway can be activated in response to Gram-negative bacteria, and it can regulate the expression of AMPs. The JAK/STAT pathway is mainly triggered by cell death, tissue repair, stress, injury or viral response rather than the actual pathogens, and may be involved in communication from the hemocytes to the fat body (Pham and Schneider 2008; Broderick et al. 2009).

The activation of a large number of targeted genes through signal pathways will lead a variety of response reactions. The first response usually occurs in the epithelial barriers such as epidermis, intestinal, and tracheal network (Moreno-García et al. 2014). Once the physical defensive line has been disrupted and led to a detrimental effect on insect, the humoral or cellular reactions will be triggered and may be spread systemically through the hemolymph. Insect

humoral and cellular reactions allow for a rapid and efficient immune response to resistance microbial infection.

1.1.2 Humoral reactions

Humoral reactions are immune components with effector molecules including antimicrobial peptides (AMPs) as well as hemolymph proteins that are mainly produced by fat body to destroy molecular structure of the pathogenic microbes. Among these effector molecules, AMPs, lysozyme, phenoloxidase (PO)-dependent melanization, and reactive oxygen species (ROS) are important biochemical components to kill invading pathogens.

1.1.2.1 Antimicrobial peptides (AMPs)

Currently, more than 1,500 AMPs with broad activities have been isolated from various organisms with over 170 AMPs have been identified in insects (Aley et al. 1994; Bulet and Stocklin 2005). The first insect AMP cecropin was isolated and characterized from bacterial immunized cecropia moth (*Hyalophora cecropia*) pupa in 1981 (Steiner et al. 1981). From this day on, the investigation of insect AMPs became a hot area to discover and study new antibiotics. The most important families are insect cecropins (linear α-helical group) and defensins (cysteine-rich group).

1.1.2.1.1 Cecropins

Insect cecropins and cecropin-like peptides are antagonistic against bacteria, filamentous fungi and yeast. It is known that cecropins are especially potent against Gram-positive bacteria strains. Unlike other insect AMPs which are constitutively present in insect salivary gland, midgut and reproductive glands, insect cecropins are usually secreted into hemolymph by microbial infection (Bulet et al. 2005). Cecropin A which is a typical example of this family as identified in *H. cecropia*. Several other cecropin peptides as well as a few cecropin-like AMPs

were identified in other Diptera and Lepidoptera insects, and social insects such as ants and termites (Table 1). Their sequences were reported with 50%-90% similarity (Hetru et al. 1998; Bulet et al. 2003). The common structure of cecropin has a long amphipathic α-helix on N-terminal, linking with a hydrophobic C-termial helix by a Gly-Pro hinge (Steiner 1982; Holak et al. 1988). Interestingly, some cecropins with an amidated C-terminal or lacking a tryptophan residue were reported with a higher efficacy against pathogens (Vizioli et al. 2000). For example, a C-terminally amidated cecropin demonstrated in *Anopheles* spp. without a tryptophan residue displayed a stronger activity against Gram-positive bacteria than cecropin A isolated from *Drosophila* spp. with the presence of a tryptophan. Other factors such as peptide size, charge, and hydrophobicity can affect their activity against pathogens according to structure-activity relationship (SAR) studies (Tossi et al. 2000).

1.1.2.1.2 Defensins

Insects defensins are with 33 to 46 amino acids containing mixed α-helix and β-sheet structure (Bulet et al. 2003). All defensins contain the same pattern with 3 to 4 disulfide bridges (Hetru et al. 1998; Rees et al. 1997). In contrast to cecropins, defensins are not frequently C-terminally amidated. To date, more than 60 defensins have been isolated from insect orders such as Odonata, Diptera, Coleoptera, Hymenoptera, and Lepidoptera. Defensins can be divided into antibacterial or antifungal defensins (Table 2). Antibacterial defensins possess abilities in inhibiting the bacterial growth or lysing bacterial cells with higher efficacy against Gram-positive bacteria by disrupting cytoplasmic membrane which led to a depolarization of inner membrane, a decreasing of ATP synthesise, and a restraint of respiration (Cociancich et al. 1993). Relatively less defensins were documented as antifungal peptide comparing to antibacterial defensins (Lamberty et al. 2001; Barbault et al. 2003; Schuhmann et al. 2003). The mode of

action (MOA) of the insect antifungal defensins may interact with fungal glucosylceramides, a unique glycosphingolipid in membranes of eukaryotic organisms to further delay hyphae growth or inhibit spore germination (Warnecke and Heinz 2003; Thevissen et al. 2004).

1.1.2.2 Lysozyme

Lysozyme is a common, heat-stable enzyme with a total weight of 14-16.5 kDa present in many organisms, including insects. It is clear that lysozyme can lyse bacteria, mainly on Gram-positive bacteria, by hydrolyzing the glycosidic linkage between *N*-acetylmuramic acid (NAM) and *N*-acetylglucosamine (NAG) of the peptidoglycan layer (Prager and Jolles 1995). Lysozymes have been identified from hemolymph of the hymenopteran, lepidopteran, orthopteran, dipteran, and etc. (Hultmark et al. 1980; Zachary and Hoffmann 1984; Ito et al. 1995; Wang et al. 2009). These reported insect lysozymes showed 75% identical residues, and a comparison of several insect lysozyme sequences with chicken and human lysozymes showed a 40% identical amino acid residues (Kanost et al. 1990; Wang et al. 2009).

1.1.2.3 Prophenoloxidases (PPOs)/POs

Hemolymph PPOs/POs has been reported in wound healing and in defense against microbes and other parasites (Taft et al. 2001; Lai et al. 2002; Liu et al., 2007). PPOs (inactive form) is a precursor enzymes of POs (active form) that circulate through the hemolymph. These molecules have a total weight of 50–60 kDa and 70–80 kDa in their active and inactive forms, respectively (González-Santoyo and Córdoba-Aguilar 2012). It contains two copper binding sites, each with three essential histidine at conserved positions (Christophides et al. 2002). Upon activation, PPOs are converted to active POs. POs further convert phenols to indole groups such as quinones, diphenols, superoxide, and hydrogen peroxide, which are subsequently polymerized to melanin (melanization) that further combating with bacteria, fungal, and viral agents.

Generally, when insects are infected by pathogens, gene expression levels of PPOs and plasma PO activity will change (Zou et al. 2008; Rund et al. 2011; González-Santoyo and Córdoba-Aguilar, 2012). Other studies reported that proteins such as PPO-activating enzyme (PPAE), PPO-activating proteinases (PAPs), serine proteinase homologs (SPHs), serpins, GNBPs, and PGRPs have been found to regulate PPO activation using *B. mori*, *M. sexta*, *D. melanogaster*, *Holotrichia diomphalia*, and various mosquitoes as models (Ashida and Brey 1997; Takehana et al., 2002; Ross et al., 2003; Yu et al. 2003; Zou et al. 2010; Jiang et al. 2011).

1.1.2.4 Reactive oxygen species (ROS)

Many toxic molecules such as ROS, reactive oxygen intermediates (ROI), reactive nitrogen intermediates (RNI) are produced to kill foreign invaders during melanization (Christensen et al. 2005; Nappi and Christensen 2005). These cytotoxic molecules include superoxide dismutase (SOD), thioredoxin, semiquinones, superoxide anion ($\cdot O_2^-$), hydroxyl radical ($\cdot OH$), hydrogen peroxide (H_2O_2) and some derivatives of nitric oxide ($\cdot NO$) is observed in mosquitos, flies, and other insects (Nappi and Christensen 2004; Christensen et al. 2005). Among these molecules, H_2O_2 is an important component because it can react with $\cdot O_2^-$, $\cdot NO$ and transition metal ions to form the highly reactive. Semiquinones are also important. They mimic the action of $\cdot O_2^-$ by reducing ferric (Fe^{3+}) and cupric (Cu^{2+}) ions, which, in turn, react with H_2O_2 to generate $\cdot OH$.

1.1.3 Cellular reactions

Cellular reactions are defined by phagocytosis, nodule formation, or encapsulation of foreign particles by circulating hemocytes such as plasmatocytes, lamellocytes or granulocytes (Schmid-Hempel 2005; Siva-Jothy et al. 2005; Strand 2008). Among the cellular reactions,

phagocytosis is a process that plasmatocytes and granulocytes attach to the foreign cell and establish a cellular layer to phagocytize small particles or larger foreign bodies (Salt 1970; Haine et al. 2008). When foreign particles cannot be removed by phagocytosis, nodule formation becomes more common to combat a high dose of invaders including fungi, bacteria, or protozoa (Ribeiro and Brehélin 2006). In this process, centrally melanized degenerating granulocytes produce a coagulum entraps substances surrounding by a sheath of blood cells (Ratcliffe and Gagen 1976; Ratcliffe and Rowley 1979). Encapsulation is a phenomenon responds to foreign particles which are larger than the hemocytes. Those foreign invaders are enclosed by several layers of hemocytes (granulocytes and plasmatocytes) (Vinson 1990; Pathak 1993; Siva-Jothy et al. 2005). Upon the activation of phenoloxidase, the layered cells became melanized mediated by the enzyme cascade (prophenoloxidase/phenoloxidase) and led to the death of foreign materials (Soderhall and Cerenius 1998; Binggeli et al. 2014).

1.2 Important Immune-Related Proteins

Insect hemolymph serves as a medium that stores and transports nutrients and ions, and plays key roles in insect physiological processes. With the development of proteomic technology, recombinant-DNA methods and sequencing technology over the past 50 years, an increasing number of proteins was identified and characterized in insects. According to the structure and function of hemolymph proteins that are common to all insects, the major groups of hemolymph proteins are storage proteins including hexamerins and arylphorins acting as amino acid sources and components of insect cuticle, lipoproteins for lipid transport, vitellogenins for embryo development, enzymes (e.g. trehalase, esterase, lipases) for sugar and lipid hydrolysis, lectins for carbohydrate binding and pathogens and parasites recognition, protease inhibitors for immune response mediation, and inducible antimicrobial proteins (Kanost et al. 1990; Lemaitre and Hoffmann 2007; Jiang et al. 2010). Hemolymph is also known as a battleground where

hemolymph proteins and hemocytes attack invading organisms such as viruses, bacteria, fungi, and parasites. In addition to immune effector proteins, it is known that a lot of insect hemolymph proteins without antimicrobial activities are reported with differently expression levels upon immune challenges or tissue damages. Changes of hemolymph protein abundance indicate their significant roles in insect immune response. According to their roles in insect immune processes, some proteins are found to recognize pathogens and propagate the signals of wounding and microbial invasion, modulate stress response and iron metabolisms, while others either act as detoxification or cytoskeletal formation.

1.2.1 Proteins engage in pattern recognition

Insect innate immune responses are initialized when pathogen-associated molecular patterns (PAMPs) are bound by pattern recognition receptors (PRRs) (Medzhitov and Janeway 2002). PRRs can serve as initiators of nodule formation and melanization, as opsonins facilitating phagocytosis, and as receptors for signal transduction pathways which lead to synthesis of AMPs. A number of PRRs such as PGRPs, thioester-containing proteins (TEPs), GNBPs, scavenger receptors (SCRs), C-type lectins (CTLs), and galectins (GALEs) have been reported in various insects (Christophides et al. 2002). Among these PRRs, PGRP plays central and diverse roles in activating insect immune reactions including melanization cascade, phagocytosis, and signal transduction pathways for production of immune effectors.

1.2.2 Proteins involve in signal modulation and amplification

After recognition of non-self elements, extracellular cascades including serine proteases or serine protease inhibitors serves as signal modulator as they either amplify or dampen signals (Christophides et al. 2002; Gorman and Paskewitz 2001). Structures of most serine protease contain a short signal peptide followed by the clip domain, a linker region of highly variable

length, and the serine protease domain. Serine protease inhibitors, known as serpins, are well-conserved proteins with 350-400 residues. Inhibitory serpins act as suicide substrates, mostly for serine and more rarely cysteine proteases. Structure of serpins contains a N-terminal region, the compact serpin core fold, and a C-terminal flexible reactive center loop which acts as bait for the target protease (Silverman et al. 2001).

1.2.3 Stress response proteins

Previous research suggested a link between insect innate immune and stress response (Suwanchaichinda and Paskewitz 1998). Molecules such as heat shock proteins (Hsp), mainly for Hsp70, and ubiquitin are stress response proteins due to their upregulation upon immune challenge when infection occurs (Nappi and Ottaviani 2000; Bartholomay et al. 2004). Hsp70 has two domains with a N-terminal nucleotide binding domain (NBD) and a substrate binding domain (SBD) (Javid et al. 2007). Ubiquitin is a small protein that has been found in all eukaryotic cells. It consists of 76 amino acids and is about 8.5 kDa. The key structure of ubiquitin contains 7 lysine residues and C-terminal tail.

1.2.4 Proteins participate in iron metabolism

Insects secrete iron metabolism proteins to sequester iron to hinder pathogen survival. An important iron metabolism protein, transferrin, was reported being upregulated in insects or insect cells challenged with bacteria (Nichol et al. 2002). Transferrins are a group of iron-binding proteins (~80 kDa) with two ferric-binding lobes. Furthermore, the fact that transferrin gene of *D. melanogaster* contains promotor region sequences which is known to bind nuclear factor-kappa B–like transcription factors suggests that transferrin may participate in an iron-withholding strategy in insects (Weinberg 1993).

1.2.5 Antioxidant proteins

Oxidative stress is concurrent with insect innate immune response. For example, cellular defenses usually result in production of cytotoxic ROI, RNI, and associated enzymes. These ROS can damage various components of host cells (Rabilloud et al. 2002) which requires host antioxidant systems to prevent cellular components from oxidative damage by removing free radicals and inhibiting other oxidative reactions (Sie 1997). Proteins such as thioredoxin, thioredoxin reductase, peroxidases, and glutathione transferase are antioxidant properties. These antioxidant enzymes were upregulated upon immune challenge (Seehuus et al. 2006; Jordan and Gibbins 2006; de Morais Guedes et al. 2005).

1.2.6 Cytoskeletal Proteins

The cytoskeletal proteins play roles in cell shape maintenance, motility, cellular division, organ formation, and intracellular transport (Bartholomay et al. 2004). In addition, the cytoskeletal proteins such as actin, actin-binding, myosin, gelsolin, and beta-tubulin were reported to change expression levels after bacterial challenge (Hudson and Cooley 2002; Scharlaken et al. 2007). This indicate their potential roles in immune cells. Evidences that the expressions of profilin and actin 5c at the early pupal stage of Drosophila in response to infection by all types of microorganisms supported the role of cytoskeletal proteins in insect immunity (Janssen and Schleicher 2001; Loseva and Engstrom 2004).

1.3 Termites as a model to study insect IC

1.3.1 Introduction of termites and their importance

Termites are now classified into the cockroach order Blattodea. So far, over 3100 species of termites have been described around the world, and there are still a few hundred more left to be described. The recent classification splits described species into 12 families such as Cratomastotermitidae, Mastotermitidae, Termopsidae, Archotermopsidae, Stolotermitidae,

Kalotermitidae, Archeorhinotermitidae, Stylotermitidae, Hodotermitidae, Rhinotermitidae, Termitidae, and Serritermitidae (Krishna et al. 2013). In the U.S., subterranean (Rhinotermitidae), drywood (Kalotermitidae), and dampwood (Hodotermitidae) termites are commonly found species.

Termites are usually small, measuring between 4 to 15 mm in length. They have prognathous head with chewing mouthparts, and compound eyes present in all winged forms. Their antennae are moniliform or filiform, usually with 10 to 30 segments. The alates are the only form with long membranous similar wings. Like ants and bees, termites are easy to tell by their caste systems includes reproductives (queens, kings, and alates), workers, and soldiers. The task of king in a colony is to continuously mate with the queen who is responsible for egg production (Korb 2008). The winged reproductives are called alates. They serve to swarm, to pair, and to start new colonies. Seasonally produced alates develop to maturity right before the rainy season and leave the nest in great swarms. The alates fly for a time and land on the ground to find a mate. Once a pair has dug a chamber in the ground, they will mate and the queen will lay eggs to produce workers. Workers are the mainstay in a colony. Although they look like alates, workers are absence of wings and genital structures. Almost of workers are blind because of lacking compound eyes. They stay in the colony and never leave except to forage for food. Workers can build and repair colony structures, tend other members, and forage food and water. The task of soldiers is to defend the colony generally against ant attack, especially the queen and the king. Soldiers generally have large heads and powerful mandibles.

Termites can be beneficial. For example, they can boost crop yields and enriching soil by increasing the amount of nitrogen as well as enable larger amounts of rainwater to soak into ground (Evans et al. 2011). In addition to their beneficial role in nature, termites can be major

agricultural and structural pest. In East Africa and North Asia, crop losses caused by termites are severe (Mitchell 2002). Many termite species can do a great damage to unprotected buildings and other wooden structures. An estimation of termite caused costs of the southwestern U.S. is approximately 1.5 billion each year in wood structure damage (Su and Scheffrahn 2000).

1.3.2 Termite IC

Since termites, especially subterranean termite species, are important wood-structural pests, control of these termites has become a very vital strategy. Although killing termites by treating insecticides on accessible infested wood are easy, it is known to be very difficult to control termites in the field due to their complex IC including innate immune reactions, social and organizational immunity, and acquired protections from nest ecology and symbionts. In comparison with many other insects, their thinner and less sclerotized cuticle make termites more vulnerable to pathogens and parasites. Therefore, individual termites tend to be more dependent on innate immune systems and social immunity to increase disease resistance. Like other insect species, termite innate immune systems are composed of humoral and cellular immune reactions, while more complicated innate immune responses such as higher degrees of specificity and longer immunological memory are expected in termites because they are the oldest eusocial insect and thus have a high probability of re-encountering the same pathogens (Cremer et al. 2007). Social immunity such as allogrooming, undertaking, and hygienic behaviors along with organizational adaptions have been explored to eliminate pathogens and parasites (Cremer et al. 2007; Fefferman et al. 2007), In addition, colony size, demography, nest architecture, symbionts, and labor division also play important roles in reducing disease transmission in termites (Naug and Camazine 2002; Rosengaus and Traniello 1993; Rosengaus et al. 2003; Rosengaus et al. 2010; Rosengaus et al. 2014).

1.3.2.1 Termite innate immune reactions

Like solitary insects, individuals in termite colonies rely on cellular and humoral reactions under pathogenic pressure although the level of IC may be influenced by social behaviors (Wilson-Rich et al. 2009). Research is on the rise about studying termite innate immunity, but relatively little information is known when comparing to solitary insects and other vertebrates. Previous studies in solitary insects such as *B. mori*, *Drosophila* spp., and *Aedes* spp. confirmed that phagocytosis is a critical mechanism contributes to eliminating pathogens (Wago 1983; Hillyer 2003; Pham et al. 2007) through engulfing foreign bodies and lysing them with the secretion of lysozyme. In termites, pilot studies evidenced the existence of cellular immunity, but there is no information elucidating the phagocytic activity of hemocytes when pathogens invade into termite hemolymph although Rosengaus et al. (2010) reported hemocytes are phagocytic when bacteria-sized fluorescent microlatex beads were injected to *Z. angusticollis* nymphs. Little attention is received in terms of encapsulation and nodule formation in termites, but pilot studies have shed light on discovering termite cellular immunity. For example, higher level of phenoloxidase activity was measured in *Z. angusticollis* when nylon monofilaments were implanted, and phenoloxidase activity differs significantly among termite species, colonies, and castes (Rosaogens et al. 2010). Encapsulation and nodule formation were also observed in response to *M. anisopliae* in the eastern subterranean termite *R. flavipes* (Chouvenc et al. 2009).

As with cellular immunity, humoral immune responses in termites are similar to solitary invertebrates. They are mediated by AMPs and enzyme cascades which are synthesized in granulocytes or fat body and secreted into the hemolymph in response to recognition of broad classes of microbes (Boman and Steriner 1981; Boman and Hultmark 1987). Although relatively less immune proteins have been reported from termites due to limited information on their

genome data, researchers still demonstrated several antimicrobial immune proteins against bacteria, fungi, and viruses from termite families including Macrotermitidae, Termopsidae, Rhinotermitidae, and Termitidae (Table 3) (Hussain and Wen 2012; Lamberty et al. 2001; Matsuura et al. 2007; Rosengaus et al. 2007; Terrapon et al. 2014). The majority of these reported immune effectors are capable of killing fungi. For example, two antimicrobial peptides (termicin and spinigerin) isolated from a fungus-growing termite *Pseudocanthotermes spiniger* were demonstrated with potent antifungal activities against yeasts and filamentous fungi (Lamberty et al. 2001). Another two unidentified proteins isolated from a pacific dampwood termite *Z. angusticollis* were reported with antagonistic activity against an entomopathogenic fungus (Rosengaus et al. 2007). In Termitidae, termite Gram-negative bacteria binding proteins (tGNBPs) with antifungal activity was also isolated (Bulmer and Crozier 2004). Additionally, molecules such as lysozyme, termicin, spinigerin, as well as a defensin-like peptide were demonstrated with antibacterial activity in various termites (Hamilton and Bulmer 2012; Bulmer et al. 2009; Matsuura et al. 2007; Hamilton et al. 2011). For example, lysozymes found in the Japanese subterranean termites *R. speratus* has bactericidal activity on entomopathogenic bacterium *B. subtilis* (Matsuura et al. 2007). Termicin and spinigerin isolated from *P. spiniger* have extended antibacterial activity against Gram-positive bacteria *B. megaterium*, *Micrococcus luteus* and *Streptococcus pyogenes*, and Gram-negative bacteria such as two strains of *Escherichia coli* (SBS363 and D22), *Klebsiella pneumoniae*, *Salmonella* Typhimurium and *Pseudomonas aeruginosa* (Lamberty et al. 2001). Additionally, a defensin-like peptide was expressed with antibacterial activity (Bulmer and Crozier 2006).

Interestingly, termites possess a unique humoral immunity advantage against pathogens coupled with social immunity when comparing to solitary insects. Some induced proteins from

dampwood termites *Z. angusticollis* after an immune challenge of *M. anisopliae* may be transferred between individuals within a colony (Rosengaus et al. 1998; Rosengaus et al. 2007). Termite lysozymes can also be spread through the colony by grooming behaviors or trophallaxis (Traniello et al. 2002).

1.3.2.2 Social and organizational immunity

In insect societies, individuals living in groups were less susceptible to be infected than isolated individuals (Rosengaus and Traniello 2001), thus social immunity is a vital component in disease resistance (Cremer et al. 2007). In termites, an antiseptic behavior, allogrooming is believed to be essential in reducing horizontal transmission of disease (Zhukovskaya et al. 2013). Isolated *Z. angusticollis* individuals were more susceptible to entomopathogenic fungus *M. anisopliae* than in groups (Rosengaus et al. 1998). In *R. flavipes*, workers can inhibit the growth of *M. anisopliae* in the alimentary tract through grooming and trophalaxis behavior (Chouvenc et al. 2009). Allogrooming has been demonstrated to spread termite Gram-negative binding proteins (tGNBPs) (Rosengaus et al. 2010).

In addition to allogrooming, corpse management/hygienic bahavior is another strategy of social immunity. Termites often bury infected nestmates and corpses to isolate them from the healthy individuals (Fefferman et al. 2007) to avoid higher infection rate within a colony (Böröczky et al. 2013). In *Z. angusticollis* colonies, healthy individuals eat both dead and diseased individuals to reduce disease transmission (Rosengaus et al. 2000; Sun and Zhou 2013). A fungus-growing species, *P. spiniger* buries dead ones to prevent potential pathogen outbreak (Chouvenc et al. 2012), while in *R. virginicus*, the existence of corpse management stimulate building behavior is induced by the existence of corpses to separate the healthy from dead ones (Ulyshen and Shelton 2012).

Recently, organizational immunity was proposed to describe how the social organization within the nest interacts with epidemiological variables to create different categories of pathogen transmission. Colonies having demographies biased towards young or old individuals had slightly higher mortality than those with heterogeneous demographies. The distribution of older individuals relative to the nest center had no significant effect on susceptibility and provided only a minor survival advantage (Naug and Smith 2007).

1.3.2.3 Acquired protection related to nest ecology, symbionts, and termite species

Termite colonies live in ground that is laden with microbiota including potential pathogens (Rosengaus et al. 2010). The cultivable nest microbial loads of dampwood termite *Z. angusticollis* are more than 800 colony forming units (CFUs)/g, of which are mostly bacteria and fungi. However, the cultivable cuticular microbial loads of drywood termites *Incisitermes minor* are much lower with about 200 CFUs/g (Rosengaus et al. 2003). The similar phenomenon was observed in the eastern subterranean termite *R. flavipes* that the cuticular microbial loads varied among colonies (Rosengaus et al. 2010). This discrepancy between nest and cuticular microbial loads suggests that both dampwood termites and subterranean termites may suppress microbial abundance on their cuticles by delivering antimicrobials through allogrooming and trophallaxis or by symbionts on termite cuticle and nest environments. In fact, nest bacteria such as *Streptomyces* spp. (Chouvenc et al. 2013), cuticular bacteria including *Bacillus sphaericus*, *Serratia marcescens*, *Cedecea davisae*, and *Pseudomonas aeruginosa* protect termites from entomopathogenic fungal and bacterial infection (Wang and Henderson 2013). The protozoa (and/or their associated bacteria) colonizing the termite hindgut synthesize multiple functional β-1, 3-glucanases, helping in digestion of ingested fungal hyphae and protection against invasion by fungal pathogens (Rosengaus et al. 2014).

Moreover, research on termites' susceptibility to an entomopathogenic fungal infection (*Metarhizium anisopliae*) reported that the ability to tolerant the pathogen varies on termite species of five families (Mastotermitidae, Termopsidae, Hodotermitidae, Kalotermitidae, Rhinotermitidae) (Chouvenc et al. 2009). Rosengaus et. al (2010) reported that *R. flavipes* showed the lowest susceptibility to *M. anisopliae* in comparing with *Coptotermes formosanus* and *I. minor*. The reason for the low susceptibility of *R. flavipes* to this pathogen is not clear, but it is hypothesized that *R. flavipes* has particularly effective immune responses to reduce susceptibility. Further studies are needed to characterize immune related chemicals and antifungal properties playing roles in termite resistance to fungal infections.

1.4 Termite Immune Gene and Protein Regulations in Response to Fungal Infection

Comparing with solitary insect, termites possess less variation on immune genes involving in pathogen recognition pathways and AMPs synthesis. Genes function as toll receptors were found less in termites than the fruit flies *D. melanogaster* although all immune-related pathways described in *D. melanogaster* and other insects were identified in *Z. nevadesis* (Weinstock et al. 2006). In addition, only three AMPs genes (attacin, diptericin, and termicin) were identified in *Z. nevadesis*. One hypothesis of the depletion of AMPs genes in *Z. nevadeisis* is to minimize deleterious effects on the microbial symbionts of the termite gut responsible for lignocellulose digestion (Terrapon et al. 2014).

1.4.1 Regulation of immune gene response to fungal pathogens

Quantitative real time polymerase chain reaction (qRT-PCR) is frequently used to study changes of target genes under different conditions. A recent study (Liu et al. 2015) reported that several immune effector genes (phenoloxidase, transferrin, and termicin) were significantly upregulated in the subterranean termite *R. chinesis* when these termites confront active immunization of the entomopathgenic fungus *M. anisopliae*. Similarly, immune genes diversity

associated with *M. anisopliae* infection was evaluated in another subterranean termite species *R. flavipes* (Gao 2014). This study revealed 182 expressed sequence tag (EST) clones that potentially represent immune responsive genes, and captured as many as 19 different mRNAs highly expressed in response to the fungal pathogen. Specifically, Gao (2014) demonstrated that a high degree of immunological specificity exists in *R. flavipes* innate immunity, and the degree of this specificity is subject to pathogen species-level due to the distinct immune-gene expression patterns following exposure to congeneric fungi (*M. anisopliae*, *M. brunneum*, *M. guizhouense* and *M. robertsii)* and to phylogenetically distant fungi (*Aspergillus flavus*, *Beauveria bassiana*).

1.4.2 Regulation of immune proteins in termites in response to fungal pathogens

Proteomics has recently become an important platform to study changes in protein expression in insect body fluids during physiological processes and under various environmental effects (de Morais Guedes et al. 2003; Chan et al. 2006; Woltedji et al. 2013). Although many studies have described compositions of insect hemolymph proteomes of the fruit fly, silkworm, white butterfly, mealworm beetle, and tobacco hornworm in response to immune challenge through technologies such as liquid chromatography-mass spectrometry (LC-MS) and isobaric tagging for relative and absolute quantification (iTRAQ) (de Morais Guedes et al. 2003; Zhang et al. 2014; Karlsson et al. 2004; He et al. 2016), knowledge regarding changes of termite proteome upon pathogen infection is relatively lacking. Recently, quantitative proteomics combined with multiple reaction monitoring (MRM)validation has been used to explore the proteome of the subterranean termites *R. chinesis* in response to active immunization of the fungal pathogen *M. anisopliae* (Liu et al. 2015). iTRAQ analysis, 62 (40 upregulated and 22 downregulated) proteins were differentially expressed and assigned to several functional categories including stress response, immune signaling, immune effector, biosynthesis,

metabolism, development, and other functions. Among them, 20 proteins were identified as immune proteins. Isocitrate dehydrogenase, glutathione *S*-transferase D1 (GSTD1), ubiquitin conjugating enzyme, and GTPase were considered as important components which involved in oxidative stress (Jo et al. 2001; Lee et al. 2002), detoxification (Low et al. 2010), ubiquitin-proteasome pathway (Aronstein et al. 2010; Yamamoto et al. 2006), as well as PO release (Bidla et al. 2007).

Over the last 20 years, the study on termite innate immunity has been steadily increasing. However, most of these studies focused on their immune responses after an entomopathgenic fungus (*M. anisopliae*) infection. Although a recent study on termite genomics of *Z. nevadensis nuttingi* provided us the first genomic insight into the genetic constructions of termite immunity (Terrapon et al. 2014), relatively less information was provided on termite antibacterial defenses. A study carried by Hussain and Wen (2012) reported no constitutive activity in the Formosan subterranean termites *C. formosanus* against bacteria (Gram-positive *B. thuringiensis* and *S. aureus* and Gram-negative *E. coli* and *Ralstonia solanacearum*). They also reported that all the bacteria strains were poor inducers resulting in no increased antimicrobial activities. Do other subterranean termites such as the eastern subterranean termites *R. flavipes* possess constitutive and inducible bactericidal compounds against bacterial agents? Or does *R. flavipes* display similar patterns as *C. formosanus*? To answer these questions, the eastern subterranean termites *R. flavipes* is chosen as a model organism to study antibacterial production against a set of pathogens. Proteomic (polyacrylamide gel electrophoresis (PAGE) and nano LC-MS/MS) and genetic technology (RT-PCR and qRT-PCR) combined with bioassays are used to fulfill our goal.

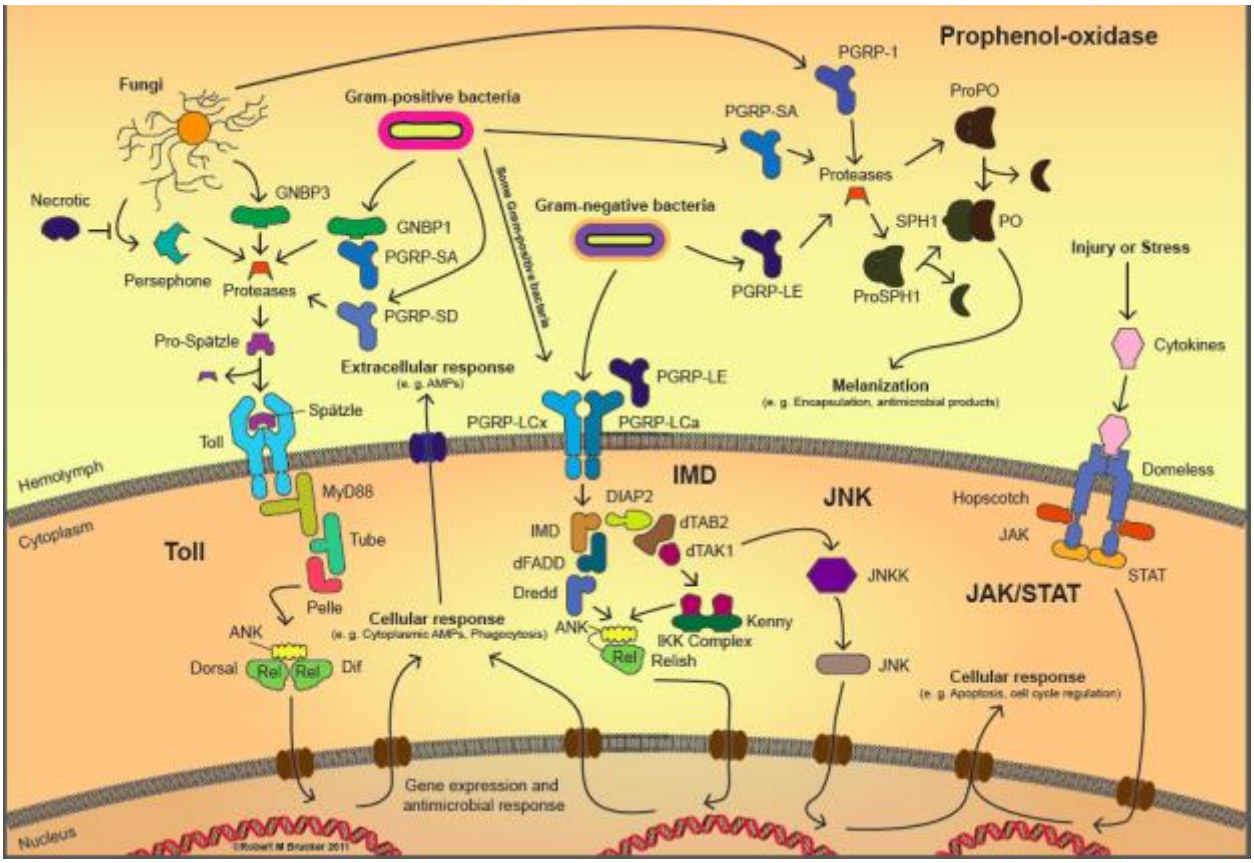

Figure 1.1 Generalized insect innate immune pathways based on *Drosophila* literature (Bordenstein Lab, NSF DEB-1046149)

Table 1.1 Protein sequences of selected α-helical AMPs (Cecropins/cecropin-like) among different insects.

Insect spp.	Identified AMPs	Protein sequences
Hyalophora cecropia (moth)	Cecropin A	KWKLFKKIEKVGQNIRDGIIKAGPAVAVVGQATQIAK *
Drosophila melanogaster (fruit fly)	Cecropin A	GWLKKIGKKIERVGQHTRDATIQGLGIAQQAANVAATAR*
Ades aegypti (mosquito)	Cecropin A	GGLKKLGKKLEGAGKRVFNAAEKALPVVAGAKALRK
Bombyx mori (silk worm)	Cecropin D	GNFFKDLEKMGQRVRDAVISAAPAVDTLAKAKALGQ*
Pachycondylas goeldii (ant)	Ponericin G2 (Cecropin-like)	GWKDWLKKGKEWLKAKGPGIVKAALQAATQ
Pseudacanthothermes spiniger (termite)	Spinigerin (Cecropin-like)	HVDKKVADKVLLLKQLRIMRLLTRL

*: C-terminal amidation.

Table 1.2 Protein sequences of selected defensins among different insects.

Insect spp.	Identified AMPs	Protein sequences
Phormia terraenovae (northen blowfly)	Defensin A	ATCDLLSGTGINHSACAAHCLLRGNRGGCNGKGVCVCRN
Drosophila melanogaster (fruit fly)	Drsomycin	ATCDLLSKWNWNHTACAGHCIAKGFKGGYCNDKAVCVCRN
Apis mellifera (bee)	Defensin	VTCDLLSFKGQVNDSACAANCLSLGKAGGHCEKGVCICRKTSFKDL WDKRF
Holotrichia diomphalia (scarab beetle)	Holotricin 1	VTCDLLSLQIKGIAINDSACAAHCLAMRRKGGSCKQGVCVCRN
Pyrrhocoris apterus (ant)	Defensin	ATCDILSFQSQWVTPNHAGCALHCVIKGYKGGQCKITVCHCRR

Table 1.3 Current knowledge of antimicrobial proteins in termites.

Name	Size (kDa)	Function	Family	Species	Origin
Gram-negative bacteria binding proteins (GNBPs)	~45	1. Recognition 2. Antifungal activity against entomopathogenic fungus	Termitidae	*Nasutitermes corniger*	Salivary glands
			Rhinotermitidae	*R.flavipes*	Surface of granulocytes
			Termitidae	*Nasutitermes* spp.	N/A
			Rhinotermitidae	*R. virginicus*	N/A
Lysozyme (termite egg recognition pheromone)	14.5	1. Evoke egg-caring and grooming behavior 2. Antibacterial activity	Rhinotermitidae	*R. speratus*	1. Eggs 2. Salivary glands
β-1, 3-glucanase	N/A	Antifungal activity against entomopathologenic fungus	Rhinotermitidae	*R. flavipes* *R. virginicus*	Salivary gland
A Constitutive protein	62-85	Antifungal activity against entomopathologenic fungus	Termopsidae	*Z. angusticollis*	Hemolymph
An induced protein	28-48	Antifungal activity against entomopathologenic fungus	Termopsidae	*Z. angusticollis*	Hemolymph
Termicin	~3.7	1. Weak activity against Gram-positive bacteria. 2. Strong activity against yeasts and a few filamentous fungi	Macrotermitinae	*P. spiniger*	1. Granulocytes 2. Salivary glands
			Rhinotermitidae	*R. virginicus*	N/A
Defensin-like peptides	N/A	Antibacterial activity against Gram-positive bacteria	Termitidae	*Nasutitermes* spp.	N/A

Spinigerin	2.5-3	1. Antibacterial activity 2. Antifungal activity 3. Effective against virus and HIV	Macrotermitinae	*P. spiniger*	1. Granulocytes 2. Salivary glands

References

Aley, S. B., Zimmerman, M., Hetsko, M., Selsted, M. E., & Gillin, F. D. (1994). Killing of Giardia lamblia by cryptdins and cationic neutrophil peptides. *Infection and immunity*, *62*(12), 5397-5403.

Aronstein, K. A., Murray, K. D., & Saldivar, E. (2010). Transcriptional responses in honey bee larvae infected with chalkbrood fungus. *BMC genomics*, *11*(1), 391.

Ashida, M., & Brey, P. T. (1995). Role of the integument in insect defense: pro-phenoloxidase cascade in the cuticular matrix. *Proceedings of the National Academy of Sciences*, *92*(23), 10698-10702.

Barbault, F., Landon, C., Guenneugues, M., Meyer, J. P., Schott, V., Dimarcq, J. L., & Vovelle, F. (2003). Solution structure of Alo-3: a new knottin-type antifungal peptide from the insect *Acrocinus longimanus*. *Biochemistry*, *42*(49), 14434-14442.

Bartholomay, L. C., Cho, W. L., Rocheleau, T. A., Boyle, J. P., Beck, E. T., Fuchs, J. F., ... & Lin, S. P. (2004). Description of the transcriptomes of immune response-activated hemocytes from the mosquito vectors *Aedes aegypti* and *Armigeres subalbatus*. *Infection and immunity*, *72*(7), 4114-4126.

Bidla, G., Dushay, M. S., & Theopold, U. (2007). Crystal cell rupture after injury in *Drosophila* requires the JNK pathway, small GTPases and the TNF homolog Eiger. *Journal of cell science*, *120*(7), 1209-1215.

Binggeli, O., Neyen, C., Poidevin, M., & Lemaitre, B. (2014). Prophenoloxidase activation is required for survival to microbial infections in *Drosophila*. *PLoS Pathog*, *10*(5), e1004067.

Boman, H. G., & Steiner, H. (1981). Humoral immunity in Cecropia pupae. In *Current topics in Microbiology and Immunology* (pp. 75-91). Springer Berlin Heidelberg.

Boman, H. G., & Hultmark, D. (1987). Cell-free immunity in insects. *Annual Reviews in Microbiology*, *41*(1), 103-126.

Böröczky, K., Wada-Katsumata, A., Batchelor, D., Zhukovskaya, M., & Schal, C. (2013). Insects groom their antennae to enhance olfactory acuity. *Proceedings of the National Academy of Sciences*, *110*(9), 3615-3620.

Brennan, C. A., & Anderson, K. V. (2004). Drosophila: the genetics of innate immune recognition and response. *Annual Reviews in Immunology*, *22*, 457-483.

Broderick, N. A., Welchman, D. P., & Lemaitre, B. (2009). *Recognition and response to microbial infection in Drosophila* (pp. 13-33). Oxford University Press: New York, NY, USA.

Bulet, P., Charlet, M., & Hetru, C. (2003). Antimicrobial peptides in insect immunity. In *Innate Immunity* (pp. 89-107). Humana Press.

Bulet, P., & Stocklin, R. (2005). Insect antimicrobial peptides: structures, properties and gene regulation. *Protein and peptide letters*, *12*(1), 3-11.

Bulmer, M. S., & Crozier, R. H. (2004). Duplication and diversifying selection among termite antifungal peptides. *Molecular Biology and Evolution*, *21*(12), 2256-2264.

Bulmer, M. S., & Crozier, R. H. (2006). Variation in positive selection in termite GNBPs and Relish. *Molecular Biology and Evolution*, *23*(2), 317-326.

Bulmer, M. S., Bachelet, I., Raman, R., Rosengaus, R. B., & Sasisekharan, R. (2009). Targeting an antimicrobial effector function in insect immunity as a pest control strategy. *Proceedings of the National Academy of Sciences*, *106*(31), 12652-12657.

Chan, Q. W., Howes, C. G., & Foster, L. J. (2006). Quantitative comparison of caste differences in honeybee hemolymph. *Molecular & Cellular Proteomics*, *5*(12), 2252-2262.

Chouvenc, T., Su, N. Y., & Robert, A. (2009). Cellular encapsulation in the eastern subterranean termite, *Reticulitermes flavipes* (Isoptera), against infection by the entomopathogenic fungus *Metarhizium anisopliae*. *Journal of invertebrate pathology*, *101*(3), 234-241.

Chouvenc, T., Robert, A., Sémon, E., & Bordereau, C. (2012). Burial behaviour by dealates of the termite *Pseudacanthotermes spiniger* (Termitidae, Macrotermitinae) induced by chemical signals from termite corpses. *Insectes sociaux*, *59*(1), 119-125.

Chouvenc, T., Efstathion, C. A., Elliott, M. L., & Su, N. Y. (2013). Extended disease resistance emerging from the faecal nest of a subterranean termite. *Proceedings of the Royal Society of London B: Biological Sciences*, *280*(1770), 20131885.

Christensen, B. M., Li, J., Chen, C. C., & Nappi, A. J. (2005). Melanization immune responses in mosquito vectors. *Trends in parasitology*, *21*(4), 192-199.

Christophides, G. K., Zdobnov, E., Barillas-Mury, C., Birney, E., Blandin, S., Blass, C., ... & Hetru, C. (2002). Immunity-related genes and gene families in *Anopheles gambiae*. *Science*, *298*(5591), 159-165.

Cociancich, S., Ghazi, A., Hetru, C., Hoffmann, J. A., & Letellier, L. (1993). Insect defensin, an inducible antibacterial peptide, forms voltage-dependent channels in *Micrococcus luteus*. *Journal of Biological Chemistry*, *268*(26), 19239-19245.

Cremer, S., Armitage, S. A., & Schmid-Hempel, P. (2007). Social immunity. *Current biology*, *17*(16), R693-R702.

de Morais Guedes, S., Vitorino, R., Domingues, R., Tomer, K., Correia, A. F., Amado, F., & Domingues, P. (2005). Proteomics of immune-challenged *Drosophila melanogaster* larvae hemolymph. *Biochemical and biophysical research communications*, *328*(1), 106-115.

Evans, T. A., Dawes, T. Z., Ward, P. R., & Lo, N. (2011). Ants and termites increase crop yield in a dry climate. *Nature Communications*, *2*, 262.

Fefferman, N. H., Traniello, J. F., Rosengaus, R. B., & Calleri II, D. V. (2007). Disease prevention and resistance in social insects: modeling the survival consequences of immunity, hygienic behavior, and colony organization. *Behavioral Ecology and Sociobiology*, *61*(4), 565-577.

Ferrandon, D., Imler, J. L., Hetru, C., & Hoffmann, J. A. (2007). The Drosophila systemic immune response: sensing and signaling during bacterial and fungal infections. *Nature Reviews Immunology*, *7*(11), 862-874.

Gao, Q. (2014). Social immunity and the expression of immune-related genes in the Eastern subterranean termite (Doctoral dissertation, The University of Western Ontario).

Geisler, R., Bergmann, A., Hiromi, Y., & Nüsslein-Volhard, C. (1992). cactus, a gene involved in dorsoventral pattern formation of Drosophila, is related to the IκB gene family of vertebrates. *Cell*, *71*(4), 613-621.

González-Santoyo, I., & Córdoba-Aguilar, A. (2012). Phenoloxidase: a key component of the insect immune system. *Entomologia Experimentalis et Applicata*, *142*(1), 1-16.

Gorman, M. J., & Paskewitz, S. M. (2001). Serine proteases as mediators of mosquito immune responses. *Insect biochemistry and molecular biology*, *31*(3), 257-262.

Haine, E. R., Moret, Y., Siva-Jothy, M. T., & Rolff, J. (2008). Antimicrobial defense and persistent infection in insects. *Science*, *322*(5905), 1257-1259.

Hamilton, C., Lay, F., & Bulmer, M. S. (2011). Subterranean termite prophylactic secretions and external antifungal defenses. *Journal of insect physiology*, *57*(9), 1259-1266.

Hamilton, C., & Bulmer, M. S. (2012). Molecular antifungal defenses in subterranean termites: RNA interference reveals in vivo roles of termicins and GNBPs against a naturally encountered pathogen. *Developmental & Comparative Immunology*, *36*(2), 372-377.

He, Y., Cao, X., Zhang, S., Rogers, J., Hartson, S., & Jiang, H. (2016). Changes in the plasma proteome of *Manduca sexta* larvae in relation to the transcriptome variations after an immune challenge: evidence for high molecular weight immune complex formation. *Molecular & Cellular Proteomics*, *15*(4), 1176-1187.

Hetru, C., Hoffmann, D., & Bulet, P. (1998). Antimicrobial peptides from insects. In: Brey PT, Hultmark D, editors. Molecular mechanisms of immune responses in insects. Chapman & Hall, p. 40-66.

Hillyer, J. F., Schmidt, S. L., & Christensen, B. M. (2003). Rapid phagocytosis and melanization of bacteria and *Plasmodium sporozoites* by hemocytes of the mosquito *Aedes aegypti*. *Journal of Parasitology*, *89*(1), 62-69.

Hoffmann, J. A. (2003). The immune response of Drosophila. *Nature*, *426*(6962), 33-38.

Holak, T. A., Engstroem, A., Kraulis, P. J., Lindeberg, G., Bennich, H., Jones, T. A., ... & Clore, G. M. (1988). The solution conformation of the antibacterial peptide cecropin A: a nuclear magnetic resonance and dynamical simulated annealing study. *Biochemistry*, *27*(20), 7620-7629.

Hudson, A. M., & Cooley, L. (2002). A subset of dynamic actin rearrangements in *Drosophila* requires the Arp2/3 complex. *The Journal of cell biology*, *156*(4), 677-687.

Hultmark, D., Steiner, H., Rasmuson, T., & Boman, H. G. (1980). Insect immunity. Purification and properties of three inducible bactericidal proteins from hemolymph of immunized pupae of *Hyalophora cecropia*. *European Journal of Biochemistry*, *106*(1), 7-16.

Hussain, A., & Wen, S. Y. (2012). Induction of immune response among formosan subterranean termites, *Coptotermes formosanus* Shiraki (Rhinotermitidae: Isoptera). *African Journal of Microbiology Research*, *6*(5), 995-1000.

Ip, Y. T., Reach, M., Engstrom, Y., Kadalayil, L., Cai, H., González-Crespo, S., ... & Levine, M. (1993). Dif, a dorsal-related gene that mediates an immune response in Drosophila. *Cell*, *75*(4), 753-763.

Ito, Y., Nakamura, M., Hotani, T., & Imoto, T. (1995). Insect lysozyme from house fly (*Musca domestica*) larvae: possible digestive function based on sequence and enzymatic properties. *The journal of biochemistry*, *118*(3), 546-551.

Janssen, K. P., & Schleicher, M. (2001). *Dictyostelium discoideum*: a genetic model system for the study of professional phagocytes: Profilin, phosphoinositides and the lmp gene family in Dictyostelium. *Biochimica et Biophysica Acta (BBA)-General Subjects*, *1525*(3), 228-233.

Javid, B., MacAry, P. A., & Lehner, P. J. (2007). Structure and function: heat shock proteins and adaptive immunity. *The Journal of Immunology*, *179*(4), 2035-2040.

Jiang, H., Vilcinskas, A., & Kanost, M. R. (2010). Immunity in lepidopteran insects. In *Invertebrate Immunity* (pp. 181-204). Springer US.

Jo, S. H., Son, M. K., Koh, H. J., Lee, S. M., Song, I. H., Kim, Y. O., ... & Song, B. J. (2001). Control of mitochondrial redox balance and cellular defense against oxidative damage by mitochondrial NADP+-dependent isocitrate dehydrogenase. *Journal of Biological chemistry*, *276*(19), 16168-16176.

Jordan, P. A., & Gibbins, J. M. (2006). Extracellular disulfide exchange and the regulation of cellular function. *Antioxidants & redox signaling*, *8*(3-4), 312-324.

Kanost, M. R., Kawooya, J. K., Law, J. H., Ryan, R. O., Van Heusden, M. C., & Ziegler, R. (1990). Insect haemolymph proteins. *Advances in insect physiology*, *22*, 299-396.

Karlsson, C., Korayem, A. M., Scherfer, C., Loseva, O., Dushay, M. S., & Theopold, U. (2004). Proteomic analysis of the *Drosophila* larval hemolymph clot. *Journal of Biological Chemistry*, *279*(50), 52033-52041.

Korb, J. (2008). Termites, hemimetabolous diploid white ants?. *Frontiers in zoology*, *5*(1), 15.

Koropatnick, T. A., Engle, J. T., Apicella, M. A., Stabb, E. V., Goldman, W. E., & McFall-Ngai, M. J. (2004). Microbial factor-mediated development in a host-bacterial mutualism. *Science*, *306*(5699), 1186-1188.

Krishna, K., Grimaldi, D. A., Krishna, V., & Engel, M. S. (2013). Treatise on the Isoptera of the world. (Bulletin of the American Museum of Natural History, no. 377).

Kuhn-Nentwig, L. (2003). Antimicrobial and cytolytic peptides of venomous arthropods. *Cellular and Molecular Life Sciences CMLS*, *60*(12), 2651-2668.

Lai, S. C., Chen, C. C., & Hou, R. F. (2002). Immunolocalization of prophenoloxidase in the process of wound healing in the mosquito *Armigeres subalbatus* (Diptera: Culicidae). *Journal of medical entomology*, *39*(2), 266-274.

Lamberty, M., Zachary, D., Lanot, R., Bordereau, C., Robert, A., Hoffmann, J. A., & Bulet, P. (2001). Insect immunity constitutive expression of a cysteine-rich antifungal and a linear antibacterial peptide in a termite insect. *Journal of Biological Chemistry*, *276*(6), 4085-4092.

Lemaitre, B., & Hoffmann, J. (2007). The host defense of *Drosophila melanogaster*. *Annu. Rev. Immunol.*, *25*, 697-743.

Lee, S. M., Koh, H. J., Park, D. C., Song, B. J., Huh, T. L., & Park, J. W. (2002). Cytosolic NADP+-dependent isocitrate dehydrogenase status modulates oxidative damage to cells. *Free Radical Biology and Medicine*, *32*(11), 1185-1196.

Liu, H., Jiravanichpaisal, P., Cerenius, L., Lee, B. L., Söderhäll, I., & Söderhäll, K. (2007). Phenoloxidase is an important component of the defense against *Aeromonas hydrophila* infection in a crustacean, *Pacifastacus leniusculus*. *Journal of Biological Chemistry*, *282*(46), 33593-33598.

Liu, L., Li, G., Sun, P., Lei, C., & Huang, Q. (2015). Experimental verification and molecular basis of active immunization against fungal pathogens in termites. *Scientific reports*, *5*.

Loseva, O., & Engström, Y. (2004). Analysis of signal-dependent changes in the proteome of *Drosophila* blood cells during an immune response. *Molecular & Cellular Proteomics*, *3*(8), 796-808.

Low, W. Y., Feil, S. C., Ng, H. L., Gorman, M. A., Morton, C. J., Pyke, J., ... & Gooley, P. R. (2010). Recognition and detoxification of the insecticide DDT by *Drosophila melanogaster* glutathione S-transferase D1. *Journal of molecular biology*, *399*(3), 358-366.

Mattoso, T. C., Moreira, D. D., & Samuels, R. I. (2012). Symbiotic bacteria on the cuticle of the leaf-cutting ant *Acromyrmex subterraneus subterraneus* protect workers from attack by entomopathogenic fungi. *Biology letters*, *8*(3), 461-464.

Matsuura, K., Tamura, T., Kobayashi, N., Yashiro, T., & Tatsumi, S. (2007). The antibacterial protein lysozyme identified as the termite egg recognition pheromone. *PLoS One*, *2*(8), e813.

Medzhitov, R., & Janeway, C. A. (2002). Decoding the patterns of self and nonself by the innate immune system. *Science*, *296*(5566), 298-300.

Mitchell, J. D. (2002). Termites as pests of crops, forestry, rangeland and structures in southern Africa and their control. *Sociobiology*, *40*(1), 47-69.

Moreno-García, M., Recio-Tótoro, B., Claudio-Piedras, F., & Lanz-Mendoza, H. (2014). Injury and immune response: applying the danger theory to mosquitoes. *Frontiers in plant science*, *5*, 451.

Nappi, A. J., & Ottaviani, E. (2000). Cytotoxicity and cytotoxic molecules in invertebrates. *Bioessays*, *22*(5), 469-480.

Nappi, A. J., & Christensen, B. M. (2005). Melanogenesis and associated cytotoxic reactions: applications to insect innate immunity. *Insect biochemistry and molecular biology*, *35*(5), 443-459.

Nichol, H., Law, J. H., & Winzerling, J. J. (2002). Iron metabolism in insects. *Annual review of entomology*, *47*(1), 535-559.

Naug, D., & Camazine, S. (2002). The role of colony organization on pathogen transmission in social insects. *Journal of Theoretical Biology*, *215*(4), 427-439.

Naug, D., & Smith, B. (2007). Experimentally induced change in infectious period affects transmission dynamics in a social group. *Proceedings of the Royal Society of London B: Biological Sciences*, *274*(1606), 61-65.

Pathak, J. P. N. (1993). Cell-mediated defense reactions in insects. In *Insect immunity* (pp. 47-58). Springer Netherlands.

Pham, L. N., Dionne, M. S., Shirasu-Hiza, M., & Schneider, D. S. (2007). A specific primed immune response in Drosophila is dependent on phagocytes. *PLoS Pathog*, *3*(3), e26.

Pham, L. N., & Schneider, D. S. (2008). Evidence for specificity and memory in the insect innate immune response. *Insect Immunology*, 97-127.

Prager, E. M., & Jolles, P. (1995). Animal lysozymes c and g: an overview. *Exs*, *75*, 9-31.

Rabilloud, T., Heller, M., Gasnier, F., Luche, S., Rey, C., Aebersold, R., ... & Lunardi, J. (2002). Proteomics analysis of cellular response to oxidative stress evidence for in vivo overoxidation of peroxiredoxins at their active site. *Journal of Biological Chemistry*, *277*(22), 19396-19401.

Ratcliffe, N. A., & Gagen, S. J. (1976). Cellular defense reactions of insect hemocytes in vivo: nodule formation and development in *Galleria mellonella* and *Pieris brassicae* larvae. *Journal of Invertebrate Pathology*, *28*(3), 373-382.

Ratcliffe, N. A., & Rowley, A. F. (1979). Role of hemocytes in defense against biological agents. *Insect hemocytes*, 331-414.

Rees, J. A., Moniatte, M., & Bulet, P. (1997). Novel antibacterial peptides isolated from a European bumblebee, *Bombus pascuorum* (Hymenoptera, Apoidea). *Insect biochemistry and molecular biology*, *27*(5), 413-422.

Ribeiro, C., & Brehélin, M. (2006). Insect haemocytes: what type of cell is that?. *Journal of insect physiology*, *52*(5), 417-429.

Rosengaus, R. B., & Traniello, J. F. (1993). Disease risk as a cost of outbreeding in the termite *Zootermopsis angusticollis*. *Proceedings of the National Academy of Sciences*, *90*(14), 6641-6645.

Rosengaus, R. B., Maxmen, A. B., Coates, L. E., & Traniello, J. F. (1998). Disease resistance: a benefit of sociality in the dampwood termite *Zootermopsis angusticollis* (Isoptera: Termopsidae). *Behavioral Ecology and Sociobiology*, *44*(2), 125-134.

Rosengaus, R. B., Traniello, J. F. A., Lefebvre, M. L., & Carlock, D. M. (2000). The social transmission of disease between adult male and female reproductives of the dampwood termite *Zootermopsis angusticollis*. *Ethology Ecology & Evolution*, *12*(4), 419-433.

Rosengaus, R. B., & Traniello, J. F. (2001). Disease susceptibility and the adaptive nature of colony demography in the dampwood termite *Zootermopsis angusticollis*. *Behavioral Ecology and Sociobiology*, *50*(6), 546-556.

Rosengaus, R. B., Moustakas, J. E., Calleri, D. V., & Traniello, J. F. (2003). Nesting ecology and cuticular microbial loads in dampwood (*Zootermopsis angusticollis*) and drywood termites (*Incisitermes minor*, *I. schwarzi*, *Cryptotermes cavifrons*). *Journal of Insect Science*, *3*(1), 31.

Rosengaus, R. B., Cornelisse, T., Guschanski, K., & Traniello, J. F. (2007). Inducible immune proteins in the dampwood termite *Zootermopsis angusticollis*. *Naturwissenschaften*, *94*(1), 25-33.

Rosengaus, R. B., Traniello, J. F., & Bulmer, M. S. (2010). Ecology, behavior and evolution of disease resistance in termites. In *Biology of termites: a modern synthesis* (pp. 165-191). Springer Netherlands.

Rosengaus, R. B., Schultheis, K. F., Yalonetskaya, A., Bulmer, M. S., DuComb, W. S., Benson, R. W., ... & Godoy-Carter, V. (2014). Symbiont-derived β-1, 3-glucanases in a social insect: mutualism beyond nutrition. *Frontiers in microbiology*, *5*, 607.

Ross, J., Jiang, H., Kanost, M. R., & Wang, Y. (2003). Serine proteases and their homologs in the *Drosophila melanogaster* genome: an initial analysis of sequence conservation and phylogenetic relationships. *Gene*, *304*, 117-131.

Rund, S. S., Hou, T. Y., Ward, S. M., Collins, F. H., & Duffield, G. E. (2011). Genome-wide profiling of diel and circadian gene expression in the malaria vector *Anopheles gambiae*. *Proceedings of the National Academy of Sciences*, *108*(32), E421-E430.

Rutschmann, S., Jung, A. C., Hetru, C., Reichhart, J. M., Hoffmann, J. A., & Ferrandon, D. (2000). The Rel protein DIF mediates the antifungal but not the antibacterial host defense in Drosophila. *Immunity*, *12*(5), 569-580.

Salt, G. (1970). The cellular defence reactions of insects (Vol. 16). Cambridge University Press.

Scharlaken, B., De Graaf, D. C., Memmi, S., Devreese, B., Van Beeumen, J., & Jacobs, F. J. (2007). Differential protein expression in the honey bee head after a bacterial challenge. *Archives of insect biochemistry and physiology*, *65*(4), 223-237.

Schmid-Hempel, P. (2005). Evolutionary ecology of insect immune defenses. *Annu. Rev. Entomol.*, *50*, 529-551.

Schuhmann, B., Seitz, V., Vilcinskas, A., & Podsiadlowski, L. (2003). Cloning and expression of gallerimycin, an antifungal peptide expressed in immune response of greater wax moth larvae, *Galleria mellonella*. *Archives of insect biochemistry and physiology*, *53*(3), 125-133.

Seehuus, S. C., Norberg, K., Gimsa, U., Krekling, T., & Amdam, G. V. (2006). Reproductive protein protects functionally sterile honey bee workers from oxidative stress. *Proceedings of the National Academy of Sciences of the United States of America*, *103*(4), 962-967.

Sies, H. (1997). Oxidative stress: oxidants and antioxidants. *Experimental physiology*, *82*(2), 291-295.

Silverman, G. A., Bird, P. I., Carrell, R. W., Coughlin, P. B., Gettins, P. G., Irving, J. I., ... & Remold-O'Donnell, E. (2001). The serpins are an expanding superfamily of structurally

similar but funtionally diverse proteins: Evolution, mechanism of inhibition, novel functions, and a revised nomenclature. *Journal of Biological Chemistry*.

Siva-Jothy, M. T., Moret, Y., & Rolff, J. (2005). Insect immunity: an evolutionary ecology perspective. *Advances in insect physiology*, *32*, 1-48.

Simone, M., Evans, J. D., & Spivak, M. (2009). Resin collection and social immunity in honey bees. *Evolution*, *63*(11), 3016-3022.

Söderhäll, K., & Cerenius, L. (1998). Role of the prophenoloxidase-activating system in invertebrate immunity. *Current opinion in immunology*, *10*(1), 23-28.

Steiner, H., Hultmark, D., Engstrom, A., Bennich, H. I., & Barman, H. G. (1981). Sequence and specificity of two antibacterial proteins involved in insect immunity. *Nature*, *292*, 246-8.

Steiner, H. (1982). Secondary structure of the cecropins: antibacterial peptides from the moth *Hyalophora cecropia*. *Febs Letters*, *137*(2), 283-287.

Strand, M. R. (2008). The insect cellular immune response. *Insect science*, *15*(1), 1-14.

Su, N. Y., & Scheffrahn, R. H. (2000). Termites as pests of buildings. In *Termites: evolution, sociality, symbioses, ecology* (pp. 437-453). Springer Netherlands.

Sun, Q., & Zhou, X. (2013). Corpse management in social insects. *International journal of biological sciences*, *9*(3), 313.

Suwanchaichinda, C., & Paskewitz, S. M. (1998). Effects of larval nutrition, adult body size, and adult temperature on the ability of *Anopheles gambiae* (Diptera: Culicidae) to melanize Sephadex beads. *Journal of Medical Entomology*, *35*(2), 157-161.

Taft, A. S., Chen, C. C., Li, J., & Christensen, B. M. (2001). Molecular cloning of two prophenoloxidase genes from the mosquito *Aedes aegypti*. *Insect molecular biology*, *10*(1), 97-103.

Takehana, A., Katsuyama, T., Yano, T., Oshima, Y., Takada, H., Aigaki, T., & Kurata, S. (2002). Overexpression of a pattern-recognition receptor, peptidoglycan-recognition protein-LE, activates imd/relish-mediated antibacterial defense and the prophenoloxidase cascade in *Drosophila* larvae. *Proceedings of the National Academy of Sciences*, *99*(21), 13705-13710.

Terrapon, N., Li, C., Robertson, H. M., Ji, L., Meng, X., Booth, W., ... & Gowin, J. (2014). Molecular traces of alternative social organization in a termite genome. *Nature communications*, *5*.

Thevissen, K., Warnecke, D. C., François, I. E., Leipelt, M., Heinz, E., Ott, C., ... & Cammue, B. P. (2004). Defensins from insects and plants interact with fungal glucosylceramides. *Journal of Biological Chemistry*, *279*(6), 3900-3905.

Tossi, A., Sandri, L., & Giangaspero, A. (2000). Amphipathic, α-helical antimicrobial peptides. *Peptide Science*, *55*(1), 4-30.

Traniello, J. F., Rosengaus, R. B., & Savoie, K. (2002). The development of immunity in a social insect: evidence for the group facilitation of disease resistance. *Proceedings of the National Academy of Sciences*, *99*(10), 6838-6842.

Turillazzi, S., Perito, B., Pazzagli, L., Pantera, B., Gorfer, S., & Tancredi, M. (2004). Antibacterial activity of larval saliva of the European paper wasp *Polistes dominulus* (Hymenoptera, Vespidae). *Insectes sociaux*, *51*(4), 339-341.

Ulyshen, M. D., & Shelton, T. G. (2012). Evidence of cue synergism in termite corpse response behavior. *Naturwissenschaften*, *99*(2), 89-93.

Vinson, S. B. (1990). How parasitoids deal with the immune system of their host: an overview. *Archives of Insect Biochemistry and Physiology*, *13*(1-2), 3-27.

Vizioli, J., Bulet, P., Charlet, M., Lowenberger, C., Blass, C., Müller, H. M., ... & Richman, A. (2000). Cloning and analysis of a cecropin gene from the malaria vector mosquito, *Anopheles gambiae*. *Insect molecular biology*, *9*(1), 75-84.

Wago, H. (1983). The important significance of filopodial elongation of phagocytic granular cells of the silkworm, *Bombyx mori*, in recognition of foreignness. *Developmental & Comparative Immunology*, *7*(3), 445-453.

Wang, W. X., Wang, Y. P., Deng, X. J., Dang, X. L., Tian, J. H., Yi, H. Y., ... & Lai, R. (2009). Molecular and functional characterization of a c-type lysozyme from the Asian corn borer, *Ostrinia furnacalis*. *Journal of insect science*, *9*(17), 1-13.

Wang, C., & Henderson, G. (2013). Evidence of Formosan subterranean termite group size and associated bacteria in the suppression of entomopathogenic bacteria, *Bacillus thuringiensis* subspecies *israelensis* and *thuringiensis*. *Annals of the Entomological Society of America*, *106*(4), 454-462.

Warnecke, D., & Heinz, E. (2003). Recently discovered functions of glucosylceramides in plants and fungi. *Cellular and Molecular Life Sciences CMLS*, *60*(5), 919-941.

Weinberg, E. D. (1993). The development of awareness of iron-withholding defense. *Perspectives in biology and medicine*, *36*(2), 215-221.

Weinstock, G. M., Robinson, G. E., Gibbs, R. A., Worley, K. C., Evans, J. D., Maleszka, R., ... & Elsik, C. G. (2006). Insights into social insects from the genome of the honeybee *Apis mellifera*. *Nature*, *443*(7114), 931-949.

Wilson-Rich, N., Spivak, M., Fefferman, N. H., & Starks, P. T. (2009). Genetic, individual, and group facilitation of disease resistance in insect societies. *Annual review of entomology*, *54*, 405-423.

Woltedji, D., Fang, Y., Han, B., Feng, M., Li, R., Lu, X., & Li, J. (2013). Proteome analysis of hemolymph changes during the larval to pupal development stages of honeybee workers (*Apis mellifera ligustica*). *Journal of proteome research*, *12*(11), 5189-5198.

Yamamoto, M., Okamoto, T., Takeda, K., Sato, S., Sanjo, H., Uematsu, S., ... & Yamaoka, S. (2006). Key function for the Ubc13 E2 ubiquitin-conjugating enzyme in immune receptor signaling. *Nature immunology*, *7*(9), 962-970.

Yu, X. Q., Jiang, H., Wang, Y., & Kanost, M. R. (2003). Nonproteolytic serine proteinase homologs are involved in prophenoloxidase activation in the tobacco hornworm, *Manduca sexta*. *Insect biochemistry and molecular biology*, *33*(2), 197-208.

Zachary, D., & Hoffmann, D. (1984). Lysozyme is stored in the granules of certain haemocyte types in Locusta. *Journal of insect physiology*, *30*(5), 405-411.

Zhang, Y., Dong, Z., Wang, D., Wu, Y., Song, Q., Gu, P., ... & Xia, Q. (2014). Proteomics of larval hemolymph in *Bombyx mori* reveals various nutrient-storage and immunity-related proteins. *Amino acids*, *46*(4), 1021-1031.

Zhukovskaya, M., Yanagawa, A., & Forschler, B. T. (2013). Grooming behavior as a mechanism of insect disease defense. *Insects*, *4*(4), 609-630.

Zou, Z., Shin, S. W., Alvarez, K. S., Bian, G., Kokoza, V., & Raikhel, A. S. (2008). Mosquito RUNX4 in the immune regulation of PPO gene expression and its effect on avian malaria parasite infection. *Proceedings of the National Academy of Sciences*, *105*(47), 18454-18459.

Zou, Z., Shin, S. W., Alvarez, K. S., Kokoza, V., & Raikhel, A. S. (2010). Distinct melanization pathways in the mosquito *Aedes aegypti*. *Immunity*, *32*(1), 41-53.

Chapter Two

Multiple antibacterial activities of proteinaceous compounds in crude extract from the eastern subterranean termites, *Reticulitermes flavipes* Kollar (Blattodea: Isoptera: Rhinotermitidae)

2.1 Abstract

Termites, the oldest eusocial insects, have evolved various defense mechanisms to resist microbial infections. In this study, the cell free crude extracts, five size-fractionated solutions (>300, 90-180, 30-90, 10-20, and <10 kDa), and heat-treated extract and heat-treated fractionated solutions were investigated against a common soil entomopathogenic bacterium *Bacillus subtilis*. The activity against *B. subtilis* was evidenced in all but the heat-treated solutions, indicating the presence of antibacterial activities, the existence of multiple active compounds in the crude extracts, and the protein nature of the active compounds. The active compounds, with the molecular sizes ranging from <10 to >300 kDa, demonstrated different levels of antibacterial activity. The greatest activity was observed in the fraction of 10-20 kDa and Ampicillin, followed by the fractions of <10 kDa and >300 kDa, and the lowest in the fraction of 30-90 kDa. This study reports that the crude extract from *R. flavipes* workers constitutively contain multiple proteins with various antibacterial activities against the susceptible bacterium *B. subtilis*.

2.2 Introduction

With roughly two million species, insects account for one of the most successful evolution groups (Adams 1999). They colonize nearly all ecological niches and feed on most of

plants and animals. Consequently, insects have evolved effective innate immune systems in confronting a large variety of potentially harmful microorganisms. Their innate immune systems may comprise of a series of cellular and humoral reactions, which differ from the adaptive immune system of vertebrates (Hultmark 2003).

The innate immune system of termites has been of great interest for discovering novel compounds against microbes, as well as exploring new approaches to control termites. Subterranean termites (Blattodea: Isoptera: Rhinotermitidae), especially species of *Reticulitermes* genus, have a wide distribution in the U.S. (except Alaska). They nest and forage underground in soil environments rich in pathogenic microbial communities (Chouvenc et al. 2008; Evans 1982). Interacting with many soil pathogens has led to the development of disease resistance mechanisms that allowed termites to survive and to develop in such environment.

Several antimicrobial proteins/peptides have been isolated or identified from subterranean termite salivary glands and hemolymph (Lamberty et al. 2001; Matsuura et al. 2007; Hamilton et al. 2011; Bulmer et al 2010). Termicin, β-1, 3-glucanase and termite Gram-negative binding proteins (tGNBPs) are reported as antifungal compounds in several *Reticulitermes* species, and lysozyme as antibacterial compound in *R. speratus* (Lamberty et al. 2001; Matsuura et al. 2007; Hamilton et al. 2011; Bulmer et al 2010). However, there has been no report on antibacterial activity from the eastern subterranean termite, *R. flavipes* Kollar *(*Isoptera: Rhinotermitidae), the most common economically important wood destroying pest in the southeastern United States.

This study has a three-fold objective: 1) to assess the presence of antibacterial activities in *R. flavipes* against a common soil entomopathogenic bacterium *Bacillus subtilis*; 2) to determine the nature of antibacterial compounds of crude extracts; and 3) to analyze the size

profile of active compounds. The ultimate goal is to discover new antibacterial compounds for development of antibiotic drugs for treating antibiotic-resistant infections.

2.3 Materials and Methods

2.3.1 Organisms

R. flavipes was collected on the Auburn University campus (Alabama, USA) between August 2012 and March 2013. Termite collections were maintained in Urban Entomology Laboratory at 25^{o}C for at least 20 days before subjected to crude extraction. Gram-positive bacterium *B. subtilis* (ATCC 6633) was obtained from Microbiology Teaching Laboratory of Auburn University and stored in skim milk at -80°C.

2.3.2 Whole Body Extraction and Size Fractionating

For each extraction, termite workers (5 g) were suspended in 25 ml of 20 mM Tris-HCl, 20 mM NaCl (pH=7.5) buffer and homogenized (Sonic Dismembrator Model 100, Fisher Scientific, Pittsburgh, PA) on ice for 30 sec. The lysed extract was centrifuged twice at 8,000 *g* (Beckman JA-21, Beckman Coulter, Inc. Brea, CA) and 4oC, each for 20 min, to remove insoluble materials. The resulting cell free extract (CFE) (15 ml) was sequentially size fractionated with Microsep^{TM} Advance Centrifugal Devices (Pall Corporation, Port Washington, NY) to obtain five fractions (>300, 90-180, 30-90, 10-20, and <10 kDa). Protein concentrations of the crude extracts and size-fractionated solutions were determined by Bradford assay (Bradford 1976) with the Bio-Rad protein assay kit (Bio-Rad, Hercules, CA). The fractionated solutions were lyophilized (Heto Lyolab 3000, Thermo Scientific, Waltham, MA) at -57oC overnight and dissolved in Milli-Q water to achieve the final protein concentration of approximately 5 mg/ml, as same as the crude extract.

2.3.3 Heating Treatment

To determine the nature of the active antibacterial compounds, a sample (5 ml) of the crude extract was subjected to heat treatment at 100^{o}C for 10 min. The resulting solution was centrifuged at 8,000 *g* (Beckman JA-21, Beckman Coulter, Inc. Brea, CA) and 4oC for 10 min to remove denatured proteins.

2.3.4 Inhibition Zone Assay

Activity of the crude extract, heated crude extract (supernatants), and size-fractionated solutions against *B. subtilis* was determined using a modified inhibition zone assay (Fig. 2.1), also named Kirby-Bauer Disk Diffusion method (Gautam et al. 2013; Bauer et al. 1966). In brief, approximately 2 x 10^{8} *B. subtilis* cells grown to log-phase (OD_{600} of 0.3) were mixed with 2.5 ml of soft agar and overlaid on a Lysogeny Broth (LB) agar plate. Four filter paper disks (5 x 5 mm) were placed uniformly on the bacterial lawn in each plate. The paper disks were treated with one of the following samples, respectively: 20 µl of the six termite CFE (crude and the five size-fractions); 20 µl of the six heat-treated termite CFE, 1 µl of ampicillin (25 mg/ml) as positive control, or 20 µl of 100 mM Tris-HCl, 100 mM NaCl (pH=7.5) buffer as a negative control. All plates were incubated at 37°C for 24 h to allow bacterial growth. The experiment was repeated three times, each with 3 replicates (N=9).

2.3.5 Statistical Analysis

The diameters (D; mm) of growth inhibition zones were measured and compared using repeated measures ANOVA (PROC GLM; α=0.05; SAS 9.2) to determine the significance among treatments.

2.4 Results and Discussions

The results are presented in Table 2.1. The clear inhibition zone in the crude extract

treatment shows the presence of activity against *B. subtilis* in *R. flavipes*. The absence of clear inhibition zone of the heat-treated crude extract indicates the proteinaceous nature of the active compounds in crude extract. However, this absence of activity cannot be used as a conclusive evidence to exclude the possibility of non-proteinaceous active molecules in the crude extract, because it is possible that the proteinaceous active molecules in the samples are too low in concentrations to show their activity in the inhibition zone assays. Future work is needed to elucidate this possibility. Previous research reported that *R. flavipes* showed robust β-(1, 3)-glucanase activity (antifungal activity) against an entomopathogenic fungus *M. anisopliae* (Hamilton and Bulmer 2012; Hamilton et al. 2011). In our study, we revealed significant antibacterial activity of the CFE and the size-fractionated solutions from naïve *R. flavipes* against *B. subtilis* by pulverizing whole termites and performing inhibition zone assay on LB agar plate. An interesting finding is that there are multiple compounds in the CFE possessing potent antibacterial property, as evidenced by the clear inhibition zones in all the five size-fractions. The molecular sizes of the active compounds range from <10 to >300 kDa. The different measurements of clear inhibition zones in the five size-fractions show that the level of antibacterial activity varies with the molecular size of the protein/peptide. The greatest antibacterial activity is displayed in the fraction of size 10-20 kDa, which has a comparable activity as Ampicillin, and the lowest activity in the fraction of size 30-90 kDa (F=26.4, P=0.016). This study is the first to report the antibacterial activities of multiple compounds existing simultaneously in a subterranean termite species.

Another interesting finding of this study is the antibacterial activity of compounds in the <10 kDa fraction. Of the known antimicrobial proteins/peptides in subterranean termite, most have antifungal activities (Matsuura et al. 2007; Hamilton et al. 2011; Bulmer et al. 2012; Bauer

et al. 1966). The only protein reported having antibacterial activity is lysozyme identified from a different termite species (*R. speratus*) (Matsuura et al. 2007). However, lysozyme has a molecular size of 14.5kDa, bigger than 10 kDa. The only documented antibacterial compound smaller than 10 kDa is spinigerin (~2.5-3 kDa). Spingerin is a broad-spectrum antibacterial peptide reported from a tropical and subtropical fungus-growing termite, *Pseudacanthotermes spiniger* (Isoptera: Macrotermitinae) (Lamberty et al. 2001). It is possible that spinigerin is present in *R. flavipes* because these genes were reported to be highly conserved. However, spinigerin is reported inactive against *B. subtilis* (Lamberty et al. 2001). Therefore, it is highly likely that the multiple antibacterial proteins/peptides, including the small peptides (<10 kDa) representing compounds that haven't been identified.

Up to date, no study has directly determined the mode of action (MOA) of the two termite-derived antimicrobial peptides, spinigerin and termicin (Lamberty et al. 2001). Because the α-helical structure of spinigerin has a strong electrostatic attraction between its three Arg residues and the negatively charged polar head groups of the phospholipids on the bacterial membrane surface, Lee et al. (2003) suggested a MOA of spinigerin breaking down membrane and consequent cell death. Da Silva et al. (2003) proposed that the antifungal properties of termicin might relate to its marked hydrophobicity and its amphipathic structure as compared to other antibacterial defensins.

In this study, unsterilized termite whole bodies were used to obtain crude extract. Therefore, the antibacterial activities may come from the proteins produced by associated bacteria on termite cuticle or symbiotic protists in termite gut, or directly relate to the termite itself (regardless of whether it is the hemolymph, specific organs or glands). Previous research identified that cuticular bacteria (*Pseudomonas aeruginosa*, *Serratia marcescens*, *Cedecea*

davisae, and *Lysinibacillus sphaericus*) of the Formosan subterranean termite, *Coptotermes formosanus* displayed antifungal activities or antibacterial effect on an entomopathogenic pathogen *B. thuringienisis* (Wang and Henderson 2013), and a bacterium (*Streptomyces* sp) associated with fecal nest protects termite against entomopathogens (Chovenc et al. 2013). Several protists isolated from the guts of several termite species (*Macrotermes michaelseni, C. formosanus,* and *R. speratus*) are reported producing antibiotics against bacteria including *Bacillus* spp., *Escherichia coli* and *Staphylococcus aureus* (Watanabe et al. 2003; Akhwale 2001; Matsui et al. 2012). Future work will identify the source or the origin of the antibacterial compounds.

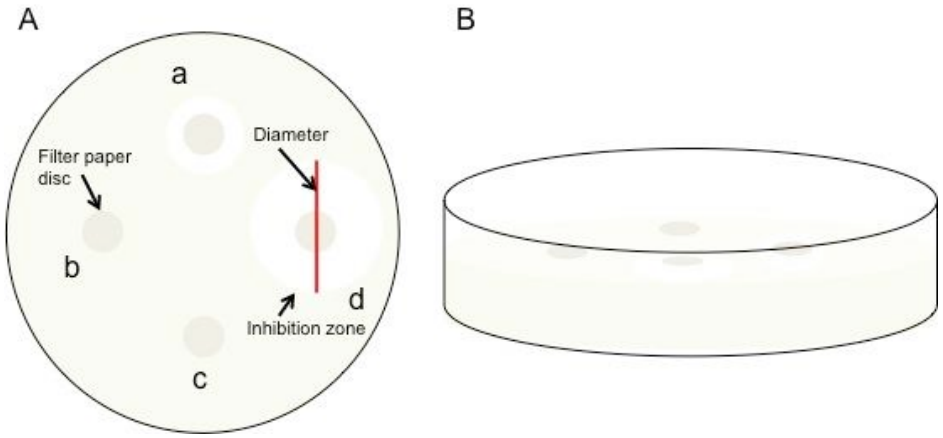

Figure 2.1 The modified inhibition zone assay. A, a top view of a bacterial lawn: (a) a filter paper disc loaded with 400 µg CFE, (b) a filter paper disc loaded with heat-treated CFE, (c) a filter paper disc loaded with 20 µl 80 mM Tris-HCl, 80 mM NaCl buffer, (d) a filter paper disc loaded with 25 µg ampicillin; B, a side view of the LB plate.

Table 2.1 Diameters (mm) of clear inhibition zone (N=9) on *B. subtilis* soft agar plate

Treatments	Diameters of inhibition zone* (Mean±SD)
>300 kDa	14.68±0.78[b]
90-180 kDa	11.96±0.54[c]
30-90 kDa	8.25±0.17[d]
10-20 kDa	20.58±0.53[a]
<10 kDa	16.32±0.83[b]
CFE	13.76±0.80[b]
Heated CFE	0[e]
100 mM Tris-HCl, 100 mM NaCl buffer	0[e]
Ampicillin	21±1.83[a]

*Different letters in the column indicate significant differences among the samples

References

Adams, T. S. (1999). Hematophagy and hormone release. *Annals of the Entomological Society of America*, *92*(1), 1-13.

Akhwale, J. K. (2014). Isolation and Characterization of antibiotic and exoenzymes producing actinobacteria from guts of fungus-cultivating termites *(Macrotermes michaelseni)* (Doctoral dissertation).

Bauer, A. W., Kirby, W. M. M., Sherris, J. C., & Turck, M. (1966). Antibiotic susceptibility testing by a standardized single disk method. *American journal of clinical pathology*, *45*(4), 493.

Bulmer, M. S., Lay, F., & Hamilton, C. (2010). Adaptive evolution in subterranean termite antifungal peptides. *Insect molecular biology*, *19*(5), 669-674.

Bradford, M. M. (1976). A rapid and sensitive method for the quantitation of microgram quantities of protein utilizing the principle of protein-dye binding. *Analytical biochemistry*, *72*(1-2), 248-254.

Chouvenc, T., Su, N. Y., & Elliott, M. L. (2008). Interaction between the subterranean termite *Reticulitermes flavipes* (Isoptera: Rhinotermitidae) and the entomopathogenic fungus Metarhizium anisopliae in foraging arenas. *Journal of Economic Entomology*, *101*(3), 885-893.

Chouvenc, T., Efstathion, C. A., Elliott, M. L., & Su, N. Y. (2013). Extended disease resistance emerging from the faecal nest of a subterranean termite. In *Proc. R. Soc. B* (Vol. 280, No. 1770, p. 20131885). The Royal Society.

Da Silva, P., Jouvensal, L., Lamberty, M., Bulet, P., Caille, A., & Vovelle, F. (2003). Solution structure of termicin, an antimicrobial peptide from the termite *Pseudacanthotermes spiniger*. *Protein science*, *12*(3), 438-446.

Evans, H. C. (1982). Entomogenous fungi in tropical forest ecosystems: an appraisal. *Ecological Entomology*, *7*(1), 47-60.

Gautam, V., Singhal, L., Arora, S., Jha, C., & Ray, P. (2013). Reliability of Kirby-Bauer disk diffusion method for detecting carbapenem resistance in *Acinetobacter baumannii-calcoaceticus* complex isolates. *Antimicrobial agents and chemotherapy*, *57*(4), 2003-2004.

Hamilton, C., Lay, F., & Bulmer, M. S. (2011). Subterranean termite prophylactic secretions and external antifungal defenses. *Journal of insect physiology*, *57*(9), 1259-1266.

Hultmark, D. (2003). Drosophila immunity: paths and patterns. *Current opinion in immunology*, *15*(1), 12-19.

Lamberty, M., Zachary, D., Lanot, R., Bordereau, C., Robert, A., Hoffmann, J. A., & Bulet, P. (2001). Insect immunity constitutive expression of a cysteine-rich antifungal and a linear antibacterial peptide in a termite insect. *Journal of Biological Chemistry*, *276*(6), 4085-4092.

Lee, K. H., Shin, S. Y., Hong, J. E., Yang, S. T., Kim, J. I., Hahm, K. S., & Kim, Y. (2003). Solution structure of termite-derived antimicrobial peptide, spinigerin, as determined in SDS micelle by NMR spectroscopy. *Biochemical and biophysical research communications*, *309*(3), 591-597.

Matsuura, K., Tamura, T., Kobayashi, N., Yashiro, T., & Tatsumi, S. (2007). The antibacterial protein lysozyme identified as the termite egg recognition pheromone. *PLoS One*, *2*(8), e813.

Matsui, T., Tanaka, J., Namihira, T., & Shinzato, N. (2012). Antibiotics production by an actinomycete isolated from the termite gut. *Journal of basic microbiology*, *52*(6), 731-735.

Wang, C., & Henderson, G. (2013). Evidence of Formosan subterranean termite group size and associated bacteria in the suppression of entomopathogenic bacteria, *Bacillus thuringiensis*

subspecies *israelensis* and *thuringiensis*. *Annals of the Entomological Society of America*, *106*(4), 454-462.

Watanabe, Y., Shinzato, N., & Fukatsu, T. (2003). Isolation of actinomycetes from termites' guts. *Bioscience, biotechnology, and biochemistry*, *67*(8), 1797-1801.

Chapter Three

Characterization of antibacterial activity of eastern subterranean termite, *Reticulitermes flavipes,* against human pathogens

3.1 Abstract

The emergence and dissemination of multidrug resistant bacterial pathogens necessitate research to find new antimicrobials against these organisms. We investigated antimicrobial production by eastern subterranean termites, *Reticulitermes flavipes,* against a panel of bacteria including three multidrug resistant (MDR) and four non-MDR human pathogens. We determined that the crude extract of naïve termites had a broad-spectrum activity against the non-MDR bacteria but it was ineffective against the three MDR pathogens *Pseudomonas aeruginosa*, methicillin-resistant *Staphylococcus aureus* (MRSA), and *Acinetobacter baumannii*. Heat or trypsin treatment resulted in a complete loss of activity suggesting that antibacterial activity was proteinaceous in nature. The antimicrobial activity changed dramatically when the termites were fed with either heat-killed *P. aeruginosa* or MRSA. Heat-killed *P. aeruginosa* induced activity against *P. aeruginosa* and MRSA while maintaining or slightly increasing activity against non-MDR bacteria. Heat-killed MRSA induced activity specifically against MRSA, altered the activity against two other Gram-positive bacteria, and inhibited activity against three Gram-negative bacteria. Neither the naïve termites nor the termites challenged with heat-killed pathogens produced antibacterial activity against *A. baumannii.* Further investigation demonstrated that hemolymph, not the hindgut, was the primary source of antibiotic activity.

This suggests that the termite produces these antibacterial activities and not the hindgut microbiota. Two-dimensional gel electrophoretic analyses of 493 hemolymph protein spots indicated that a total of 38 and 65 proteins were differentially expressed at least 2.5-fold upon being fed with *P. aeruginosa* and MRSA, respectively. Our results provide the first evidence of constitutive and inducible activities produced by *R. flavipes* against human bacterial pathogens.

3.2 Introduction

In recent years, insects have been recognized for having potent immune defenses that produce constitutive and inducible antimicrobial compounds to combat various pathogens (Haine et al. 2008). Thus, they have been targeted as a potential source of antimicrobial compounds (Dossey 2010; Slocinska et al 2008). Insects possess complex immune responses that act synergistically to provide protection against microbial infections (Tzou et al. 2002). When pathogens break through morphological barriers, insects evoke innate immune responses comprised of cellular and humoral reactions. Cellular reactions are hemocyte-mediated and include phagocytosis and encapsulation, while humoral reactions involve the production of antimicrobial proteins and activation of enzymatic cascades (Lavin and Strand 2002). Over the last few decades, more than 150 insect antimicrobial peptides/proteins (AMPs) have been identified from naïve, microbe-challenged, or injured insects (Yi et al. 2014). Reported insect AMPs include lysozymes, cecropins, attacins, defensins, and proline rich peptides (Yi et al. 2014; Bulet et al. 1999).

Recently, several constitutive antimicrobial proteins and peptides have been identified from three termite families: Termopsidae (Rosengaus et al 2007), Rhinotermitidae (Bulmer et al. 2010; Hamilton and Bulmer 2012; Matsuura et al. 2007; Zeng et al. 2014), and Termitidae (Bulmer et al. 2009; Bulmer and Crozier 2004; Bulmer and Crozier 2006; Lamberty et al. 2001). The majority of these molecules have antifungal activities and only a few, including termicin,

defensin-like peptides, spinigerin, and lysozymes, have weak antibacterial activities (Bulmer et al. 2009; Lamberty et al. 2001). Hussain et al. (2012) reported induction of antibacterial activity from the whole body homogenates of *Coptotermes formosanus* Shiraki upon exposure with various bacteria, including a human pathogen *Staphylococcus aureus*. However, exposure to different bacteria did not stimulate activity against the inducing organisms except for *Bacillus thuringiensis.*

Subterranean termites (Blattodea: Isoptera: Rhinotermitidae), especially the *Reticulitermes* species, are widely distributed in the United States. These termites have developed disease resistance mechanisms that facilitated their survival and propagation as they nest and forage in soil (Chovenc et al. 2013). Termite-produced AMPs, termicin (initially isolated from a fungus-growing termite) and tGNBPs (termite gram-negative binding proteins), have been described in the eastern subterranean termite *R. flavipes* and the dark southern subterranean termite *R. virginicus* (Bulmer et al. 2010; Hamilton and Bulmer 2012; Bulmer et al. 2009). GNBP2 has β-1, 3-glucanase activity in termites and contributes to external antifungal defense (Bulmer et al. 2009). We previously reported the discovery of constitutive antibacterial activity from the cell-free extract (CFE) of *R. flavipes* against a common Gram-positive soil-borne entomopathogenic bacterium, *B. subtilis* (Zeng et al. 2014). In this study, we determined the presence, characteristics, and levels of constitutive and inducible antibacterial activities in *R. flavipes* against a panel of human bacterial pathogens including three common multidrug resistant nosocomial pathogens and five non-MDR pathogens.

3.3 Materials and Methods

3.3.1 Termite maintenance and induction of antimicrobial activity

R. flavipes were collected on the Auburn University campus as previously described (Zeng et al. 2014; Hu and Appel 2004) and workers were maintained in Urban Entomology

Laboratory at 25 ± 2°C for at least 20 days before being subjected to experiments. To examine the potentially inducible antibacterial activity, two heat-killed MDR pathogens, Gram-negative *P. aeruginosa* and Gram-positive MRSA, were selected to stimulate the immune response. Bacteria were grown in Lysogeny Broth (LB) (Bertani 1951) at 37°C with aeration overnight, subcultured, and grown in fresh LB to early-mid log-phase (OD_{600} = 0.3 ± 0.05). Twenty-four ml of heat-killed bacterial suspension was obtained as follows: cells from 48 ml of culture was harvested via centrifugation at 13,200 rpm for 5 min, washed twice with 48 ml of milli-Q (MQ) water, resuspended in 24 ml of MQ water (~6 x 10^8 cells/ml), and heat-killed at 100°C for 10 min. *R. flavipes* workers were surface sterilized with 70% ethanol to eliminate surface microbes immediately before being subjected to testing. To immunize the workers, a group of 3 g of surface-sterilized termites (8 groups per treatment) was introduced into Petri plates (15 cm × 2.5 cm) provisioned with sterile filter papers (12.5 cm in diameter, Whatman #1; 1 filter paper per Petri dish) moistened with 3 ml of heat-killed *P. aeruginosa* or MRSA suspension, respectively. Sterile filter papers were moisturized with the same amount of MQ water and were used as negative controls. The termites were allowed to feed in Petri plates for 24 hours and then harvested for analysis.

3.3.2 Preparation of whole body and size-fractionated CFE

Surface sterilized naïve and heat-killed pathogen challenged termite workers (24 g each) were suspended, separately, in 120 ml of 20 mM Tris-HCl, 20 mM NaCl (pH = 7.5) buffer and homogenized as previously described (Zeng et al. 2014). The crude CFE was quickly frozen in liquid nitrogen and lyophilized (Heto Lyolab 3000, Thermo Fisher Scientific, Pittsburgh, PA) at -57°C overnight before being dissolved in MQ water to achieve the final concentration of

approximately 20 mg/ml protein concentration as determined by the Bradford assay (Bio-Rad, Hercules, CA) (Bradford 1976).

Additionally, a sample of each crude CFE (15 ml) was sequentially size fractionated with Microsep^{TM} Advance Centrifugal Devices (Pall Corporation, Port Washington, NY) with the molecular weight cut-offs (MWCO) of 100K, 30K, 10K, and 3K. This separated the CFE into five fractions containing proteins with approximate molecular weight of >300 kDa, 90-180 kDa, 30-90 kDa, 10-20 kDa, and <10 kDa, respectively. The fractionated solutions were lyophilized and dissolved in MQ water to achieve the final protein concentration of approximately 20 mg/ml to match that of the crude extract. All samples were stored at -80°C until the antibacterial assays.

3.3.3 Protein denaturation

To denature proteins, 5 ml of the lyophilized crude extract of each treatment was heated to 100°C for five minutes as previously described (Zeng et al. 2014). Trypsin digestion was performed as follows. To 100 µl of lyophilized crude extract for each treatment, 5 µl of 200 mM dithiothreitol (DTT) in 100 mM NH_4HCO_3 was added and incubated for 30 min at room temperature. Then, 4 µl of the 1M iodoacetamide alkylating reagent was added to the sample, mixed, and incubated for 45 min at room temperature. Finally, 50 µl of trypsin (0.2 µg/µl in 100 mM NH_4HCO_3) was added to the sample and incubated overnight at 37°C.

3.3.4 Termite hemolymph collection and hindgut extraction

Hemolymph was immediately drawn (~0.05-0.1 µl/individual) from surface sterilized termites by inserting a sterile insect needle into the dorsal intersegmental membrane of cold-immobilized insects. Any sample contaminated with the gut or fat was discarded. The extracted hemolymph (~200-400 µl) was transferred to a microcentrifuge tube containing 1 ml of 20 mM Tris-HCl, 20 mM NaCl (pH = 7.5) buffer and kept on ice. Hindguts for the same individuals

were separated and rinsed in 5 ml of 20 mM Tris-HCl, 20 mM NaCl (pH = 7.5) buffer before being homogenized in 1ml of buffer on ice. The hemolymph and gut extracts were centrifuged at 12,000 rpm at 4°C for 5 min to acquire the cell-free samples. The protein concentration of each sample was measured and was adjusted to the final concentration of 25 mg/ml by either dilution or concentration following lyophilization.

3.3.5 Antibacterial assay

Antibacterial activity of each extract against a panel of selected bacteria (Table 1) was determined using a modified inhibition zone assay as previously described (Zeng et al. 201). For every assay, each bacterium was freshly grown from a frozen stock. Briefly, a colony from a freshly streaked plate was inoculated into LB medium, grown overnight at 37°C with shaking at ~220 rpm, subcultured the next day into fresh LB medium and grown at 37°C with shaking at ~220 rpm to early log-phase of growth (OD_{600} = 0.3 ± 0.05), and diluted to ~2.5×10^7 CFU/ml. The antibacterial activities of crude extracts were examined by placing eight sterilized filter paper disks (5 × 5 mm) uniformly on the bacterial lawn in each plate. The paper disks were treated with one of the following eight samples, respectively: 20 µl of three crude extracts (naïve, *P. aeruginosa*-challenged, and MRSA-challenged) at a concentration of approximately 20 mg/ml (= 400 µg/disk), 20 µl of three heat-treated crude extracts (naïve, *P. aeruginosa*-challenged, and MRSA-challenged), 1 µl of ampicillin (= 25 µg/disk) as the positive control, and 20 µl of 80 mM Tris-HCl, 80 mM NaCl buffer as the negative control. The antibacterial activities of size-fractionated extracts, hemolymph, and gut extract were determined using the same assay. All plates were incubated at 37°C for 24 h to allow bacterial growth and the zones of clearing were measured. Every assay was repeated three times, each with 3 replicates, to acquire an N of 9 for each treatment.

3.3.6 Statistical analysis

The diameters (D; mm) of inhibition zones were compared using the ANOVA and Tukey's method (PROC GLM; $\alpha = 0.05$; SAS 9.2) to determine all possible pairwise differences among treatments. The ANOVA (PROC GLM; $\alpha = 0.05$; SAS 9.2) was used to determine the difference in activities of the same treatment on each tested bacterium.

3.3.7 Gel electrophoretic analysis of proteins

Protein profiles of the MWCO of 30K and 100K fractionated samples of termite CFE were analyzed by polyacrylamide gel electrophoreses (PAGE) including both non-denaturing Native PAGE and denaturing SDS-PAGE. Approximately 20 μg of protein samples were loaded per lane. The protein ladders for Native PAGE (14-500 kDa) and SDS-PAGE (10-250 kDa) were purchased from Sigma-Aldrich (St Louis, MI) and Life Technologies (Green Island, NY), respectively. In addition, non-size fractionated hemolymph samples were analyzed on SDS-PAGE. The proteins on PAGE were stained with Coomassie brilliant blue R-250 (Bio-Rad, Hercules, CA) for visualization.

Two-dimensional gel electrophoretic analysis of the proteins in hemolymph was performed by the Kendrick Labs, Inc. (Madison, WI). Approximately 200 μg of total protein per sample was used to separate the proteins between pI of 3 to 10 for the first dimension and molecular weight of 14-220 kDa for the second dimension. Duplicate gels were run for each sample, stained with Sypro®Ruby (Bio-Rad), and scanned on a Typhoon FLA 9000 scanner (GE Healthcare, Piscataway, NJ). A total of 493 spots were analyzed using Progenesis SameSpots software (version 4.5, 2011, TotalLab, UK) and Progenesis PG240 software (version 2006, TotalLab, UK). The quantity of each spot was calculated as spot percentages (individual spot density divided by total density of all measured spots). The quantity differences between MRSA-

challenged versus naïve and *P. aeruginosa*-challenged versus naïve were analyzed using two-sample t-test.

3.4 Results

3.4.1 Broad-spectrum constitutive antibacterial activity of *R. flavipes*

In order to understand the biological range of antibacterial activity of *R. flavipes* CFE, we tested a panel of non-MDR and MDR human bacterial pathogens for their susceptibility. Table 3.1 shows the panel of bacteria used in this study which includes both gram-positive and gram-negative bacteria. The CFE prepared from the whole body of naïve termite displayed significant inhibitory activity against the five non-MDR bacteria (*Staphylococcus aureus*, *Streptococcus pyogenes*, *Escherichia coli* O157:H7, *Salmonella enterica* serovar Typhimurium, and *E. coli* K-12) but it was inactive against the three MDR pathogens (methicillin resistant *S. aureus* or MRSA, *Pseudomonas aeruginosa*, and *Acinetobacter baumannii*) (Table 3.2). Of the five susceptible bacteria, the strongest inhibitory effect was against *S. aureus*, followed by *E. coli* O157:H7 and *S.* Typhimurium. The weakest activity was against *S. pyogenes*. As expected, ampicillin inhibited the growth of all but the three MDR pathogens. We observed no obvious correlation between Gram-staining and the effectiveness of the termite CFE on growth inhibition. The antibacterial activity of termite CFE disappeared completely when it was heat-denatured (Table 3.2) or treated with trypsin (data not shown). These data suggest that the antibacterial activity of *R. flavipes* is likely to be proteinaceous in nature.

3.4.2 MDR-induced alteration in antibacterial activities of *R. flavipes*

In addition to the constitutive antibacterial activity, we determined that *R. flavipes* possesses inducible antibacterial activities. Feeding termites with heat-killed *P. aeruginosa* or MRSA altered their antibacterial activities and stimulated specific anti-MDR activity as illustrated in Figure 3.1. In both cases, the termites produced new antibacterial activity that was

effective against the inducer bacterium. Specifically, termite challenged by heat-killed *P. aeruginosa* produced activity against both *P. aeruginosa* and MRSA while maintaining or slightly increasing antibacterial activity against bacteria listed in Table 3.1. Termites challenged by heat-killed MRSA produced anti-MRSA activity while maintaining activity against two non-MDR Gram-positive pathogens. Interestingly, antibacterial activity against Gram-negative bacteria listed in Table 1 was completely abolished in MRSA-challenged termites (Figure 3.1). Neither *P. aeruginosa* nor MRSA induced antibacterial activity against *A. baumannii* in *R. flavipes* (data not shown).

3.4.3 Size fractionation of antibacterial activities

We previously demonstrated that multiple fractions of size-fractionated *R. flavipes* CFE had antibacterial activity against the soil-borne entomopathogenic *B. subtilis* (Zeng et al. 2014). This indicated that *R. flavipes* produced multiple proteins with anti-*B. subtilis* activity. In continuing our characterization, we tested size-fractionated CFE from the naïve, *P. aeruginosa* challenged, and MRSA challenged *R. flavipes* against the panel of bacteria listed in Table 3.1. We determined that all antibacterial activities of three groups of termites against this panel of bacteria were contained in fractions with proteins larger than 90 kDa in molecular weight (MWCO filters of 30K and 100K; Supplementary Figure 3.1). However, many of these large proteins appeared to be composed of smaller subunits because they migrated as proteins of 25-90 kDa on denaturing SDS-PAGE (Supplementary Figure 3.2). In all three groups of termites, the MWCO 100K fractions containing proteins of >300 kDa demonstrated greater activity against the susceptible bacteria than the MWCO of 30K fractions with 90-180 kDa proteins (Figure 3.2). These data support our previous finding that *R. flavipes* possesses multiple proteins with antibacterial activity.

The *P. aeruginosa*-induced antibacterial activities against the seven susceptible bacteria were all due to the protein fraction from the MWCO 100K filter except against the inducer bacterium. The anti-*P. aeruginosa* activity was present in both the MWCO 100K and 30K fractions, indicating the possibility of induction of multiple anti-*P. aeruginosa* proteins. In addition, the *P. aeruginosa*-challenged termites exhibited more effective antibacterial activity in the MWCO 100K protein fraction against those non-MDR bacteria than did the naïve termites. The increased activity in the MWCO 100K fraction was especially evident against *E. coli* K-12 and *S. aureus,* indicating that the induction of antibacterial activity by *P. aeruginosa* was independent of the Gram staining-based classification of bacteria. Interestingly, *P. aeruginosa* induced greater anti-MRSA activity in the MWCO 100K fraction than did MRSA.

Similar to *P. aeruginosa* induction, the MRSA-induced antibacterial activity was contained in the MWCO 100K fraction with the exception of anti-MRSA activity which was present in both the MWCO 30K and 100K fractions.

3.4.5 Origin of *R. flavipes* antibacterial activity

In order to determine whether the antibacterial activities were of termite origin or of the gut microbiota, we prepared extracts from the hindgut and compared the activity to the hemolymph. As illustrated in Figure 3.3, the antibacterial activity against our panel of bacteria were only observed in the hemolymph of the naïve, *P. aeruginosa*-challenged, or MRSA-challenged. Hindgut extracts from the same termites showed no perceived antibacterial activities (data not shown). The antibacterial activity profile of the hemolymph resembled that of the whole-body extract shown in Figure 3.1. Our data suggest that both constitutive and inducible antibacterial activities of *R. flavipes* are likely of termite origin and reside in hemolymph.

3.4.6 Protein profiles of termite hemolymph

We analyzed the hemolymph protein profiles of naïve, *P. aeruginosa*-challenged, and MRSA-challenged termites via both one-dimensional and two-dimensional gel electrophoreses to identify differentially expressed proteins. On one-dimensional 8% Native PAGE, we observed very little difference between the naïve, MRSA-challenged, and *P. aeruginosa*-challenged termites for both 100K and 30K MWCO fractionated samples (Supplementary Figure 3.1). On denaturing 8% SDS-PAGE, we observed subtle differences between the three samples and between the 100K and 30K MWCO fractionated samples (Supplementary Figure 3.2). Specifically, there was a slight upregulation of ~50 kDa, ~110 kDa and ~150-200 kDa proteins, and a slight downregulation of ~35 kDa, ~55 kDa in MRSA-challenged termites. For *P. aeruginosa*-challenged termites, we observed a slight upregulation of ~80 kDa, ~50 kDa, and ~35 kDa proteins and a slight downregulation of >250 kDa and ~60 kDa proteins. When the hemolymph samples were analyzed on 8% SDS-PAGE, we observed two abundant proteins between ~60-85 kDa that appeared to be conserved among the naïve, *P. aeruginosa*-challenged, and MRSA-challenged termites. We also observed some differences between three samples but especially for *P. aeruginosa*-challenged termites in which we saw disappearance of a prominent band of ~250 kDa and appearance of ~35 kDa, ~50 kDa, and ~65 kDa (Supplementary Figure 3.3).

It was clear from our analyses that termite hemolymph was too complex to be accurately analyzed via one-dimensional PAGE. Thus, we performed two-dimensional electrophoretic analyses of the naïve, *P. aeruginosa*-challenged, and MRSA-challenged termite hemolymphs. Based on our data, the termite hemolymph contains approximately 493 proteins that are visible on two-dimensional gel stained with Sypro®Ruby. A comparison of the hemolymph proteins

between the naïve (Figure 3.4A) and the *P. aeruginosa*-challenged termites (Figure 3.4B) indicated that 38 proteins were differentially expressed at least 2.5-fold ($P<0.05$). Of these, 18 proteins were upregulated and 20 proteins were downregulated (Supplementary Table 1). A comparison of the naïve termites (Figure 3.5A) and the MRSA-challenged termites (Figure 3.5B) showed that 65 proteins were differentially expressed at least 2.5-fold ($P<0.05$). Of these, 11 proteins were upregulated and 54 proteins were downregulated (Supplementary Table 3.2)

In *P. aeruginosa*-challenged termites, the highest upregulated protein (approximately 11-fold increase) had MW of approximately 37 kDa. The 20 downregulated proteins displayed no discernable pattern in size. In MRSA-challenged termites, the majority of upregulated proteins (11 spots) had MW of approximately 18 to 58 kDa while downregulated proteins (53 spots) were all larger than 28 kDa. The alteration of hemolymph protein profile in response to bacterial challenge support our assertion that *R. flavipes* contains both constitutive and inducible antibacterial proteins.

We compared some of the differentially expressed hemolymph proteins to previously identified insect immune proteins based on their relative pI and MW. The results are shown in Tables 3 and 4 for *P. aeruginosa*-induced and MRSA-induced proteins, respectively. Among the *P. aeruginosa*-induced proteins, six proteins of approximately 30-55 kDa proteins had similar pI and MW to previously identified insect immune proteins. We did not find any insect immune proteins of ≥100 kDa in the literature that had similar pI and MW as the spots we identified (Supplementary Table 3.1). Among the MRSA-induced proteins, we found three proteins of approximately 29-60 kDa in MW that had similar pI and MW to previously identified insect immune proteins. Similar to *P. aeruginosa*-induced proteins, we did not find any insect immune proteins of ≥100 kDa in the literature that had similar pI and MW as the spots we identified in

our MRSA-challenged hemolymph samples (Supplementary Table 3.2).

3.5 Discussion

The current study demonstrates that the eastern subterranean termite, *R. flavipes*, produces innate and inducible antibacterial activities that are effective against several human pathogens including two MDRs. The list of pathogens found to be susceptible to naïve *R. flavipes'* extract includes bacteria that cause gastroenteritis (*E. coli* O157:H7 and *S.* Typhimurium), and common opportunistic and nosocomial pathogens (*S. aureus* and *S. pyogenes*). The presence of innate antibacterial proteins in *R. flavipes* parallels the results found in a fungus-growing termite *Pseudacanthotermes spiniger* and a pacific dampwood termite *Zootermopsis angusticollis* (Rosengaus et al. 2007; Lamberty et al. 2001). Recent analysis of *Z. nevadensis* genome revealed that multiple effector immune response genes, including GNBPs, attacin, diptericin and termicin, are encoded in this termite (Terrapon et al. 2014). It is likely that similar products may be found in the hemolymph of *R. flavipes* since there is a high degree of genetic conservation among termites. Interestingly, in contrast to other studies, including our own study demonstrating fractions of MWCO of 3K and 10K of naïve *R. flavipes* CFE inhibiting growth of the entomopathogenic *B. subtilis* (Zeng et al. 2014), all of the activities against the infectious human pathogens we identified in this study were larger than 90 kDa contained within the MWCO of 30K and 100K fractions. However, based on our SDS-PAGE analyses, some of the larger proteins appear to be multisubunit complexes as they denatured into smaller proteins.

Constitutive defense mechanisms of insects usually rely on the response of hemocytes and several enzyme cascades such as phenoloxidase to defend against potential pathogens (Haine et al. 2008). Although the exact identity or the molecular mechanisms of innate antibacterial activities of *R. flavipes* have yet to be characterized, we identified the hemolymph as the source

of these activities. This suggests that the antibacterial activities seen in naïve termites are a part of *R. flavipes'* constitutive immune system.

In addition to the constitutive antibacterial activities against several non-MDR human pathogens, we successfully demonstrated induction of specific activities using two MDR human pathogens as antagonists. Induction of antimicrobial activity in insects is not new. In 2012, Hussain et al. (2012) described a low level induction of antibacterial activity in the Formosan subterranean termite, *C. formosanus*, when the termite was immersed in suspensions of an entomopathogenic fungus (*M. anisopliae*) or several bacteria. However, of the bacteria used in the study (*S. aureus*, *B. thuringiensis*, *E. coli*, and *Ralstonia solanacearum*), only *B. thuringiensis*, which produces anti-insect toxins, induced antimicrobial activity. Interestingly, our results suggest that both Gram-positive and Gram-negative bacteria can be strong inducers, and antibacterial responses can be observed 24 h after heat-killed bacteria challenge. This is supported by a recent study showing that specific combinations of immune genes in *R. flavipes* were expressed in responding to the exposure of various infective fungal spores (Gao 2014). Other studies have demonstrated specific response of the American cockroach, *Periplaneta Americana* (Faulhaber and Karp 1992), and the bumblebee, *Bombus terrestris* (Sadd and Schmid-Hempel 2006), to Gram-negative and Gram-positive bacteria. However, our study is the first one to demonstrate induction of specific activities in termite against MDR human pathogens.

The pattern of induced antibacterial activity based on the bacterium used as the antagonist suggests a complex phenomenon. *P. aeruginosa*-challenge induced anti-*P. aeruginosa* activity while maintaining or slightly increasing antibacterial activities across a broad spectrum of bacteria tested. In contrast, MRSA-challenge induced the activity against the antagonist while maintaining or slightly increasing activity only against two Gram-positive bacteria, *S. aureus* and

S. pyogenes. Thus, these induction patterns appear to reduce the possibility of peptidoglycan or lipopolysaccharide serving as the major antagonist for *R. flavipes* against these bacteria. Both *P. aeruginosa* and MRSA possess peptidoglycan while only *P. aeruginosa* possesses lipopolysaccharide. Interestingly, heat-killed *S. aureus* failed to induce anti-MRSA activity (data not shown), thereby lending support that peptidoglycan is unlikely to be the inducer. Thus, MRSA likely invoked some immune response in *R. flavipes* that is specific to MRSA that is missing in *S. aureus* (*i.e.* staphyloccal cassette chromosome *mec* or SCC*mec*) (Ito et al. 2001; Katayama et al. 2000), while *P. aeruginosa* invoked a response that is effective against a multitude of bacteria.

Termites contain a complex microbiota in their alimentary tract that could have contributed to the observed inducible antibacterial activity (Haine et al. 2008; Parker et al. 2013). We suspected that the microbial symbionts from the hindgut, as well as termite immune proteins, could be the source of the antibacterial activity (Chouvenc et al. 2009; Rosengaus et al. 2014) in our assays. However, our comparative analysis of the hemolymph versus the hindgut localized all of the observable antibacterial activity to the hemolymph, suggesting termite cells as the origin of antibacterial activity. Our finding agrees with a previous study that reported the inability of oral ingestion of fungal spores and bacteria to induce innate gut defenses in *R. flavipes* (Sen et al. 2015). The authors of that study speculated a lack of inducible genes being present on the microarray or weak innate defense in this termite.

Several antimicrobials have been identified from termites including termicin, spinigerin, lysozymes, tGNBPs, and transferrin (Rosengaus et al. 2007; Matsuura et al. 2007; Bulmer and Crozier 2004; Bulmer and Crozier 2006; Lamberty et al. 2001; Thompson et al. 2003). However, given the small molecular weight of most these previously identified peptides/proteins ≤15 kDa),

it is likely that we have discovered novel proteins or protein complexes, with antibacterial activity since most of our activity is limited to proteins of ≥90 kDa. This finding agrees with previous studies demonstrating various protein complexes functioning as antimicrobial effectors with large molecular weight (>150 kDa) in insects, plants, and microorganisms (Anju et al. 2015; Beck et al. 1996; Benz et al. 2014; James et al. 1996; Sitohy et al. 2014). Because our hemolymph samples were CFE and the induced antibacterial proteins appeared to be involved in humoral reaction, it is possible that these proteins were induced by Relish (Bulmer and Crozier 2006). Based on recent identification of differentially expressed proteins involved in stress response, immune signaling, biosynthesis and other functions in *R. chinensis* following an entomopathogenic fungal infection (Liu et al. 2015), mechanisms of insect immunity regulation appear to be complex.

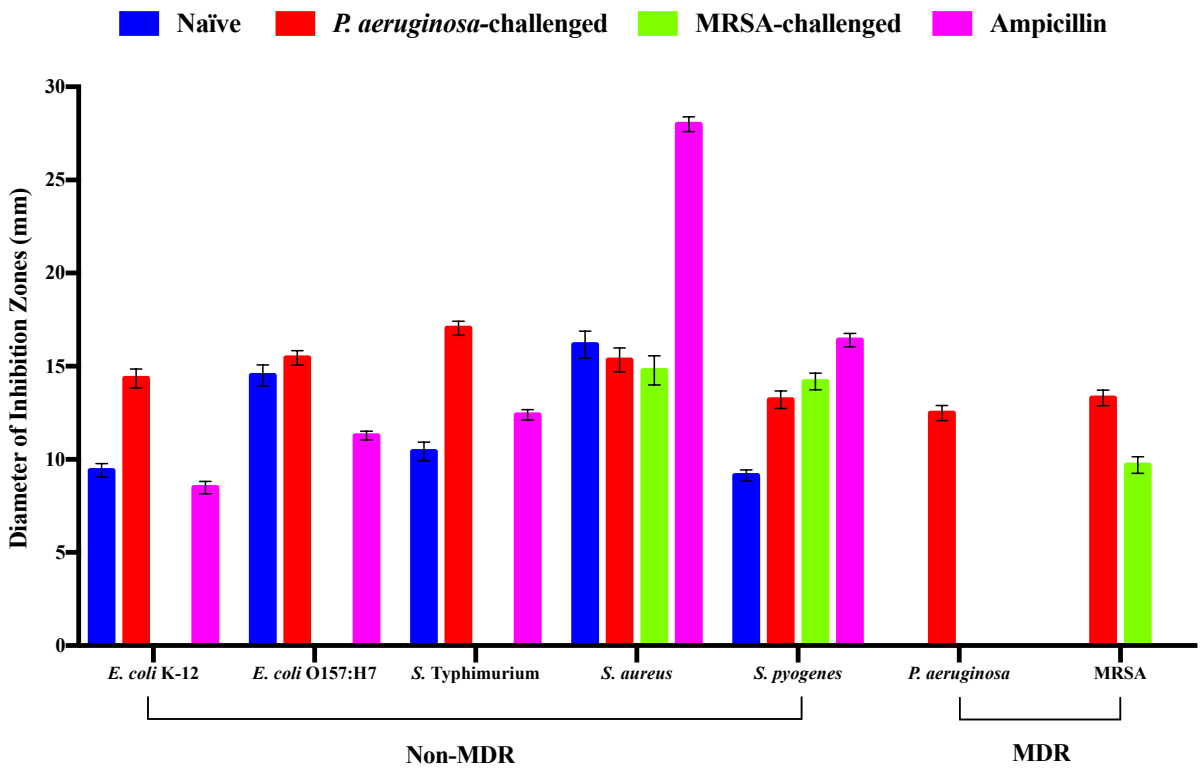

Figure 3.1 Antibacterial activities of cell free extracts of *R. flavipes*. Approximately 400 µg of CFE of the naïve, *P. aeruginosa*-challenged, and MRSA-challenged *R. flavipes* was applied respectively to each filter disk on a bacterial lawn. The zone of inhibition of growth was measured following incubation for 24 hours at 37°C. Ampicillin was used as the positive control at 25 µg per filter disk and 20 µl of buffer was used as the negative control. The data shown are a compilation of three independent experiments done in triplicate for a total N of 9 per sample (ANOVA, $F_{27, 224=2635.47}$, $P < 0.0001$). Data for *A. baumannii* are not shown because the termite extracts were ineffective against the bacterium.

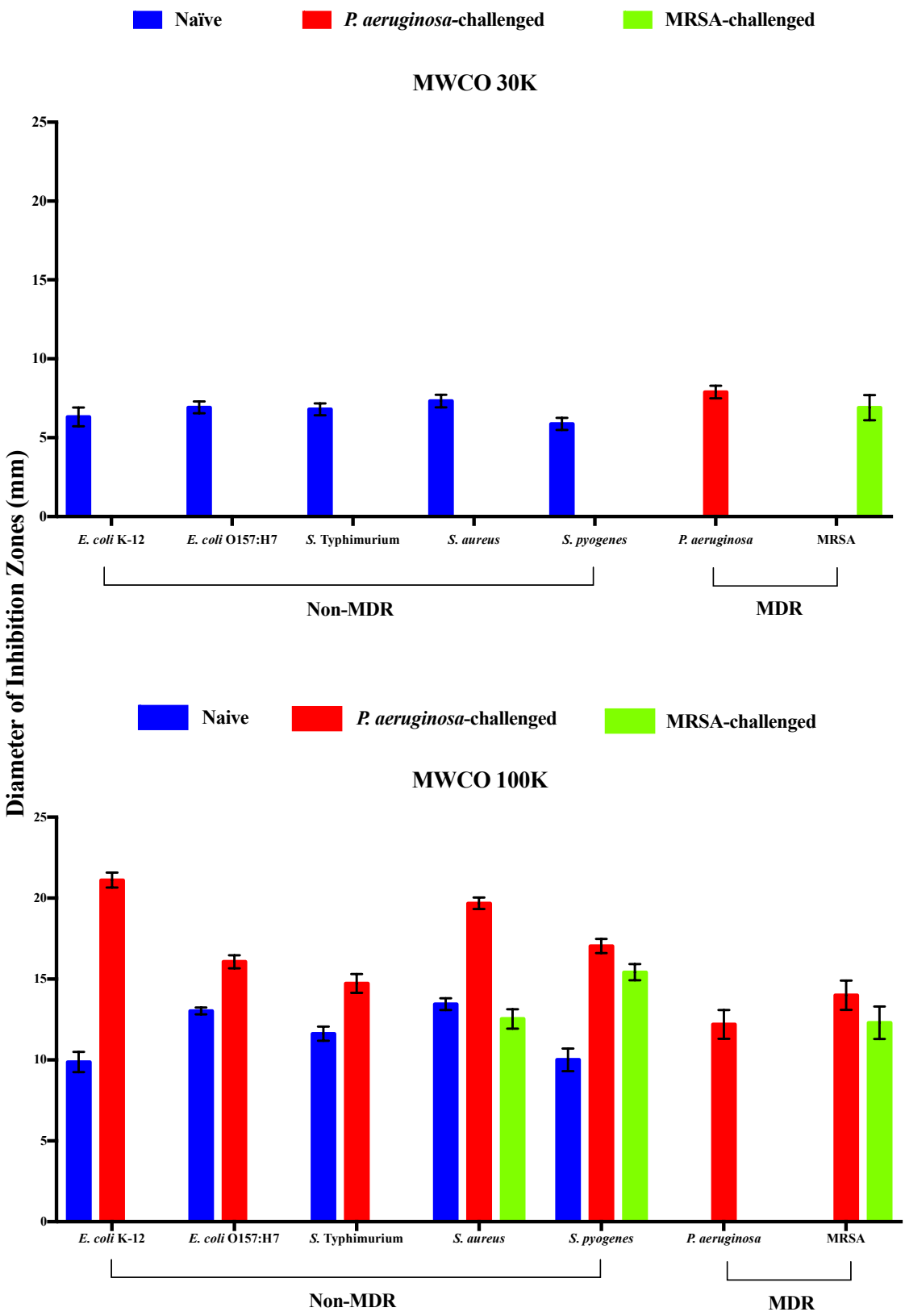
Naïve
P. aeruginosa-challenged
MRSA-challenged
MWCO 30K
Diameter of Inhibition Zones (mm)
25
20
15
10
5
0
E. coli K-12
E. coli O157:H7
S. Typhimurium
S. aureus
S. pyogenes
P. aeruginosa
MRSA
Non-MDR
MDR
Naive
P. aeruginosa-challenged
MRSA-challenged
MWCO 100K
25
20
15
10
5
0
E. coli K-12
E. coli O157:H7
S. Typhimurium
S. aureus
S. pyogenes
P. aeruginosa
MRSA
Non-MDR
MDR

Figure 3.2 Antibacterial activity of size-fractionated cell free extracts of *R. flavipes.*

Antibiotic activity was measured as diameter of inhibition zones caused by respective application of approximately 400 μg of size-fractionated CFE from the naïve, *P. aeruginosa*-challenged, and MRSA-challenged *R. flavipes* on a bacterial lawn. The data shown are a compilation of three independent experiments done in triplicate for a total N of 9 per sample (ANOVA, $F_{27, 224=2635.47}$, $P < 0.0001$). (A) MWCO 30K (90-180 kDa) fraction. (B) MWCO 100K (>300 kDa) fraction. Data for fractions of < 10 kDa, 10-20 kDa, 30-90 kDa are not shown because they did not demonstrate antibacterial activities.

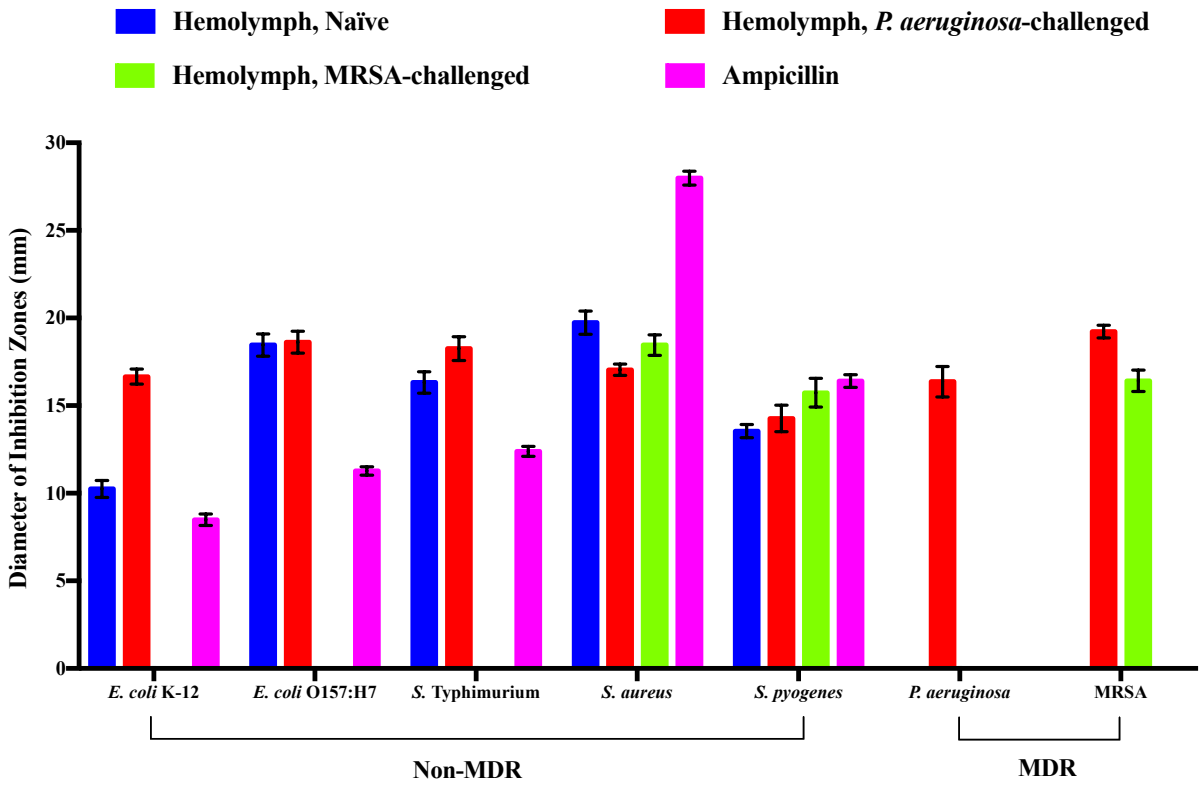

Figure 3.3 Antibacterial activity of *R. flavipes* hemolymph. Approximately 400 µg of hemolymph extract from the naïve, *P. aeruginosa*-challenged, and MRSA-challenged *R. flavipes* was applied respectively on a bacterial lawn. The zone of inhibition was measured. Ampicillin was used as the positive control at 25 µg per filter disk. The data shown are a compilation of three independent experiments done in triplicate for a total N of 9 per sample (ANOVA, $F_{41, 336}$=9762.44, P<0.0001).

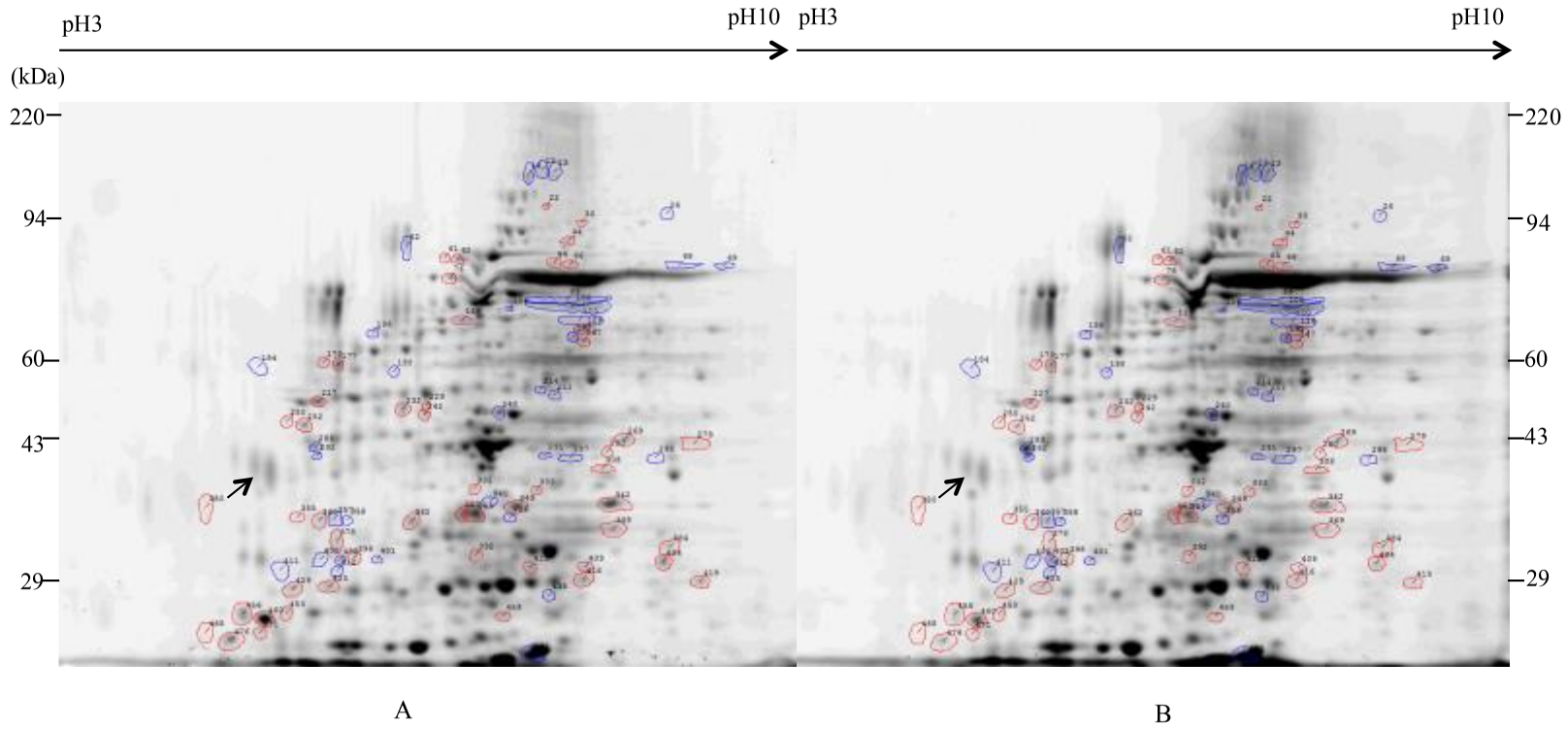

Figure 3.4 Two-dimensional electrophoretic analysis of hemolymph proteins from naïve and *P. aeruginosa*-challenged *R. flavipes*. Approximately 200 µg of hemolymph proteins were separated by two-dimensional gel electrophoresis and visualized with Sypro®Ruby. Blue circles indicate protein spots that are upregulated in *P. aeruginosa* challenged termite while red circles indicate protein spots that are downregulated. (A) Naïve termites. (B) *P. aeruginosa*-challenged termites.

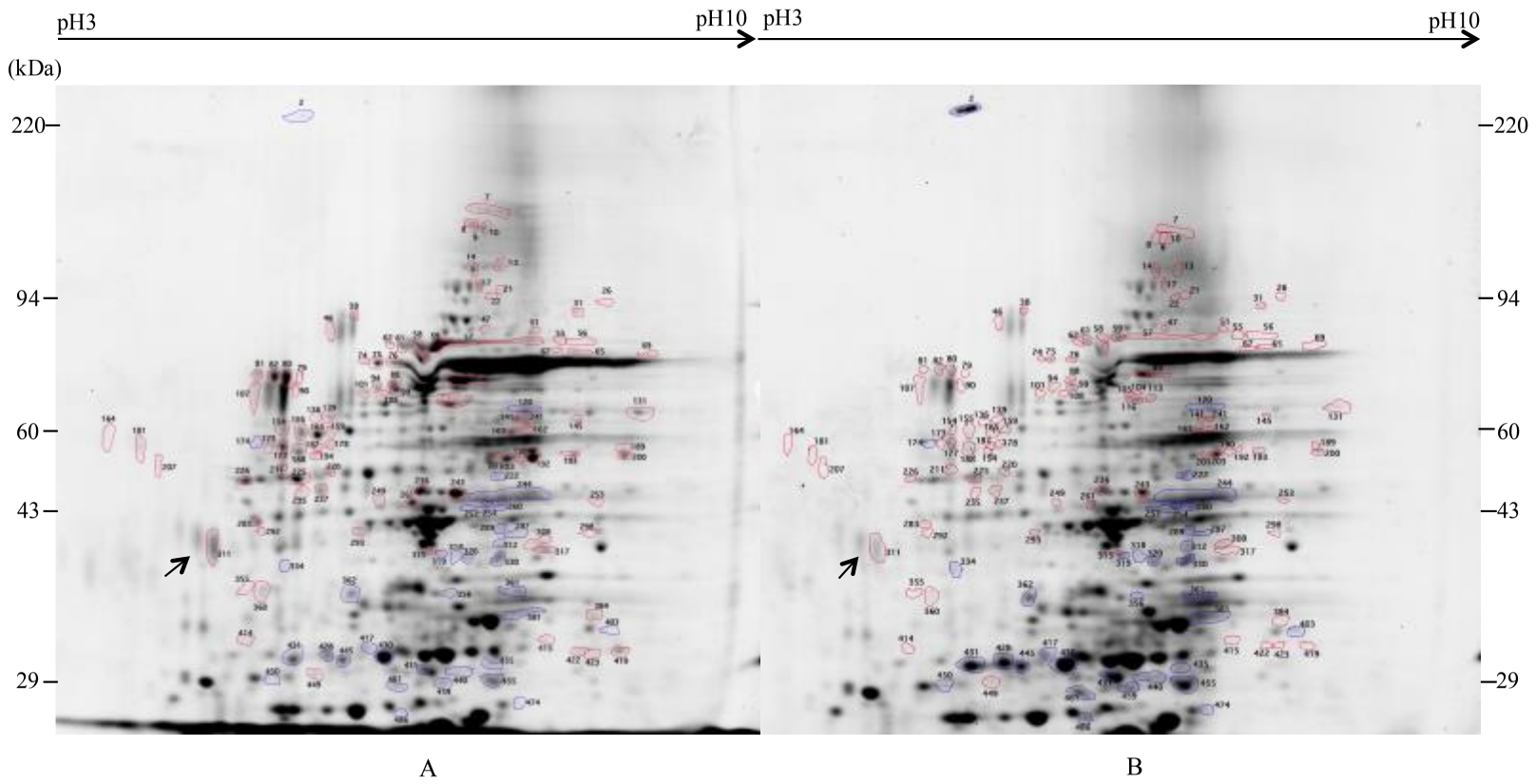

Figure 3.5 Two-dimensional electrophoretic analysis of hemolymph proteins from naïve and MRSA-challenged *R. flavipes*. Approximately 200 µg of hemolymph proteins were separated by two-dimensional gel electrophoresis and visualized with Sypro®Ruby. Blue circles indicate protein spots that are upregulated in MRSA challenged termite and red circles indicate protein spots that are downregulated. (A) Naïve termites. (B) MRSA-challenged termites.

Table 3.1 List of the tested bacteria.

Bacterium	Gram Stain	Multi-Drug Resistant	Source or Reference
Staphylococcus aureus	+	No	ATCC 12600 via Robert Miller
Methicillin-resistant *Staphylococcus aureus* (MRSA)	+	Yes	James Barbaree
Streptococcus pyogenes	+	No	ATCC 19615 via Robert Miller
Pseudomonas aeruginosa (PAO1)	-	Yes	[22]
Escherichia coli O157:H7 (CDC B1409-C1)	-	No	ATCC 43889
E. coli K-12 (MG 1655)	-	No	ATCC 700926
Salmonella enterica serovar Typhimurium (LT2)	-	No	[23] via Jorge Escalante-Semerena
Acinetobacter baumannii (AYE)	-	Yes	ATCC BAA-1710 [24]

Table 3.2 Antibacterial activity of CFE of naïve termites.

Bacteria			Termite crude extract (400 µg)	Ampicillin (25 µg)	Heat-treated crude extract	Control*
Non-infectious		*E. coli*	9.41 ± 0.37^{d}	8.49 ± 0.33^{e}	0	0
Infectious	**Non-MDR**	*S. aureus*	16.16 ± 0.73^{a}	27.99 ± 0.4^{a}	0	0
		S. pyogenes	9.14 ± 0.30^{d}	16.41 ± 0.36^{b}	0	0
		E. coli O157:H7	14.51 ± 0.57^{b}	11.28 ± 0.24^{d}	0	0
		S. Typhimurium	10.42 ± 0.50^{c}	12.39 ± 0.28^{c}	0	0
	MDR	MRSA	0	0	0	0
		P. aeruginosa	0	0	0	0
		A. baumannii	0	0	0	0

Different letters within a column indicate significant difference in inhibition zone diameters at significance level of $\alpha = 0.05$ (ANOVA, $F_{4, 40(\text{CrudeExtract})}=1854.68$, $P < 0.0001$; $F_{6, 56(\text{Ampicillin})}=2960.78$, $P < 0.0001$). The experiment was performed three independent times with triplicate samples for a total N of 9 for each treatment. The diameter of zone of inhibition was measured following 24 h incubation at 37ºC. *Control: 80 mM Tris-HCl, 80 mM NaCl buffer.

Table 3.3 Comparison of *P. aeruginosa*-induced termite hemolymph proteins to insect immune proteins.

Spot	Fold change	pI	MW (Da)	Insect immune proteins	pI	MW (Da)	Reference
491	3.7	7.1	17661	Antibacterial peptide (*Bombyx mori*)	6.8	18,777	Suetsugu et al. 2013
491	3.7	7.1	17661	Attacin-like immune protein	7.0	17,588	http://www.ncbi.nlm.nih.gov/protein/AHB11276.1
491	3.7	7.1	17661	Gloverin 4 (*Bombyx mori*)	6.8	18,777	Suetsugu et al. 2013
358	7.2	5.7	36011	Toll (*Sitophilus oryzae*)	5.2	37,609	Masson et al. 2015
400	2.9	5.6	32736	Immune-related Hdd13 (*Hyphantria cunea*)	5.7	29,691	Shin et al. 1998
402	3.1	5.7	32692	Antimicrobial protein 6 Tox precursor (*Galleria mellonella*)	5.7	32,542	Brown et al. 2009
358	7.2	5.7	36011	Immune-related Hdd1 (*Hyphantria cunea*)	5.2	35,611	Shin et al. 1998
283	3.2	5.6	42081	Termite GNBPs (*Nasutitermes coniger*)	5.6	42,323	Bulmer et al. 2009
214	3.8	7.2	52154	β-1,3-glucan-binding protein/Gram negative bacteria-binding protein precursor (*Hyphantria cunea*)	7.1	53,014	Sun et al. 1990

The pI and the MW of termite hemolymph proteins are based on the Kendrick Labs' analysis of the two-dimensional gels. We used arbitrary cutoff values of ≤0.5 in pI and ≤5 kDa between our hemolymph proteins and previously reported insect proteins to determine potential relationship.

Table 3.4 Comparison of MRSA-induced termite hemolymph proteins to insect immune proteins.

Spot	Fold change	pI	MW (Da)	Insect immune proteins	pI	MW (Da)	Reference
486	7.7	6.6	18,674	Antibacterial peptide (*Bombyx mori*)	6.4	18,821	Suetsugu et al. 2013
486	7.7	6.6	18,674	Gloverin 2 (*Bombyx mori*)	6.4	18,821	Suetsugu et al. 2013
486	7.7	6.6	18,674	Gloverin 4 (*Bombyx mori*)	6.8	18,777	Suetsugu et al. 2013
428	3	6.0	26,359	Attacin-E (*Hyalophora cecropia*)	6.1	25,438	Sun et al. 1991
450	2.5	5.7	27,591	Possible antimicrobial peptide (*Bombyx mori*)	6.3	27,469	Taniai et al. 2006
440	3	7.1	29,320	Phospholipase A2B precursor (*Tribolium castaneum*)	7.6	29,425	Shrestha et al. 2010
440	3	7.1	29,320	Spz1A, partial (*Manduca sexta*)	7.6	29,195	An et al. 2010
440	3	7.1	29,320	Scolexin A (*Manduca sexta*)	7.0	30,373	Finnerty et al. 1999
254	6.3	7.2	44,637	Putative hemolin (*Hyphantria cunea*)	6.7	46,119	Shin et al. 1996
174	2.7	5.5	58,639	Gram-negative bacteria binding protein 3 (*Drosophila melanogaster*)	6.0	55,322	Kim et al. 2000

The pI and the MW of termite hemolymph proteins are based on the Kendrick Labs' analysis of the two-dimensional gels. We used arbitrary cutoff values of ≤0.5 in pI and ≤5 kDa between our hemolymph proteins and previously reported insect proteins to determine potential relationship.

References

Anju, K. M., Archana, M. M., Mohandas, C., & Nambisan, B. (2015). Purification and identification of an antibacterial protein from the symbiotic bacteria associated with novel entomopathogenic nematode, *Rhabditis* (*Oscheius*) sp. *World Journal of Microbiology and Biotechnology*, *31*(4), 621-632.

Adams, M. D., Goglin, K., Molyneaux, N., Hujer, K. M., Lavender, H., Jamison, J. J., ... & Hujer, A. M. (2008). Comparative genome sequence analysis of multidrug-resistant *Acinetobacter baumannii*. *Journal of bacteriology*, *190*(24), 8053-8064.

An, C., Jiang, H., & Kanost, M. R. (2010). Proteolytic activation and function of the cytokine Spätzle in the innate immune response of a lepidopteran insect, *Manduca sexta*. *Febs Journal*, *277*(1), 148-162.

Beck, G., Cardinale, S., Wang, L., Reiner, M., & Sugumaran, M. (1996). Characterization of a defense complex consisting of interleukin 1 and phenol oxidase from the hemolymph of the tobacco hornworm, *Manduca sexta*. *Journal of Biological Chemistry*, *271*(19), 11035-11038.

Benz, J., & Meinhart, A. (2014). Antibacterial effector/immunity systems: it's just the tip of the iceberg. *Current opinion in microbiology*, *17*, 1-10.

Bertani, G. (1951). STUDIES ON LYSOGENESIS I.: The Mode of Phage Liberation by Lysogenic *Escherichia coli*1. *Journal of bacteriology*, *62*(3), 293.

Bradford, M. M. (1976). A rapid and sensitive method for the quantitation of microgram quantities of protein utilizing the principle of protein-dye binding. *Analytical biochemistry*, *72*(1-2), 248-254.

Brown, S. E., Howard, A., Kasprzak, A. B., Gordon, K. H., & East, P. D. (2009). A peptidomics study reveals the impressive antimicrobial peptide arsenal of the wax moth *Galleria mellonella*. *Insect biochemistry and molecular biology*, *39*(11), 792-800.

Bulmer, M. S., Bachelet, I., Raman, R., Rosengaus, R. B., & Sasisekharan, R. (2009). Targeting an antimicrobial effector function in insect immunity as a pest control strategy. *Proceedings of the National Academy of Sciences*, *106*(31), 12652-12657.

Bulmer, M. S., & Crozier, R. H. (2004). Duplication and diversifying selection among termite antifungal peptides. *Molecular Biology and Evolution*, *21*(12), 2256-2264.

Bulmer, M. S., & Crozier, R. H. (2006). Variation in positive selection in termite GNBPs and Relish. *Molecular Biology and Evolution*, *23*(2), 317-326.

Bulet, P., Hetru, C., Dimarcq, J. L., & Hoffmann, D. (1999). Antimicrobial peptides in insects; structure and function. *Developmental & Comparative Immunology*, *23*(4), 329-344.

Bulmer, M. S., Lay, F., & Hamilton, C. (2010). Adaptive evolution in subterranean termite antifungal peptides. *Insect molecular biology*, *19*(5), 669-674.

Chouvenc, T., Efstathion, C. A., Elliott, M. L., & Su, N. Y. (2013, November). Extended disease resistance emerging from the faecal nest of a subterranean termite. In *Proc. R. Soc. B* (Vol. 280, No. 1770, p. 20131885). The Royal Society.

Chouvenc, T., Su, N. Y., & Robert, A. (2009). Inhibition of Metarhizium anisopliae in the alimentary tract of the eastern subterranean termite Reticulitermes flavipes. *Journal of invertebrate pathology*, *101*(2), 130-136.

Dossey, A. T. (2010). Insects and their chemical weaponry: new potential for drug discovery. *Natural product reports*, *27*(12), 1737-1757.

Faulhaber, L. M., & Karp, R. D. (1992). A diphasic immune response against bacteria in the American cockroach. *Immunology*, *75*(2), 378.

Finnerty, C. M., Granados, R. R., & Karplus, P. A. (1999). The insect immune protein scolexin is a novel serine proteinase homolog. *Protein science*, *8*(1), 242-248.

Gao, Q. (2014). Social immunity and the expression of immune-related genes in the Eastern subterranean termite (Doctoral dissertation, The University of Western Ontario).

Haine, E. R., Moret, Y., Siva-Jothy, M. T., & Rolff, J. (2008). Antimicrobial defense and persistent infection in insects. *Science*, *322*(5905), 1257-1259.

Hamilton, C., & Bulmer, M. S. (2012). Molecular antifungal defenses in subterranean termites: RNA interference reveals in vivo roles of termicins and GNBPs against a naturally encountered pathogen. *Developmental & Comparative Immunology*, *36*(2), 372-377.

Holloway, B. W., Krishnapillai, V., & Morgan, A. F. (1979). Chromosomal genetics of *Pseudomonas*. *Microbiological reviews*, *43*(1), 73.

Hussain, A., & Wen, S. Y. (2012). Induction of immune response among formosan subterranean termites, *Coptotermes formosanus* Shiraki (Rhinotermitidae: Isoptera). *African Journal of Microbiology Research*, *6*(5), 995-1000.

Hu, X. P., & Appel, A. G. (2004). Seasonal variation of critical thermal limits and temperature tolerance in Formosan and eastern subterranean termites (Isoptera: Rhinotermitidae). *Environmental entomology*, *33*(2), 197-205.

Ito, T., Katayama, Y., Asada, K., Mori, N., Tsutsumimoto, K., Tiensasitorn, C., & Hiramatsu, K. (2001). Structural comparison of three types of staphylococcal cassette chromosome mec integrated in the chromosome in methicillin-resistant *Staphylococcus aureus*. *Antimicrobial agents and chemotherapy*, *45*(5), 1323-1336.

James, S. G., Holmström, C., & Kjelleberg, S. (1996). Purification and characterization of a novel antibacterial protein from the marine bacterium D2. *Applied and Environmental Microbiology*, *62*(8), 2783-2788.

Katayama, Y., Ito, T., & Hiramatsu, K. (2000). A new class of genetic element, staphylococcus cassette chromosome mec, encodes methicillin resistance in *Staphylococcus aureus*. *Antimicrobial Agents and Chemotherapy*, *44*(6), 1549-1555.

Kim, Y. S., Ryu, J. H., Han, S. J., Choi, K. H., Nam, K. B., Jang, I. H., ... & Lee, W. J. (2000). Gram-negative bacteria-binding protein, a pattern recognition receptor for lipopolysaccharide and β-1, 3-glucan that mediates the signaling for the induction of innate immune genes in *Drosophila melanogaster* cells. *Journal of Biological Chemistry*, *275*(42), 32721-32727.

Lamberty, M., Zachary, D., Lanot, R., Bordereau, C., Robert, A., Hoffmann, J. A., & Bulet, P. (2001). Insect immunity constitutive expression of a cysteine-rich antifungal and a linear antibacterial peptide in a termite insect. *Journal of Biological Chemistry*, *276*(6), 4085-4092.

Lavine, M. D., & Strand, M. R. (2002). Insect hemocytes and their role in immunity. *Insect biochemistry and molecular biology*, *32*(10), 1295-1309.

Lilleengen, K. (1948). Typing of *Salmonella* Typhimurium by Means of Bacteriophage: An Experimental Bacteriologic Study for the Purpose of Devising a Phage-typing Method to be Used as an Aid in Epidemiologic and Epizootologic Investigations in Outbreaks of Typhimurium Infection (Doctoral dissertation, Ivar Hœggström).

Liu, L., Li, G., Sun, P., Lei, C., & Huang, Q. (2015). Experimental verification and molecular basis of active immunization against fungal pathogens in termites. *Scientific reports*, *5*, 15106.

Masson, F., Vallier, A., Vigneron, A., Balmand, S., Vincent-Monégat, C., Zaidman-Remy, A., & Heddi, A. (2015). Systemic infection generates a local-like immune response of the bacteriome organ in insect symbiosis. *Journal of innate immunity*, *7*(3), 290-301.

Matsuura, K., Tamura, T., Kobayashi, N., Yashiro, T., & Tatsumi, S. (2007). The antibacterial protein lysozyme identified as the termite egg recognition pheromone. *PLoS One*, *2*(8), e813.

Parker, B. J., Spragg, C. J., Altincicek, B., & Gerardo, N. M. (2013). Symbiont-mediated protection against fungal pathogens in pea aphids: a role for pathogen specificity?. *Applied and environmental microbiology*, *79*(7), 2455-2458.

Rosengaus, R. B., Cornelisse, T., Guschanski, K., & Traniello, J. F. (2007). Inducible immune proteins in the dampwood termite *Zootermopsis angusticollis*. *Naturwissenschaften*, *94*(1), 25-33.

Rosengaus, R. B., Schultheis, K. F., Yalonetskaya, A., Bulmer, M. S., DuComb, W. S., Benson, R. W., ... & Godoy-Carter, V. (2014). Symbiont-derived β-1, 3-glucanases in a social insect: mutualism beyond nutrition. *Frontiers in microbiology*, *5*, 607.

Sadd, B. M., & Schmid-Hempel, P. (2006). Insect immunity shows specificity in protection upon secondary pathogen exposure. *Current Biology*, *16*(12), 1206-1210.

Sen, R., Raychoudhury, R., Cai, Y., Sun, Y., Lietze, V. U., Peterson, B. F., ... & Boucias, D. G. (2015). Molecular signatures of nicotinoid-pathogen synergy in the termite gut. *PloS one*, *10*(4), e0123391.

Shin, S. W., Park, S. S., Park, D. S., Kim, M. G., Kim, S. C., Brey, P. T., & Park, H. Y. (1998). Isolation and characterization of immune-related genes from the fall webworm, *Hyphantria cunea*, using PCR-based differential display and subtractive cloning. *Insect biochemistry and molecular biology*, *28*(11), 827-837.

Shrestha, S., Park, Y., Stanley, D., & Kim, Y. (2010). Genes encoding phospholipases A 2 mediate insect nodulation reactions to bacterial challenge. *Journal of insect physiology*, *56*(3), 324-332.

Sitohy, M. Z., Osman, A. O., & Mahgoub, S. A. (2014). Bioactive proteins against pathogenic and spoilage bacteria. *Functional Foods in Health and Disease*, *4*(10), 451-462.

Slocinska, M., Marciniak, P., & Rosinski, G. (2008). Insects antiviral and anticancer peptides: new leads for the future?. *Protein and peptide letters*, *15*(6), 578-585.

Sun, S. C., Lindstrom, I., Boman, H. G., Faye, I., & Schmidt, O. (1990). Hemolin: an insect-immune protein belonging to the immunoglobulin superfamily. *Science*, *250*(4988), 1729.

SUN, S. C., LINDSTRÖM, I., LEE, J. Y., & FAYE, I. (1991). Structure and expression of the attacin genes in *Hyalophora cecropia*. *European journal of biochemistry*, *196*(1), 247-254.

Suetsugu, Y., Futahashi, R., Kanamori, H., Kadono-Okuda, K., Sasanuma, S. I., Narukawa, J., ... & Sezutsu, H. (2013). Large scale full-length cDNA sequencing reveals a unique genomic landscape in a lepidopteran model insect, *Bombyx mori*. *G3: Genes| Genomes| Genetics*, *3*(9), 1481-1492.

Taniai, K., Lee, J. H., & Lee, I. H. (2006). *Bombyx mori* cell line as a model of immune-system organs. *Insect molecular biology*, *15*(3), 269-279.

Terrapon, N., Li, C., Robertson, H. M., Ji, L., Meng, X., Booth, W., ... & Gowin, J. (2014). Molecular traces of alternative social organization in a termite genome. *Nature communications*, *5*.

Thompson, G. J., Crozier, Y. C., & Crozier, R. H. (2003). Isolation and characterization of a termite transferrin gene up-regulated on infection. *Insect molecular biology*, *12*(1), 1-7.

Tzou, P., De Gregorio, E., & Lemaitre, B. (2002). How Drosophila combats microbial infection: a model to study innate immunity and host–pathogen interactions. *Current opinion in microbiology*, *5*(1), 102-110.

Yi, H. Y., Chowdhury, M., Huang, Y. D., & Yu, X. Q. (2014). Insect antimicrobial peptides and their applications. *Applied microbiology and biotechnology*, *98*(13), 5807-5822.

Zeng, Y., Hu, X. P., Yu, X. Q., & Suh, S. J. (2014). Multiple antibacterial activities of proteinaceous compounds in crude extract from the eastern subterranean termite, *Reticulitermes flavipes* Kollar (Blattodea: Isoptera: Rhinotermitidae). *Adv. Res*, *2*, 455-461.

Supplementary Data

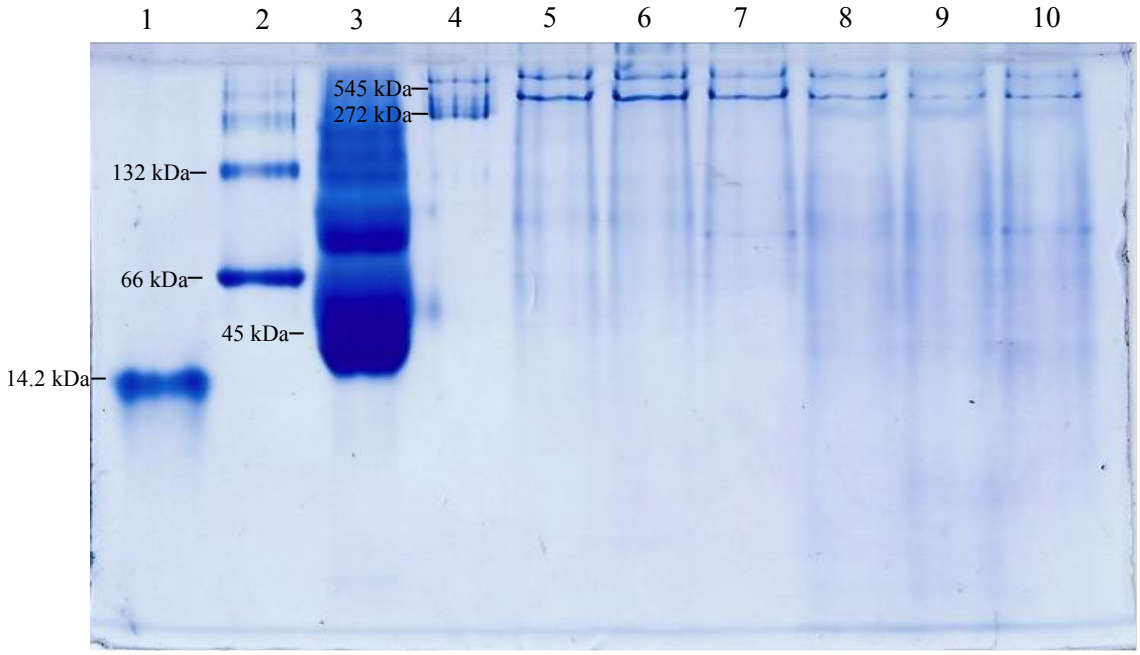

Supplementary Figure 3.1 8% Non-denaturing PAGE analysis of MWCO of 30K and 100K size-fractionated samples of termite CFE. Lanes 1-4: Protein ladders of α-lactalbumin from bovine milk, albumin from bovine serum, albumin from chicken egg white, and urease from jack bean, respectively. Lanes 5-7: MWCO of 100K fractions from *P. aeruginosa*-challenged, MRSA-challenged, and naïve termites, respectively. Lanes 8-10: MWCO of 30K fractions from *P. aeruginosa*-challenged, MRSA-challenged, and naïve termites, respectively.

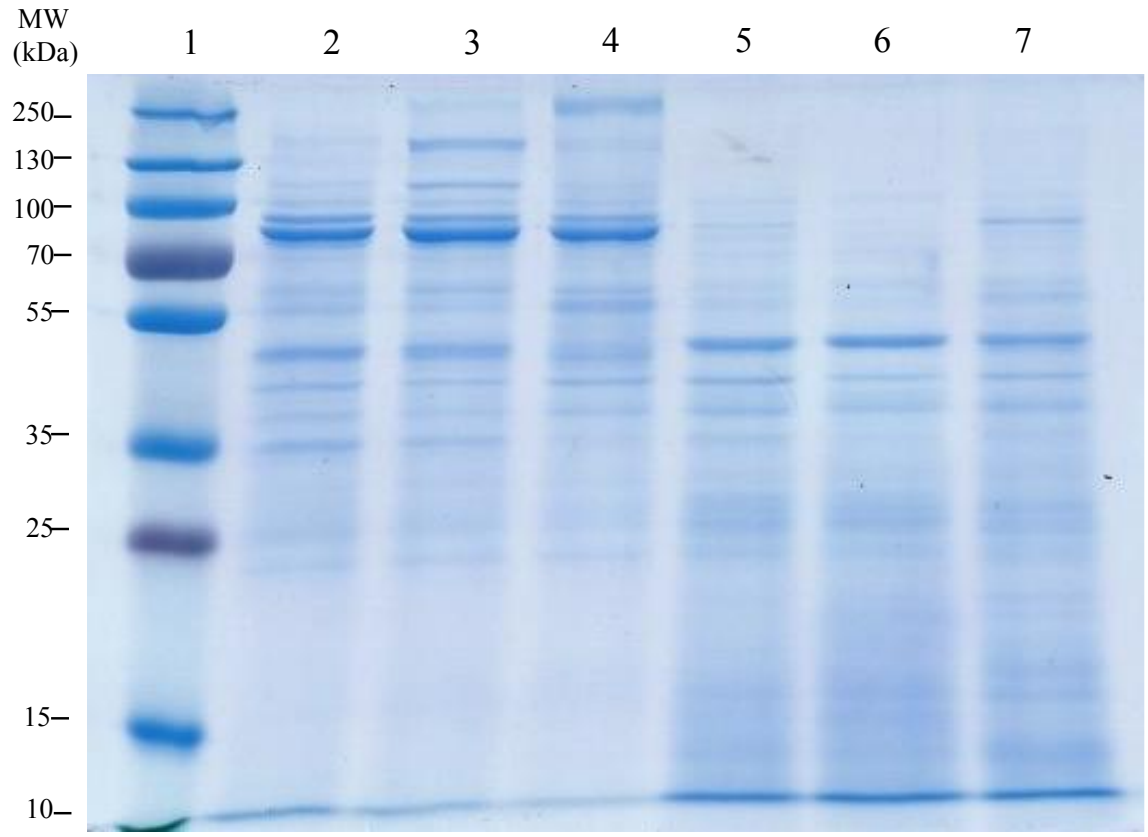

Supplementary Figure 3.2 8% SDS-PAGE analysis of MWCO of 30K and 100K size-fractionated samples of termite CFE. Lane 1: Protein ladder (10-250 kDa); Lanes 2-4: MWCO of 100K fractions from *P. aeruginosa*-challenged, MRSA-challenged, and naïve termites, respectively. Lanes 5-7: MWCO of 30K fractions from *P. aeruginosa*-challenged, MRSA-challenged, and naïve termites, respectively.

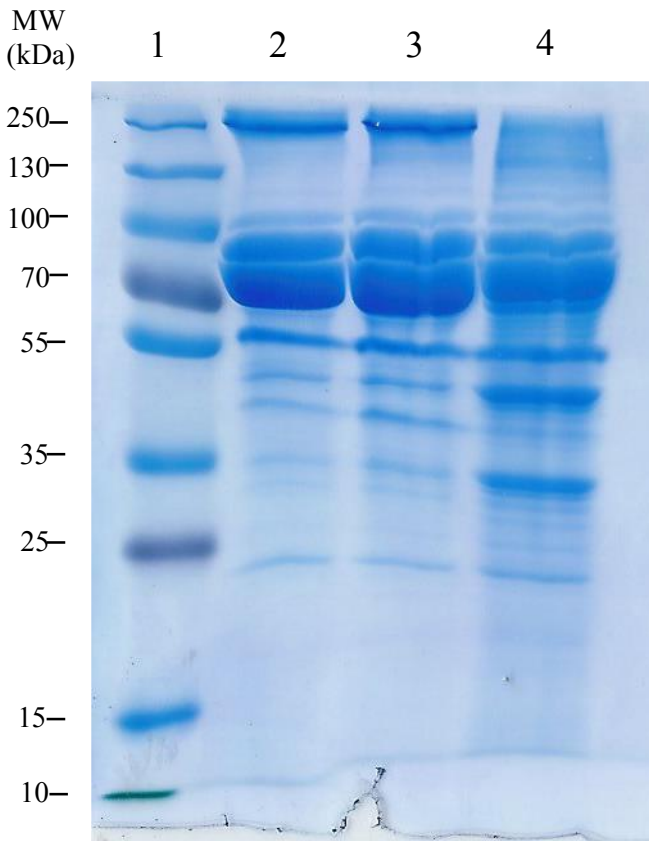

Supplementary Figure 3.3 8% SDS-PAGE analysis of hemolymph proteins. Lane 1: Protein Ladder (10-250 kDa); Lanes 2-4: Hemolymph proteins from naïve, MRSA-challenged, and *P. aeruginosa*-challenged termites, respectively.

Supplementary Table 3.1 Differentially expressed hemolymph proteins in *P. aeruginosa*-challenged termites with at least 2.5-fold change.

Spot #	pI	MW (Da)	*P. aeruginosa* vs Naïve Difference	T-test of *P. aeruginosa* vs Naïve
491	7.1	17,661	3.7	0.017
471	5.2	22,326	-2.8	0.009
468	4.6	22,510	-6	0.013
460	5.2	25,510	-2.6	0.012
419	8	30,979	-3	0.007
411	5.3	31,862	3.2	0.008
409	7.5	32,180	-7.2	0.006
402	5.7	32,692	3.1	0.023
400	5.6	32,736	2.9	0.045
378	5.7	34,264	-2.6	0.022
369	7.7	35,253	-3.1	0.023
360	5.6	35,967	-2.9	0.031
362	6.2	36,011	-2.7	0.027
358	5.7	36,011	7.2	0
356	7	36,270	5.1	0.011
349	7	37,206	-2.6	0.035
340	6.8	37,568	11.2	0.001
333	7.2	38,453	-2.7	0.024
332	6.7	38,649	-2.7	0.003
298	7.9	41,015	2.8	0.005
297	7.4	41,045	2.8	0.006

292	5.6	41,338	3.3	0.011
290	7.6	41,527	-3.8	0.013
283	5.6	42,081	3.2	0.006
279	8	42,290	-3.4	0.178
229	6.3	49,342	-2.9	0.018
214	7.2	52,154	3.8	0.042
184	5.2	57,852	4.4	0.025
173	5.6	58,751	-4	0.19
147	7.5	63,573	-9.6	0.004
69	8.1	82,559	3.9	0.03
68	8	82,792	3.4	0.023
44	7.4	88,830	-2.9	0.011
30	7.5	93,453	-3.7	0.268
26	7.9	99,201	2.7	0.003
22	7.3	104,801	-3	0.038
13	7.3	131,601	3.1	0.02
12	7.2	132,401	2.6	0.015

The pI and the MW of termite hemolymph proteins are based on the Kendrick Labs' analysis of the two-dimensional gels.

Supplementary Table 3.2 Differentially expressed hemolymph proteins in MRSA-challenged termites with at least 2.5-fold change.

Spot #	pI	MW (Da)	MRSA vs Naïve Difference	T-test of MRSA vs Naïve
486	6.6	18,674	7.7	0.007
461	6.6	25,506	2.6	0.019
428	6	26,359	3	0.01
450	5.7	27,591	2.5	0.013
449	5.9	28,081	-3.4	0.004
440	7.1	29,320	3	0.017
422	7.8	30,857	-7.4	0.006
419	8	30,979	-6.5	0.007
403	8	32,692	6.7	0.008
381	7.5	34,163	3.6	0.043
319	6.9	39,471	2.5	0.014
315	6.8	39,774	-6.2	0.025
308	7.6	40,162	-2.8	0.007
298	7.9	41,015	-2.8	0.043
283	5.6	42,081	-4.2	0.011
254	7.2	44,637	6.3	0.035
249	6.4	46,320	-2.7	0.024
243	7	47,295	-3.1	0.014
237	5.9	48,296	-2.6	0.002
235	5.8	48,521	-2.5	0.001
222	7.3	51,064	4	0.005
201	7.4	54,533	-8.2	0.031
193	7.8	55,951	-4	0.003
194	5.9	56,053	-10.4	0.001
192	7.7	56,066	-2.8	0.008
189	8	57,477	-6.2	0.007
187	5.9	57,515	-4.2	0.002
174	5.5	58,639	2.7	0.019
163	7.4	60,547	-2.7	0.016
162	7.5	60,683	-4.1	0.038
165	5.9	61,318	-9.4	0.001
155	5.8	62,372	-4.6	0.001

154	5.7	62,636	-2.6	0.014
142	7.5	63,946	-7.5	0.013
145	7.8	64,758	-4.6	0.01
131	8.1	67,007	-2.8	0.002
113	7.1	69,385	-2.8	0.001
108	6.5	70,937	-2.5	0.036
105	6.9	71,205	-4.3	0.026
107	5.5	71,465	-2.7	0.04
104	7	71,473	-4.8	0.036
101	6.3	71,875	-3.6	0
94	6.4	72,947	-3.5	0.005
82	5.6	76,473	-3.9	0.015
81	5.5	76,605	-5.7	0.001
80	5.7	76,736	-4.1	0.001
79	5.8	77,264	-4.9	0.01
76	6.5	79,378	-2.6	0.012
75	6.4	79,512	-3.8	0.004
74	6.3	79,780	-4.5	0.033
70	6.8	81,924	-3.7	0.03
67	7.8	82,792	-9.2	0.03
62	6.6	84,068	-4.4	0
61	6.5	84,470	-4.4	0.007
59	6.8	84,872	-6.6	0.005
58	6.7	85,274	-5.5	0.014
57	7.3	85,295	-3.6	0.013
56	7.8	85,820	-5.3	0.011
55	7.7	85,820	-6.6	0.015
51	7.6	87,794	-13.4	0.003
47	7.3	88,558	-2.6	0.026
22	7.3	104,801	-6.5	0.04
17	7.2	114,401	-3	0.049
7	7.3	169,600	-3	0.042
164	Nd	Nd	-2.5	0.041

The pI and the MW of termite hemolymph proteins are based on the Kendrick Labs' analysis of the two-dimensional gels

Chapter Four

Hemolymph protein profile changes in MDR-challenged and naïve *Reticulitermes flavipes* workers

4.1 Abstract

Hemolymph plays key roles in insect innate immune defenses in addition to other functions. In our effort to continue seeking new therapeutic approaches against the two common multidrug resistant opportunistic bacterial pathogens, *Pseudomonas aeruginosa* and methicillin-resistant *Staphylococcus aureus*, we investigated hemolymph proteins changes in *P. aeruginosa* and MRSA immuned termite groups in comparison with naïve control group. The hemolymph protein profiles were determined using Nano liquid-chromatography-MS/MS analysis. Mass spectrometry (MS) analysis identified a total of 578 proteins, with 245 proteins being shared by all three groups, and 58, 56 and 50 unique proteins in naïve, MRSA-challenged and *P. aeruginosa*-challenged termites, respectively. Furthermore, we observed 36 and 80 proteins that appeared to be differentially expressed at least 2.5-fold in response to MRSA and *P. aeruginosa*-challenge, respectively. MRSA-challenge significantly increased the intensity of 9 proteins, and 2 of them were involved in immune-related processes. *P. aeruginosa*-challenge significantly upregulated 23 proteins, while 9 proteins engaged in immune-related processes including iron metabolism, antioxidant-related response**,** general stress response, and immune effectors. Both hierarchical clustering and principle component analysis indicated that MDR-challenged and naïve termite hemolymph samples are partitioned into separate clusters according to treatment,

confirming the differential abundances of these proteins in isolated categories of up- or down-regulated proteins. These findings provide an insight concerning protein compositional changes in defending bacterial challenge.

4.2 Introduction

Insect hemolymph serves as a connective tissue responsible for transporting nutrients, ions, and hormones throughout the body, allowing occurrence of physiological processes, and controlling systemic changes in innate immune pathways which aid in the response to various pathogens and parasites (Kanost et al. 1990; Vierstraete et al. 2003; Flatt et al. 2008; Chan et al. 2009; He et al. 2016). With the rapid development of molecular technology over the past 50 years, more and more insect hemolymph proteins were unraveled for their structure and function. For example, hexamerins and arylphorins act as amino acid sources and components of insect cuticles, lipophorins and other enzymes function as lipid transportation and hydrolysis, vitellogenins play important role in embryo development, cytokines facilitate intercellular communications, and etc. In addition, the discovery of insect immune proteins of hemolymph such as effector molecules, enzyme cascades, antioxidant proteins, and etc. provides the evidence that hemolymph is a vital source for defending pathogen infections or tissue damage (Kim and Kim 2005; Bulet et al. 2004; Evans et al. 2006).

Proteomics has recently become an important platform for studying changes in hemolyphm proteome during physiological processes and under various environmental effects (Guedes et al. 2003; Chan et al. 2006). In the aspects of studying insect biology, proteomics has been widely used to examine hemolymph composition during insect developmental stages (Woltedji et al. 2013). However, relatively less and thorough studies of hemolymph proteomes focused on their role in insect innate immunity. Some studies have described compositions of hemolymph proteomes of various insects such as fruit fly, silkworm, white butterfly, and tobacco

hornworm in response to immune challenges (Guedes et al. 2003; Zhang et al. 2014; Karlsson et al. 2004; He et al. 2016). In termites, Liu et al. (2015) used quantitative iTRAQ proteomics combined with MRM validation to explore the hemolymph proteomes of the active immunized subterranean termites *Reticulitermes chinensis* by an entomopathgenic fungus *Metarhizium anisopliae*. However, the knowledge on changes of the hemolymph proteome in termite upon bacterial infection is lacking.

Our previous study has demonstrated the existence of constitutive and inducible bactericidal activities in the hemolymph of the eastern subterranean termites *R. flavipes* when the insect was fed with heat-killed multidrug-resistant bacterial pathogens (MDRs) *Pseudomonas aeruginosa* or methicillin-resistant *Staphylococcus aureus* (MRSA) (Zeng et al. 2016). The reported broad-spectrum constitutive antagonistic activities against both Gram-positive and Gram-negative pathogens as well as inducible anti-MDR activities indicated the presence of novel antibiotics in *R. flavipes*. In this study, we used a proteomic approach (nano liquid-chromatography with tandem mass spectrometry (LC-MS/MS)) combing multi-level methods to determine the changes of hemolymph protein profiles of naïve versus *P. aeruginosa*- or MRSA-challenged *R. flavipes* in the purpose of identification of antibacterial proteins in *R. flavipes*. In addition, we found many immune-related proteins involved in iron metabolism, antioxidant-related response**,** and stress response were regulated after MDR challenges. Our results shed lights on termite antimicrobial discovery and improve the current understanding of physiological and immunological functions of termite hemolymph proteins in response to bacterial pathogens.

4.3 Materials and Methods

4.3.1 Hemolymph sample collection

Reticulitermes flavipes workers were reared with filter papers (12.5 cm in diameter, Whatman #1) in Urban Entomology Laboratory at 25 ± 2°C for at least 20 days. Three groups of

workers (4 g of surface sterilized termites per group) were introduced into Petri plates (15 cm × 2.5 cm) provisioned with sterile filter papers (1 filter paper per Petri dish) moistened with 3 ml of milli-Q (MQ) water, heat-killed *Psedomonas aeruginosa* or Methicillin-resistant *Staphylococcus aureus* (MRSA) suspension, respectively. Each bacterial suspension contains approximately 1.8 x 10^9 cells. After 24 h feeding, all termite individuals from each treatment were collected, and the cell-free hemolymph was extracted using the method described in Zeng et al. (2016). For each treatment, termite immunization and hemolymph extraction were performed in triplicates independently. In addition, to confirm the protein profiles of hemolymph on one-dimensional protein gel, we further analyzed the cell-free hemolymph samples on a 8% SDS-PAGE gel (Zeng et al. 2016). The remaining hemolymph of each treatment was frozen and stored at -80 °C.

4.3.2 Trypsin digestion and nano LC-MS/MS analysis

Trypsin digestion and nano LC-MS/MS analysis were performed in the Mass Spectrometry & Proteomics Resource of the W.M. Keck Foundation Biotechnology Resource Laboratory of Yale School of Medicine. Trypsin digestion was performed as follows. Each hemolymph sample was dried and reconstituted in 40 µl 8M urea, 0.4M NH_4HCO_3, reduced in 4.0 µl 45 mM dithiothreitol (DTT), and incubated at 37 ºC for 30 minutes. Then, samples were alkylated in 4.0 µl 100mM iodoacetamide and incubated in the dark at room temperature for 30 minutes, followed by digestion with 10 µl 0.5mg/ml trypsin with incubation at 37 ºC for 16 hours. Acquired solutions were desalted using a C18 macrospin column (The Nest Group, #SMM SS18V) with 2 x 160 µl 0.1% trifluoroacetic acid (TFA), 80% acetonitrile. Eluted sample was dried and dissolved in 10 µl 70% formic acid (FA) and 340 µl 0.1% TFA. Protein concentrations (A260/280) were determined by Nanodrop measurements (Thermo Scientific Nanodrop 2000 UV-Vis Spectrophotometer) before injected for mass spectrometric analysis.

LC-MS/MS analysis was performed on a Thermo Scientific Q Exactive Plus mass spectrometer equipped with a Waters nanoAcquity UPLC system utilizing a binary solvent system (Buffer A: 100% water, 0.1% formic acid; Buffer B: 100% acetonitrile, 0.1% formic acid). Trapping was performed at 5 µl/min with 97% A for 3 min using a Waters Symmetry® C18 (180 µm x 20 mm) trap column. Peptides were separated using an ACQUITY UPLC PST (BEH) C18 nanoACQUITY Column (1.7 µm, 75 µm x 250 mm at 37 ºC) and eluted at 330 nl/min with the following gradient (3% B at initial conditions; 5% B at 1 minute; 30% B at 140 minutes; 50% B at 155 minutes; 90% B at 160-170 min; return to initial conditions at 171 minutes). MS was acquired in profile mode over the 300-1,500 m/z range using 1 microscan, 70,000 resolution, AGC target of 3E6, and a full max ion time of 45 ms. Data dependent MS/MS were acquired in centroid mode using 1 microscan, 17,500 resolution, AGC target of 1E5, full max IT of 100 ms, 1.7 m/z isolation window, and a normalized collision energy of 28. Up to 20 MS/MS were collected per MS scan on species with an intensity threshold of 1E4, charge states 2-6, peptide match preferred, and dynamic exclusion set to 20 seconds.

4.3.3 Protein identification and compilation of search results

All MS/MS samples were analyzed using Sequest (Thermo Fisher Scientific, San Jose, CA, USA; version 2.1.0.81) and X!Tandem (The GPM, thegpm.org; version CYCLONE (2010.12.01.1)). Sequest was set up to search against a proteome database including insects, *R. flavipes*, *P. aeruginosa*, and MRSA from NCBI (https://www.ncbi.nlm.nih.gov/guide/proteins/), assuming the digestion enzyme trypsin. X!Tandem was set up to search a subset of the database also assuming the digestion enzyme trypsin. The following parameters were used in search with Sequest and X!Tandem: fragment ion mass tolerance of 0.02 Da, parent ion tolerance of 10 parts per million (PPM); carbamidomethyl of cysteine as a fixed modification, and deamidation of

asparagine, oxidation of methionine as well as acetyl of the N-terminus as variable modifications in Sequest; Glu->pyro-Glu of the N-terminus, ammonia-loss of the N-terminus, Gln->pyro-Glu of the N-terminus, deamidated of asparagine, oxidation of methionine and acetyl of the N-terminus as variable modifications in X!Tandem.

Scaffold software (v4.6.1, Proteome Software Inc., Portland, OR) was used to validate MS/MS based peptide and protein identifications. Peptide probabilities from X!Tandem were assigned by the Peptide Prophet algorithm (Keller 2002) with Scaffold delta-mass correction. Peptide Probabilities from X!Tandem and Sequest were assigned by the Scaffold Local FDR algorithm. Protein probabilities were assigned by the Protein Prophet algorithm (Nesvizhskii et al. 2003). Protein probabilities and identifications were accepted if they could be established at greater than 95% peptide probability and contained at least two identified peptides to achieve a false discovery rate (FDR; the ratio between the false peptide-spectrum matches (PSM) and the total number of PSMs above the score threshold) less than 5.0%. Proteins that sharing significant peptide evidence were grouped into clusters.

4.3.4 Function prediction and statistical analysis

The accepted protein identifications were used as queries to search the insect protein collections at NCBI using Blast2GO PRO to predict functions due to their advanced functional analysis to the genomics research of non-model species (Conesa et al. 2005). BLASTp-fast searches were done with an expectation value maximum of 1E-3. In order to compare the abundances of the accepted proteins across different treatments, the original protein dataset was first reduced to eliminate proteins that only present in one replicate with too few spectral counts. The acquired subsets of the protein database (409 proteins in MRSA-challenged and naïve termites; 419 proteins in *P. aeruginosa*-challenged and naïve termites) were analyzed using

Quasi-Poisson likelihood model combined with a FDR adjustment to identify differences in protein levels based on spectral counts. Significantly expressed proteins were determined with a quasi *p*-value of less than 0.05 and at least 2.5-fold difference in spectral counts (log_2(rate1/rate2) higher than 1.32 or lower than -1.32) (Li et al. 2010). To evaluate variations of hemolymph proteins between *P. aeruginosa-challenged* or MRSA-challenged and naïve groups, and to visualize strong patterns in our dataset, unsupervised hierarchical clustering was performed using Ward's method with Pearson correlation as similarity metric. This clustering technique organized all data elements into a dendrogram representing the discovered classes. In addition, a principal component analysis (PCA) was applied to the protein expression data to better visualize the dataset after class prediction analysis and the top components were used to illustrate the similarity in protein expression profiles among samples. Hierarchical clustering analysis and PCA was performed on identified significantly expressed proteins. All statistical analyses were performed using R software.

4.4 Results

4.4.1 Descriptive data

Protein database search showed that 22,338 spectra matched those of trypsinolytic peptides at ≥98% probabilities to achieve 0.10% Decoy FDR. The matching spectra corresponded to 181 clusters containing a total of 578 proteins with at least two peptides at ≥95% probability to achieve 1.6% Decoy FDR (Supplementary table 1). Of the 578 proteins, 245 proteins were shared by naïve, MRSA-challenged, and *P. aeruginosa* challenged termites. 87 proteins were shared by naïve and MRSA-challenged termites, 41 proteins were shared by naïve and *P. aeruginosa*-challenged termites, and 27 proteins were found in the two MDR-challenged groups. Furthermore, 58, 56 and 50 unique proteins were detected in the hemolymph in naïve,

MRSA-challenged and *P. aeruginosa*-challenged termites, respectively (Figure 4.1A; Supplementary Tables 2-7). About 87% of these proteins had molecular weight (MW) between 10 to 80 kDa (Figure 4.1B) which corresponds to the dominant bands showed in SDS-PAGE gel (Supplementary Figure 4.1). The smallest protein was 8 kDa (antioxidant enzyme) and the largest protein was 2068 kDa (uncharacterized protein).

According to total spectrum count, the 19 most highly expressed hemolymph proteins included 4 storage proteins (hexamerin I, hexamerin II, apolipophorins, apolipophorin-like protein), 9 immune-related proteins (2 transferrins, catalase, ferrintin, alpha-tubulin, retinal dehydrogenase 2, aldo-keto reductase, gram-negative bacteria, and phenoloxidase 2), and 6 other proteins (2 actins, hypothetical protein L798_04756, endogenous cellulase, chain W molecular models of averaged rigor crossbridges from tomograns of insect flight muscle, and arginine kinase) (Figure 4.2).

4.4.3 Gene ontology of hemolymph proteins

Protein functional analysis was performed using Blast2Go. The analysis indicated that the majority of the hemolymph protein sequences (87.2%) could be associated with biological processes and molecular functions. On the basis of their biological processes, the expressed proteins were annotated into 10 categories. The most represented categories were proteins associated with organic substance metabolic process (17%), primary metabolic process (16.6%), cellular metabolic process (16.4%), followed by proteins related to single-organism metabolic process (12.5%), single-organism cellular process (11.1%), and nitrogen compound metabolic process (9.4%). Proteins associated with biosynthetic process (6.2%), catabolic process (4.3%), response to stress (3.2%), and the establishment of localization (3.2%) were also represented in Figure 4.3. In terms of molecular functions, protein binding and catalytic activity were annotated

into two major categories (Figure 4.4). The predicted binding activity included protein binding (4.2%), ion binding (8.1%), carbohydrate derivate binding (14.4%), small molecule binding (15.1%), organic cyclic compound binding (16.9%), and heterocyclic compound binding (16.9%). The predicted catalytic activity included transferase activity (5.8%), oxidoreductase activity (6.7%), and hydrolase activity (11.9%).

4.4.4 Differentially expressed proteins in MDR-challenged *R. flavipes*

4.4.4.1 up- and down-regulated hemolymph proteins in *R. flavipes* after MRSA-challenge

MRSA-challenged termites showed 36 hemolymph proteins were significantly expressed, and 9 of them were induced; MRSA-challenge also down-regulated 27 proteins exists in naïve termites (Table 4.1). The majority of the regulated proteins are involved in metabolic process, cell movements, and cellular changes. Among the induced (up-regulated) proteins, 2 are related to immune responses: transferrin (iron metabolism) and catalase (detoxification). Among the down-regulated proteins, 13 are related to immune responses (i.e. response to stress, cytoskeletal modeling, detoxification, and immune effectors). These molecules included beta-glucosidase, papilin, C-type lysozyme, apolipophorin, beta-glucuronidase, peroxiredoxin-6, isocitrate dehydrogenase, cathepsin L-like protein, hsp 90, and etc.

Hierarchical clustering of the 6 samples based on the expression profiles of these 36 discriminatory proteins essentially separated samples into two main clusters corresponding to the MRSA-challenged and naïve termite (Figure 4.5). The clustering analysis partitioned proteins into two main groups of 9 and 27 proteins over- and under-expressed in MRSA-challenged hemolymph samples, respectively, as compared to naïve termites (Figure 4.5). Similarity in protein expression profiles among the 6 samples was summarized in a biplot of the first two principal components of the PCA (Figure 4.6). The first principal component (PC1), explaining

the largest variation (89.9%), clearly differentiated MRSA-challenged and naïve termite hemolymph samples.

4.4.4.2 up- and down-regulated hemolymph proteins in *R. flavipes* after *P. aeruginosa*-challenge

Interestingly, we identified 80 differently expressed hemolymph proteins after *P. aeruginosa*-challenge using nano LC-MS/MS (Table 4.2). These proteins are annotated to metabolism, development, stress response, immune signaling, immune effectors and other functions. Heat-killed *P. aeruginosa* feeding significantly increased the spectrum count of 11 proteins. Among the 11 upregulated proteins, we detected 10 proteins (actin, sorbitol dehydrogenase, transferrin, catalase, malate dehydrogenase, and heat shock proteins, etc.) that were related to immune response with a fold change of ≥ 2.5 folds. In contrast to the up-regulated proteins of *P. aeruginosa*-challenged termite samples, there were 59 proteins being down-regulated with 89 proteins not detected after *P. aeruginosa*-challenge. Most of the downregulated proteins involve in metabolic process and stress response.

Like MRSA-challenged termite hemolymph samples, hierarchical clustering (Figure 4.7) of these 80 discriminatory proteins in *P. aeruginosa*-challenged and naïve termites essentially separated samples into two main clusters corresponding to the treatment. PCA analysis of these 6 samples were summarized by the first two principal components, explaining 95.8% of the variations.

4. 5 Discussions

This study, for the first time, described the hemolymph proteomes of MDR-challenged *R. flavipes* workers and compared with the hemolymph proteome of naïve termites. We used nano LC-MS/MS to perform a deep analysis of the hemolymph proteome and identified a total of 578

proteins (Supplementary Table 1). Among the detected proteins, most of them were involved in metabolism process as evidenced in Figure 4.2-4.4. This result suggests that hemolymph is an important source for nutrient and ion storage and transportation, a battleground for cellular and humoral immunity, and the network for metabolism reorganization upon bacterial challenge (Guedes et al. 2005; Zdybicka-Barabas and Cytryńska 2013; He et al. 2016).

Interestingly, we found three immune effectors, phenoloxidase (PO), Gram-negative binding protein (GNBP), lysosomal aspartic protease constitutively present and remained at a similar expression level in MDR-challenged termites compared to naïve termites. POs play a crucial role in formation of melanin and reactive oxygen species (ROS) to defend microbes and other parasites (Taft et al. 2001; Lai et al. 2002; Liu et al., 2007). GNBPs are recognition proteins with antimicrobial activity due to the presence of β-1, 3-glucanases structure (Bulmer et al. 2009). Therefore, it is likely that these two molecules are contributors of previously reported constitutively antibacterial activities found in *R. flavipes* (Zeng et al. 2016). Nevertheless, the protein expression levels of POs and GNBPs seem contradictory with other studies demonstrated that the transcriptomic levels of POs and GNBPs were overexpressed after immune challenge (Rodriguez-Andres et al. 2012; Gonzalez-Santoyo et al. 2012; Liu et al. 2015). Another induced molecule, lysosomal aspartic protease has multi-domains of aspartyl protease including pepsins, cathepsins, and renins, and it is potentially a contributor to the bactericidal activity against a broad range of susceptible bacteria (Thorne et al. 1976; Hamilton et al. 2011; Hussain et al. 2016).

We observed 36 and 80 hemolymph proteins that appeared to be differently expressed with a fold change of ≥ 2.5 in response to MRSA and *P. aeruginosa*-challenge, respectively. Many of these differentially expressed proteins were involved in immune-related process such as

cytoskeletal modeling, iron metabolism, antioxidant-related immune response**,** stress response, and immune effectors. Upon infection, insects need to produce a large number of ROS to kill pathogens, but excessive ROS can result in damage to the host organism (Law 2002; Nicol et al. 2002; Liu et al. 2015). Therefore, it is necessary that proteins related to antioxidant activities were required to remove excessive ROS for maintaining host homeostasis (Sies 1997; Li et al. 2010; Dubovskiy et al. 2013). In our study, the significantly upregulated malate dehydrogenase, sorbitol dehygrogenase, and catalase provide evidence that *R. flavipes* responded to MDR-challenge led to oxidative stress. In addition to antioxidant system, iron metabolism is vital to hinder pathogen survival in insects by sequestering iron (Yoshiga et al. 1999; Yun et al. 1999). An upregulation of transferrin (isolate free iron ions) observed in MDR-challenged termites provide the evidence that these two molecules might relate to antibacterial activity of hemolymph due to a lack of ionic iron (Thompson et al. 2003; Altincicek et al. 2007; Wang et al. 2009). In addition, numerous stress-responsive molecules including heat shock proteins as well as ubiquitin were detected due to bacterial infection served as stressors in MDR-challenged *R. flavipes* (Table 4.1&4.2). These data indicated that there might be a link between the innate immunity and stress responses in *R. flavipes* upon the occurrence of infections.

In MRSA-challenged termites, we found two upregulated proteins (catalase and transferrin) were involved in insect immune responses, which supported previous findings on upregulation of these molecules upon immune challenge (Yoshiga et al. 1999; Bartholomay et al. 2004; Zug and Hammerstein 2015). Importantly, two proteins (beta-glucuronidase and C-type lysozyme) with hydrolase activity were vanished after MRSA-challenge in comparison with naïve termites. Beta-glucuronidase is a proteinaceous compound with hydrolase activity targeting on O-glycosyl compounds, and c-type lysozyme is defined by its enzymatic hydrolysis

of peptidoglycan with basically activity against certain Gram-positive bacteria and extent weak activity with some Gram-negative bacteria (Yu et al. 2002; Wang et al. 2009). It is very likely that the disappearance of these two molecules may correspond to the loss of activity against Gram-negative bacteria observed in our previous observation after MRSA-challenge (Zeng et al. 2016). To test this hypothesis, further investigation on three-dimensional structure of the two proteins and reconstituting the antibacterial activity should be considered.

Of the differently expressed hemolymph proteins in *P. aeruginosa*-challenged termites, 10 upregulated proteins involve in immune response, with majority of them being categorized in cytotoxic molecule production, antioxidant-related immune response, and iron metabolism (actins, tublins, transferrin, dehydrogenases, and catalase and etc.) (Table 4.2). Actin, alpha- and beta-tubulin are cytoskeletal elements that help maintain cell shape and participate in cellular division, and intracellular transport (Bartholomay et al. 2004; Vierstraete et al. 2004; Scharlaken et al. 2007; Li et al. 2011; Randolt et al. 2008;), and their expression levels were reported to be upregulated in various insects in response to bacterial challenge (Loseva et al. 2004; Woltedji et al. 2013). Comparing with MRSA-challenged termites, the abundance of actins and tublins were significantly increased in *P. aeruginosa*-challenged termites (Table 4.1&4.2). This suggests that termites tend to produce more cytoskeletal elements in response to Gram-negative bacterial challenge than Gram-positive bacterial challenge. A recent study demonstrated that insect actin can mediate bacterial cell killing through phagocytosis or direct antibacterial action when it binds to the surface of bacterial cells (Sandiford et al. 2015). Thus, it is likely that actin identified in our study is the possible antibacterial molecule to inhibit the growth of *P. aeruginosa* and other susceptible bacteria (Zeng et al. 2016).

In conclusion, the results achieved in this study increased the present knowledge of the

termite immune response primed by oral ingestion of *P. aeruginosa* or MRSA, supported essentially on proteomic approaches showing protein regulation after MDR challenge. In addition, the identified potential immune effectors provide insights for the potential new targets of antimicrobial discovery against a set of human pathogens, especially against *P. aeruginosa* and MRSA.

A.

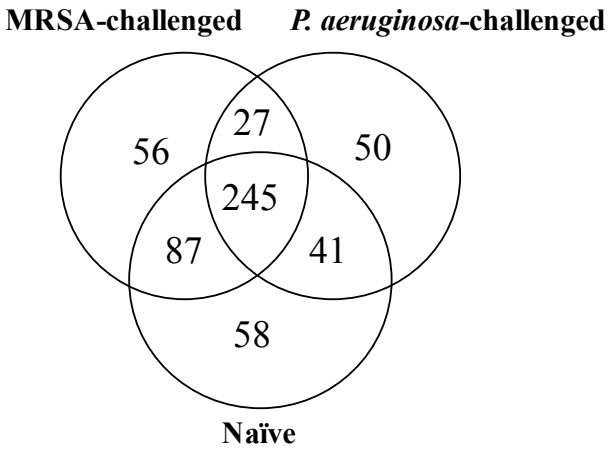

B.

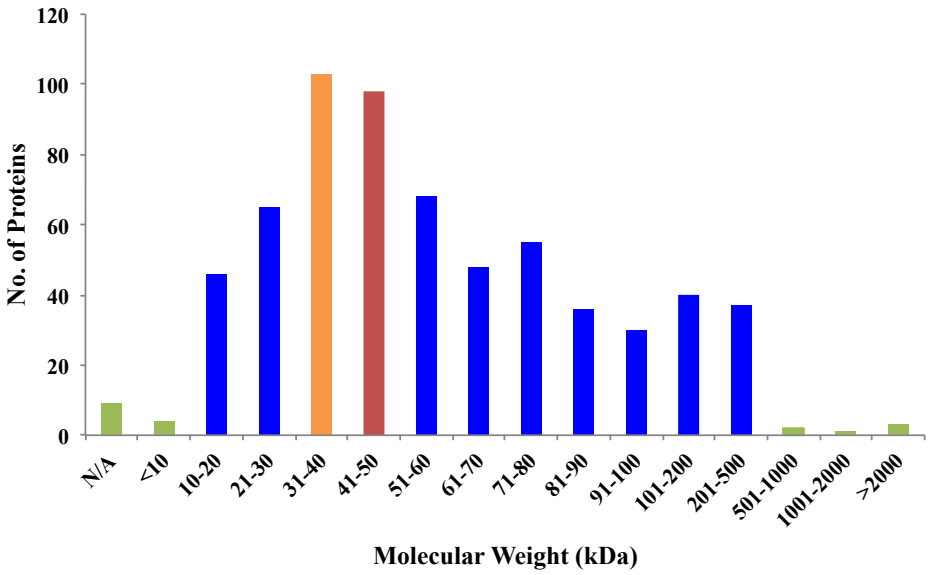

Figure 4.1 Comparison of proteins identified in naïve and MDR challenged *R. flavipes* (A) and size distribution of proteins in terms of molecular weight ranges (B).

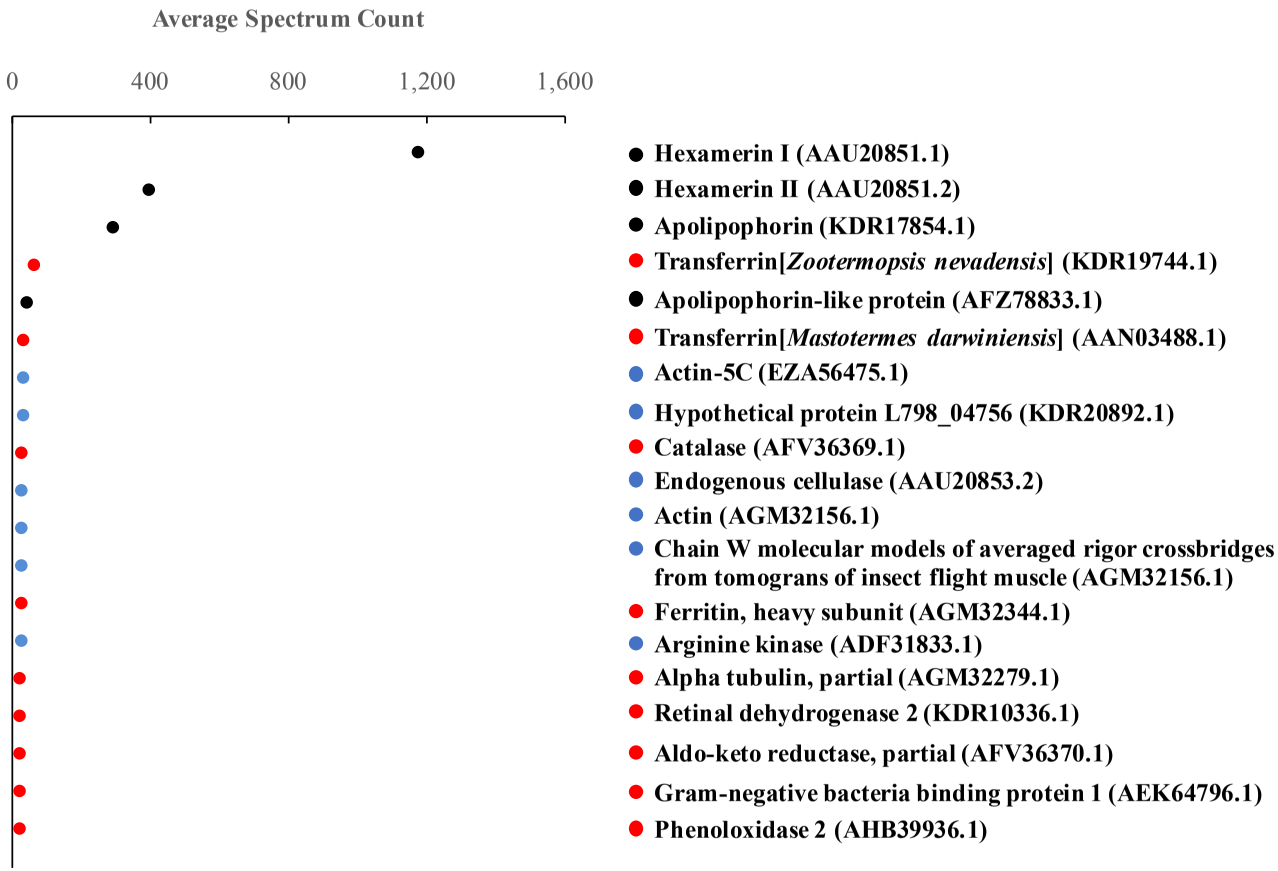

Figure 4.2 Nineteen most abundant proteins in *R. flavipes* hemolymph. The abundance value of each protein was estimated as spectral count**.** Colors show the protein category: storage protein, black; immune-related protein, red; other proteins, blue.

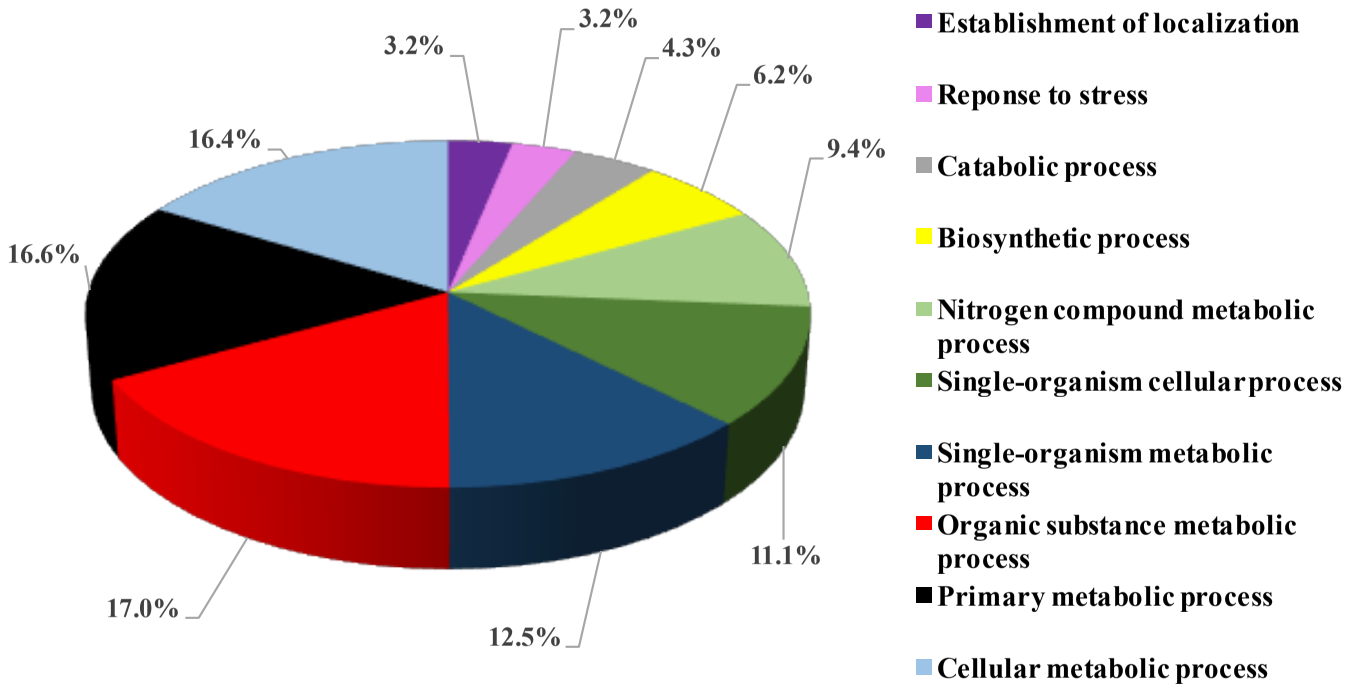

Figure 4.3 Protein categorization by gene ontology based on biological processes.

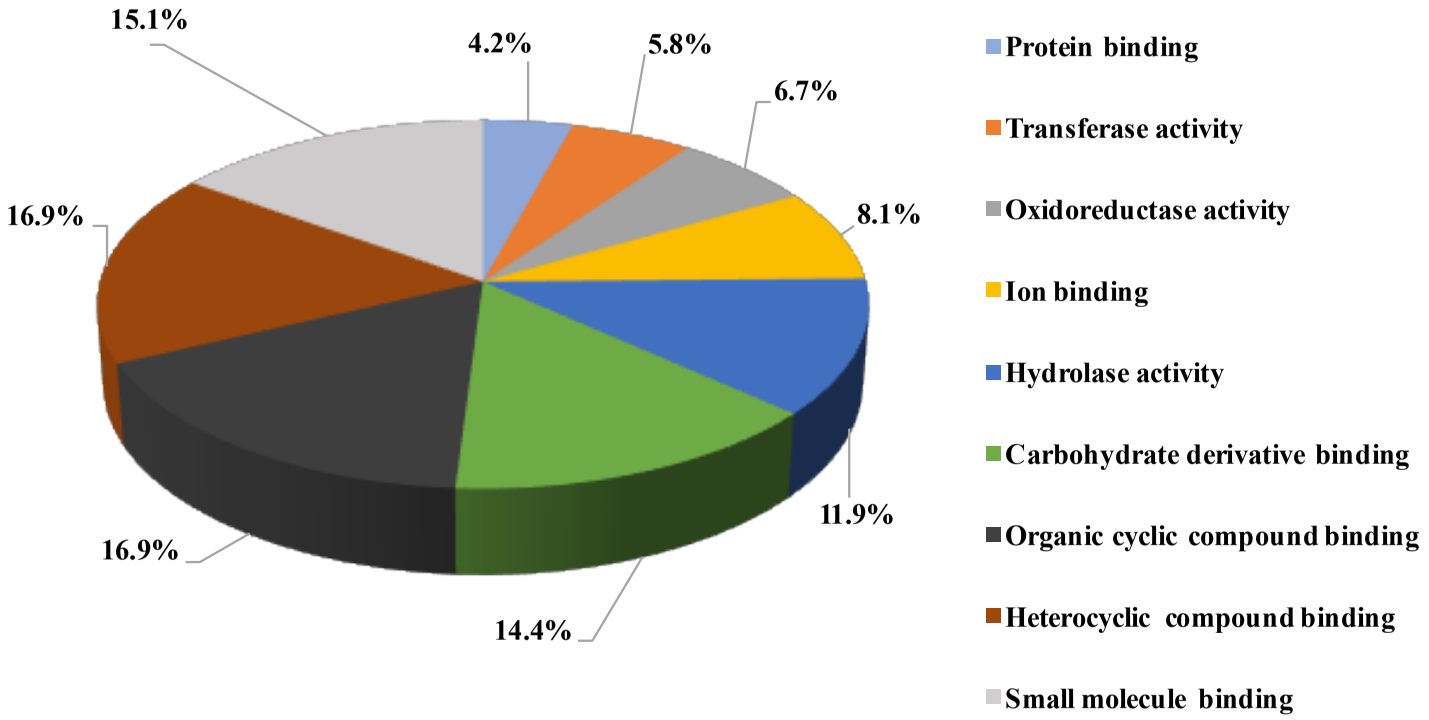

Figure 4.4 Protein categorization by gene ontology based on molecular functions.

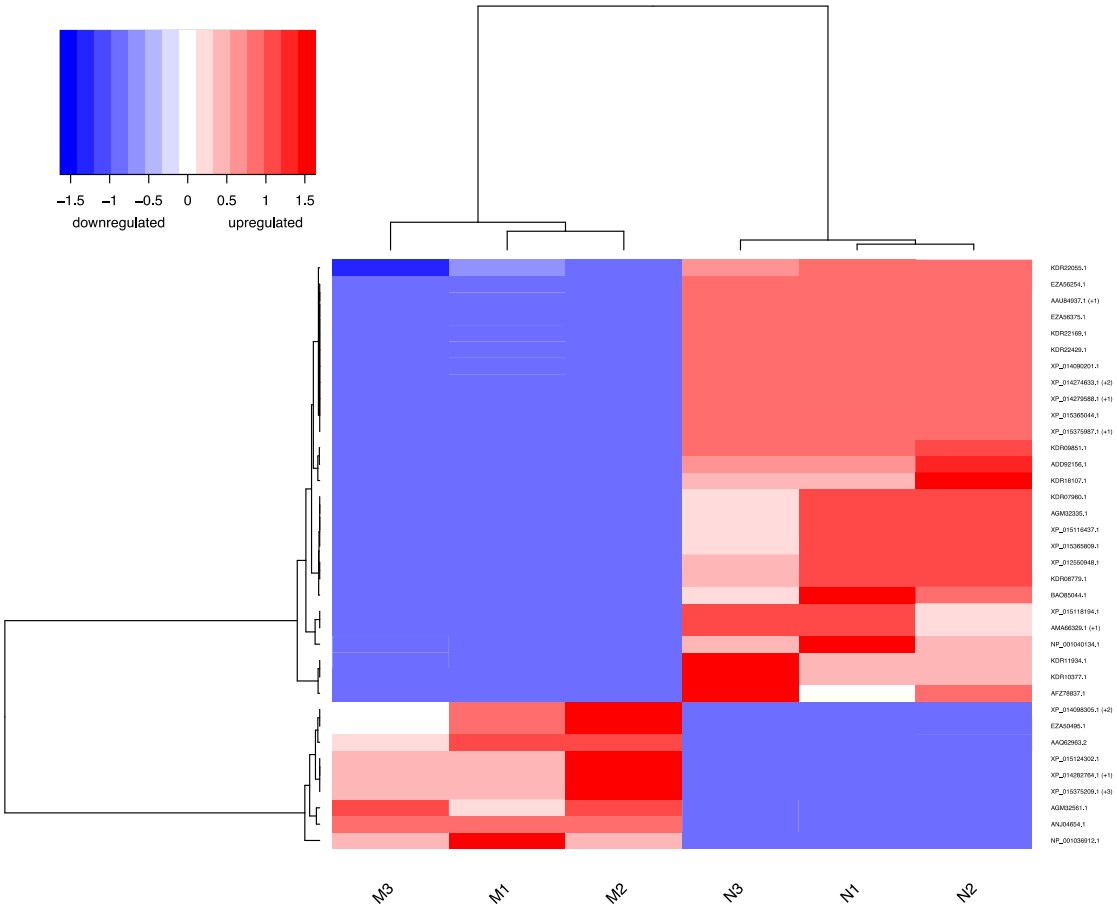

Figure 4.5 Hierarchical clustering analysis based on 36 proteins significantly changed in abundances between MRSA-challenged and naïve termites within the dataset. Both samples and proteins were clustered using Ward's method, and with Pearson correlation as similarity metric. The samples are shown horizontally (columns), the proteins vertically (rows). The dendrograms represent the distances between clusters. Protein expression levels are represented in the color scale of blue (downregulated) to red (upregulated).

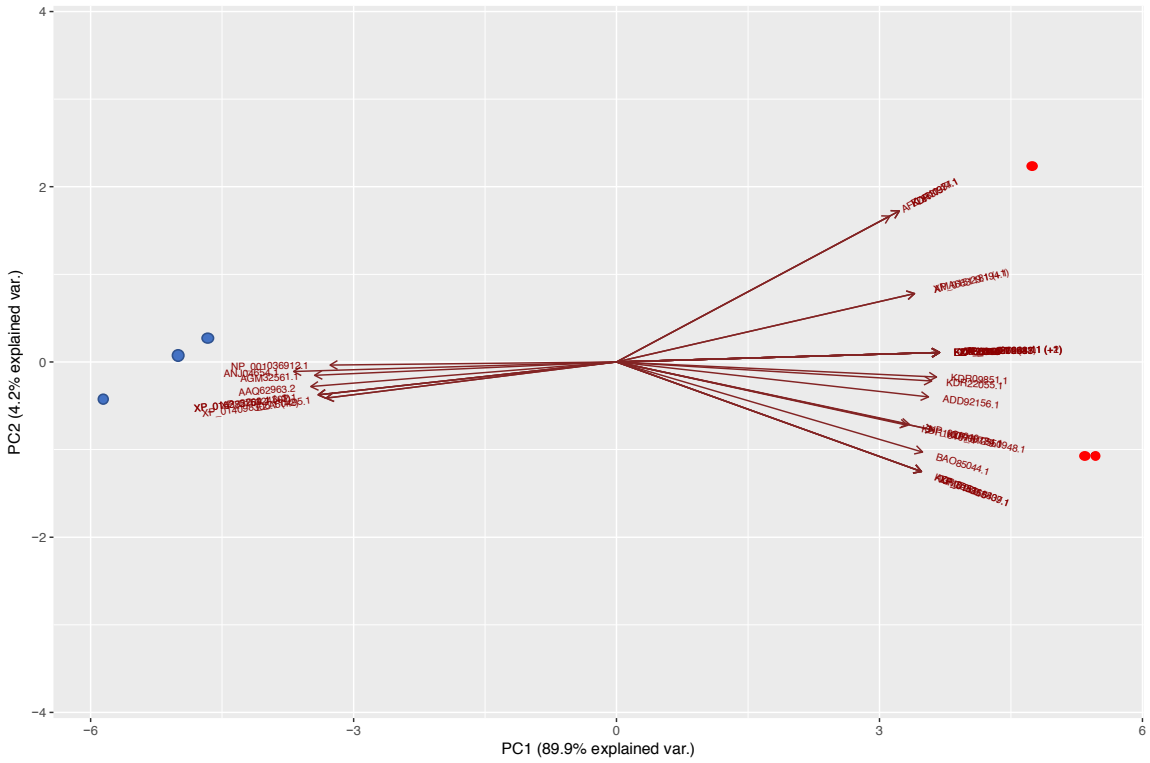

Figure 4.6 Principal component analysis based on the expression profiles of 36 proteins significantly changed in abundances between MRSA-challenged and naïve termites. Blue and red dots represent MRSA-challenged termite hemolymph samples and naïve termite hemolymph samples, respectively. Each axis represents a principal component (PC1 and PC2) with the percentage of the total variance it explains. The next two components (PC3 and PC4) explained 2.7% and 1.8% of total variance, respectively.

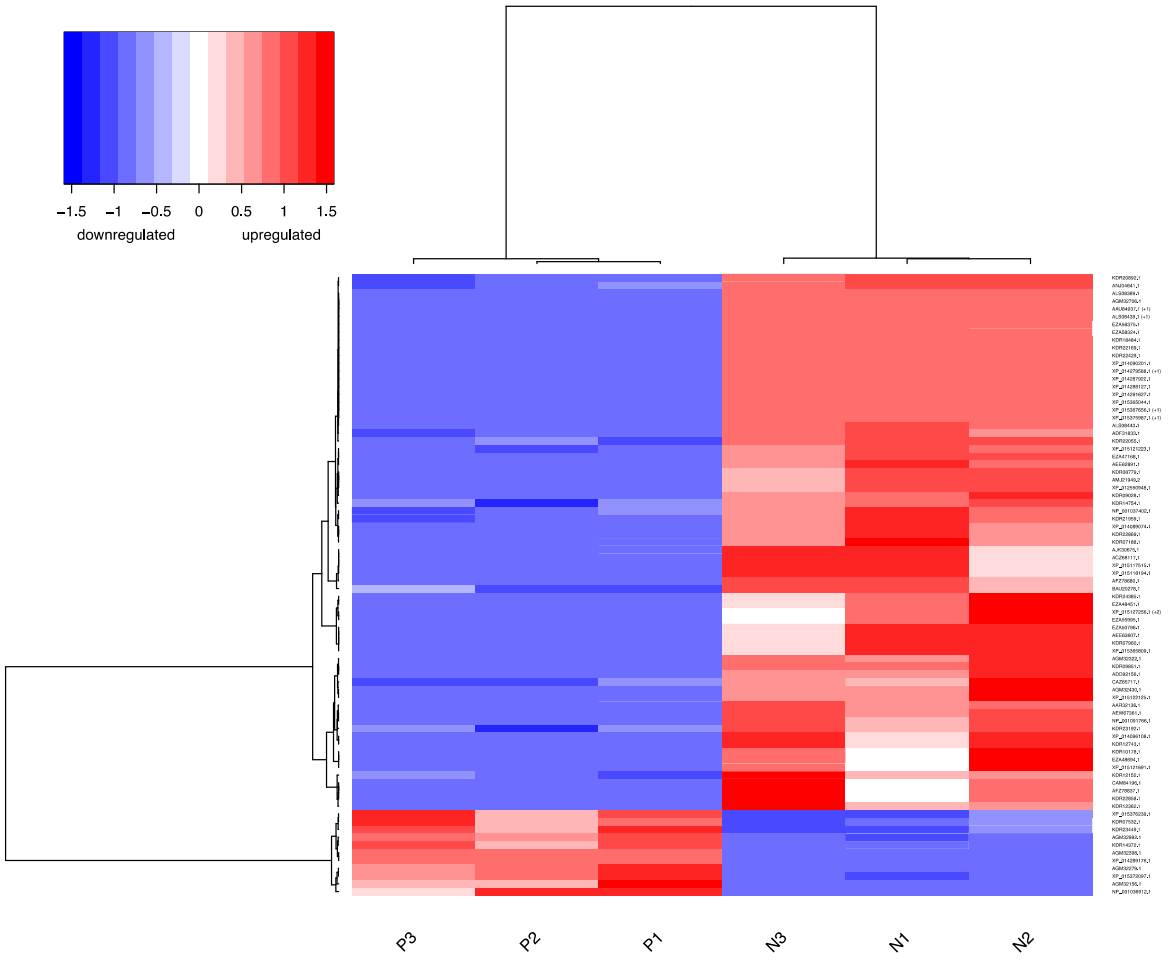

Figure 4.7 Hierarchical clustering analysis based on 80 proteins significantly changed in abundances between *P. aeruginosa*-challenged and naïve termites within the dataset. Both samples and proteins were clustered using Ward's method, and with Pearson correlation as similarity metric. The samples are shown horizontally (columns), the proteins vertically (rows). The dendrograms represent the distances between clusters. Protein expression levels are represented in the color scale of blue (downregulated) to red (upregulated).

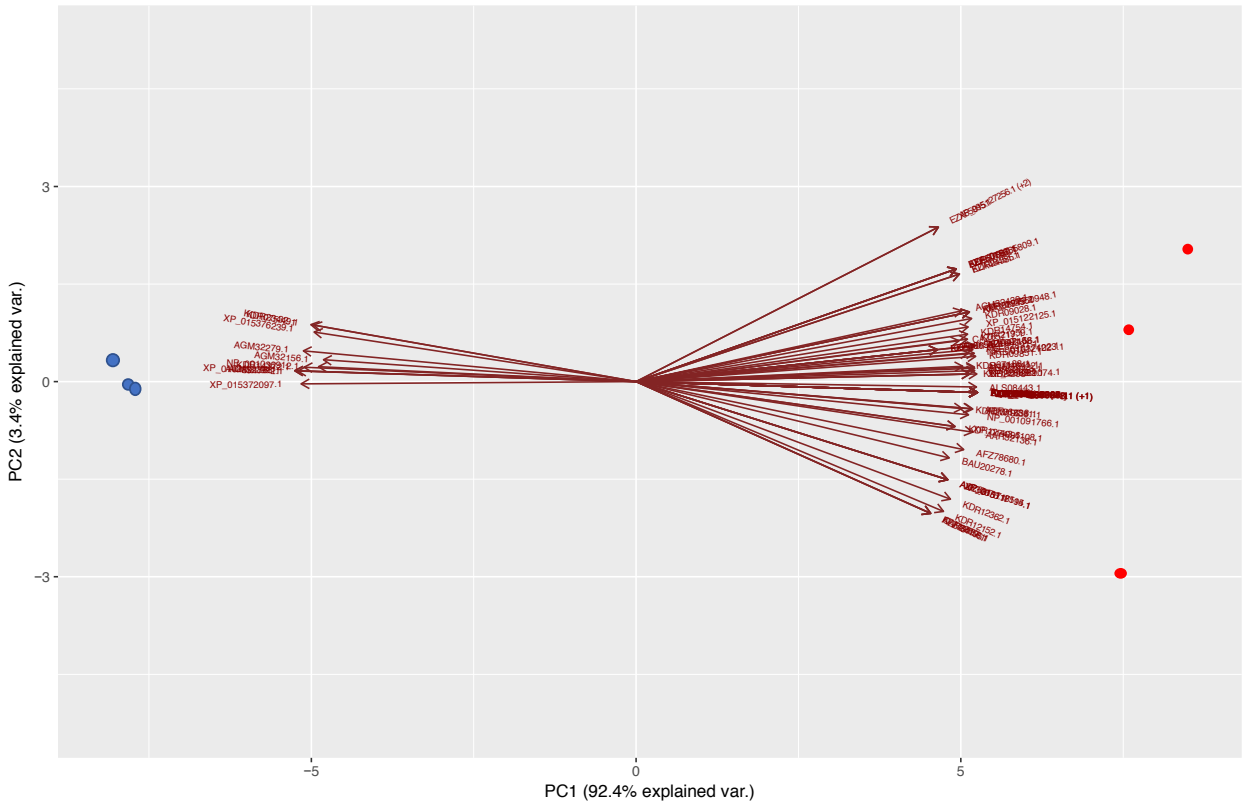

Figure 4.8 Principal component analysis based on the expression profiles of 80 proteins significantly changed in abundances between *P. aeruginosa*-challenged and naïve termites. Blue and red dots represent *P. aeruginosa*-challenged termite hemolymph samples and naïve termite hemolymph samples, respectively. Each axis represents a principal component (PC1 and PC2) with the percentage of the total variance it explains. The next two components (PC3 and PC4) explained 3.0% and 0.59% of total variance, respectively.

Table 4.1 Differently expressed proteins from hemolymph proteins of *R. flavipes* after MRSA challenge when compared to naïve termites.

Protein	Accession Number	Poisson.FDR *p*-value	Quasi.FDR *p*-value	Rate Ratio
mitochondrial ATP synthase alpha subunit	ANJ04654.1	0.1938	<0.0001	33.62
transferrin	AAQ62963.2	0.0909	0.0193	32.91
Calponin-likey domain containing protein	AGM32561.1	0.0909	0.0193	32.91
catalase	NP_001036912.1	0.1375	0.0308	32.59
PREDICTED: myosin heavy chain, muscle isoform X26	XP_014282764.1 (+1)	0.1375	0.0308	32.59
PREDICTED: ATP synthase subunit alpha	XP_015124302.1	0.1375	0.0308	32.59
REDICTED: myosin heavy chain, muscle isoform X3	XP_015375209.1 (+3)	0.1375	0.0308	32.59
Myosin heavy chain, muscle	EZA50495.1	0.0696	0.0469	31.73
REDICTED: myosin heavy chain, muscle isoform X3	XP_014098305.1 (+2)	0.0696	0.0469	31.73
beta-glucosidase	ADD92156.1	0.2069	0.0193	-1.74
papilin	KDR22055.1	0.0049	0.0308	-1.79
beta-glucosidase	BAO85044.1	0.1375	0.0308	-2.00
C-type lysozyme-2	AFZ78837.1	0.0696	0.0469	-31.73
apolipophorin	KDR18107.1	0.0272	0.0308	-32.15
Peroxiredoxin-6	KDR10377.1	0.1375	0.0308	-32.59
Lambda-crystallin-like protein	KDR11934.1	0.1375	0.0308	-32.59
isocitrate dehydrogenase	NP_001040134.1	0.1375	0.0308	-32.59
cathepsin L-like protein	AGM32335.1	0.0909	0.0193	-32.91
hsp 90	AMA66329.1 (+1)	0.0909	0.0193	-32.91
hypothetical protein	KDR07960.1	0.0909	0.0193	-32.91

L798_01615 PREDICTED: isocitrate				
isocitrate dehydrogenase	XP_015116437.1	0.0909	0.0193	-32.91
PREDICTED: pyruvate kinase-like	XP_015118194.1	0.0909	0.0193	-32.91
PREDICTED: bifunctional purine biosynthesis protein PURH	XP_015365809.1	0.0909	0.0193	-32.91
beta-glucosidase	KDR08779.1	0.0272	0.0050	-33.59
beta-glucuronidase	XP_012550948.1	0.0272	0.0050	-33.59
putative fructose 1,6-bisphosphate aldolase	AAU84937.1 (+1)	0.1938	<0.0001	-33.62
Alpha-L-fucosidase	EZA56254.1	0.1938	<0.0001	-33.62
Multifunctional protein ADE2	EZA56375.1	0.1938	<0.0001	-33.62
Cytosolic carboxypeptidase-like protein 5, partial	KDR22169.1	0.1938	<0.0001	-33.62
PREDICTED: cofilin/actin-depolymerizing factor homolog	XP_014090201.1	0.1938	<0.0001	-33.62
Peroxiredoxin-6	XP_014274633.1 (+2)	0.1938	<0.0001	-33.62
PREDICTED: alpha,alpha-trehalose-phosphate synthase [UDP- forming] isoform X1	XP_014279588.1 (+1)	0.1938	<0.0001	-33.62
PREDICTED: alpha,alpha-trehalose-phosphate synthase [UDP-forming]-like isoform X1	XP_015365044.1	0.1938	<0.0001	-33.62
PREDICTED: glycogen phosphorylase isoform X1	XP_015375987.1 (+1)	0.1938	<0.0001	-33.62
Multifunctional protein ADE2,	KDR09851.1	0.0018	0.0008	-34.29

partial Protein yellow	KDR22429.1	0.0696	<0.0001	-34.62

Table 4.2 Differently expressed proteins from hemolymph proteins of *R. flavipes* after *P. aeruginosa*-challenge when compared to naïve termites.

Protein	Accession Number	Poisson.FDR p-value	Quasi.FDR p-value	Rate Ratio
arginine kinase, partial (mitochondrion)	ALS08443.1	<0.0001	<0.0001	-37.12
arginine kinase, partial (mitochondrion)	ALS08389.1	<0.0001	<0.0001	-36.62
arginine kinase, partial (mitochondrion)	ALS08439.1 (+1)	<0.0001	<0.0001	-36.62
ferrtin	AGM32322.1	<0.0001	0.0007	-35.55
Arginine kinase	EZA47168.1	<0.0001	0.0004	-35.40
Glutamine synthetase 2 cytoplasmic	KDR18484.1	0.0034	<0.0001	-35.20
VHDL receptor	AAR32136.1	<0.0001	0.0006	-34.98
uncharacterized protein	AGM32706.1	0.0198	<0.0001	-34.62
Translationally-controlled tumor protein-like protein	EZA58324.1	0.0198	<0.0001	-34.62
Protein yellow	KDR22429.1	0.0198	<0.0001	-34.62
aldose reductase-like	XP_014287922.1	0.0198	<0.0001	-34.62
dehydrogenase	XP_014291627.1	0.0198	<0.0001	-34.62
PREDICTED: alpha-L-fucosidase isoform X1	XP_015367656.1 (+1)	0.0198	<0.0001	-34.62
Selenium-binding protein 1-A	KDR09028.1	0.0001	0.0017	-34.50
unknown	AEE62891.1	0.0000	0.0007	-34.43
Multifunctional protein ADE2, partial	KDR09851.1	0.0003	0.0005	-34.29
beta-glucosidase	AEW67361.1	0.0011	0.0008	-34.05

beta-glucosidase	ADD92156.1	0.0020	0.0010	-33.91
Glutathione S-transferase	KDR22869.1	0.0020	0.0010	-33.91
PREDICTED: enolase	XP_014089074.1	0.0020	0.0010	-33.91
putative fructose 1,6-bisphosphate aldolase	AAU84937.1 (+1)	0.1132	<0.0001	-33.62
Multifunctional protein ADE2	EZA56375.1	0.1132	<0.0001	-33.62
Cytosolic carboxypeptidase-like protein 5, partial	KDR22169.1	0.1132	<0.0001	-33.62
PREDICTED: cofilin/actin-depolymerizing factor homolog	XP_014090201.1	0.1132	<0.0001	-33.62
PREDICTED: alpha,alpha-trehalose-phosphate synthase [UDP- forming] isoform X1	XP_014279588.1 (+1)	0.1132	<0.0001	-33.62
heat shock protein	XP_014288127.1	0.1132	<0.0001	-33.62
PREDICTED: alpha,alpha-trehalose-phosphate synthase [UDP-forming]-like isoform X1	XP_015365044.1	0.1132	<0.0001	-33.62
PREDICTED: glycogen phosphorylase isoform X1	XP_015375987.1 (+1)	0.1132	<0.0001	-33.62
aldo-keto reductase 1	AMJ21949.2	0.0061	0.0020	-33.59
Beta-glucuronidase	KDR08779.1	0.0061	0.0020	-33.59
fructose 1,6-bisphosphate aldolase	NP_001091766.1	0.0061	0.0020	-33.59
Beta-glucuronidase	XP_012550948.1	0.0061	0.0020	-33.59
PREDICTED: plasma alpha-L-fucosidase-like	XP_015122125.1	0.0124	0.0030	-33.40
Teneurin-3	KDR07188.1	0.0002	0.0030	-32.96
enolase	ACZ68117.1	0.0351	0.0077	-32.91

unknown	AEE63607.1	0.0351	0.0077	-32.91
putative enolase, partial	AJK30675.1	0.0351	0.0077	-32.91
Teneurin-3	EZA50796.1	0.0351	0.0077	-32.91
hypothetical protein L798_01615	KDR07960.1	0.0351	0.0077	-32.91
Regucalcin	KDR12743.1	0.0351	0.0077	-32.91
PREDICTED: ribose-phosphate pyrophosphokinase	XP_014096108.1	0.0351	0.0077	-32.91
PREDICTED: enolase	XP_015117515.1	0.0351	0.0077	-32.91
XP_015118194.1	XP_015118194.1	0.0351	0.0077	-32.91
PREDICTED: bifunctional purine biosynthesis protein PURH	XP_015365809.1	0.0351	0.0077	-32.91
Superoxide dismutase	KDR12362.1	0.0003	0.0079	-32.85
SCP-like extracellular domain containing protein 2	AGM32430.1	0.0011	0.0069	-32.61
heat shcok protein	EZA48451.1	0.0034	0.0077	-32.32
c-type lysozyme	AFZ78837.1	0.0198	0.0223	-31.73
hexamerin 1	CAM84196.1	0.0198	0.0223	-31.73
Ribose-phosphate pyrophosphokinase	EZA48694.1	0.0198	0.0223	-31.73
Filamin-B	EZA55995.1	0.0198	0.0223	-31.73
Ribose-phosphate pyrophosphokinase 2, partial	KDR10178.1	0.0198	0.0223	-31.73
Neurotrypsin	KDR22858.1	0.0198	0.0223	-31.73
PREDICTED: ribose-phosphate pyrophosphokinase 1 isoform X1	XP_015121691.1	0.0198	0.0223	-31.73

PREDICTED: filamin-A isoform X1	XP_015127256.1 (+2)	0.0198	0.0223	-31.73
Hemocytin, partial	KDR23192.1	0.0361	0.0384	-2.46
hypothetical protein L798_04756, partial	KDR20892.1	0.0000	0.0004	-2.38
PREDICTED: arginine kinase isoform X1	XP_015121223.1	0.0000	0.0014	-2.18
Prostaglandin reductase 1	KDR24385.1	0.0627	0.0150	-2.00
hypothetical protein L798_11509	KDR14754.1	0.0034	0.0217	-1.95
glutathione S-transferase	AFZ78680.1	0.0927	0.0045	-1.87
arginine kinase	NP_001037402.1	0.0008	0.0077	-1.74
Papilin	KDR22055.1	0.0019	0.0047	-1.66
Plasma alpha-L-fucosidase	KDR21959.1	0.0198	0.0079	-1.58
arginine kinase	ADF31833.1	0.0001	0.0022	-1.56
Beta-ureidopropionase	KDR12152.1	0.0198	0.0450	-1.53
putative chemosensory protein	BAU20278.1	0.1696	0.0473	-1.46
arginine kinase	ANJ04641.1	0.0024	0.0029	-1.38
arginine kinase 2	CAZ65717.1	0.0400	0.0223	-1.32
actin	AGM32156.1	<0.0001	0.0255	1.61
Tubulin alpha chain	KDR23449.1	0.0003	0.0223	1.68
tubulin alpha chain	XP_015376239.1	<0.0001	0.0217	1.84
Tubulin alpha	KDR07532.1	0.0001	0.0167	1.85
alpha-tubulin	AGM32992.1	<0.0001	0.0012	1.96
alpha tubulin	AGM32279.1	<0.0001	0.0045	2.50
tubulin beta	XP_015372097.1	<0.0001	0.0091	3.63

catalase	NP_001036912.1	0.0020	0.0077	32.47
Malate dehydrogenase	KDR14372.1	0.0061	0.0020	33.59
sorbitol dehydrogenase-like	XP_014289176.1	0.1132	<0.0001	33.62
enolase	AGM32398.1	0.0034	<0.0001	35.20

References

Altincicek, B., Knorr, E., & Vilcinskas, A. (2008). Beetle immunity: Identification of immune-inducible genes from the model insect *Tribolium castaneum*. *Developmental & Comparative Immunology, 32*(5), 585-595.

Bartholomay, L. C., Cho, W. L., Rocheleau, T. A., Boyle, J. P., Beck, E. T., Fuchs, J. F., ... & Lin, S. P. (2004). Description of the transcriptomes of immune response-activated hemocytes from the mosquito vectors *Aedes aegypti* and *Armigeres subalbatus*. *Infection and immunity*, *72*(7), 4114-4126.

Bulet, P., Stöcklin, R., & Menin, L. (2004). Antimicrobial peptides: from invertebrates to vertebrates. *Immunological reviews*, *198*(1), 169-184.

Chan, Q. W., Howes, C. G., & Foster, L. J. (2006). Quantitative comparison of caste differences in honeybee hemolymph. *Molecular & Cellular Proteomics*, *5*(12), 2252-2262.

Conesa, A., Götz, S., García-Gómez, J. M., Terol, J., Talón, M., & Robles, M. (2005). Blast2GO: a universal tool for annotation, visualization and analysis in functional genomics research. *Bioinformatics*, *21*(18), 3674-3676.

de Morais Guedes, S., Vitorino, R., Tomer, K., Domingues, M. R. M., Correia, A. F., Amado, F., & Domingues, P. (2003). *Drosophila melanogaster* larval hemolymph protein mapping. *Biochemical and biophysical research communications*, *312*(3), 545-554.

de Morais Guedes, S., Vitorino, R., Domingues, R., Tomer, K., Correia, A. F., Amado, F., & Domingues, P. (2005). Proteomics of immune-challenged *Drosophila melanogaster* larvae hemolymph. *Biochemical and biophysical research communications*, *328*(1), 106-115

Dubovskiy, I. M., Whitten, M. M., Yaroslavtseva, O. N., Greig, C., Kryukov, V. Y., Grizanova, E. V., ... & Butt, T. M. (2013). Can insects develop resistance to insect pathogenic fungi?. *PloS one*, *8*(4), e60248.

Evans, J. D., Aronstein, K., Chen, Y. P., Hetru, C., Imler, J. L., Jiang, H., ... & Hultmark, D. (2006). Immune pathways and defence mechanisms in honey bees *Apis mellifera*. *Insect molecular biology*, *15*(5), 645-656.

Flatt, T., Heyland, A., Rus, F., Porpiglia, E., Sherlock, C., Yamamoto, R., ... & Silverman, N. (2008). Hormonal regulation of the humoral innate immune response in *Drosophila melanogaster*. *Journal of Experimental Biology*, *211*(16), 2712-2724.

González-Santoyo, I., & Córdoba-Aguilar, A. (2012). Phenoloxidase: a key component of the insect immune system. *Entomologia Experimentalis et Applicata*, *142*(1), 1-16.

Hamilton, C., Lejeune, B. T., & Rosengaus, R. B. (2011). Trophallaxis and prophylaxis: social immunity in the carpenter ant Camponotus pennsylvanicus. *Biology letters*, *7*(1), 89-92.

He, Y., Cao, X., Zhang, S., Rogers, J., Hartson, S., & Jiang, H. (2016). Changes in the plasma proteome of *Manduca sexta* larvae in relation to the transcriptome variations after an immune challenge: evidence for high molecular weight immune complex formation. *Molecular & Cellular Proteomics*, *15*(4), 1176-1187.

Hussain, A., Rizwan-ul-Haq, M., Al-Ayedh, H., & AlJabr, A. M. (2016). Susceptibility and Immune Defence Mechanisms of Rhynchophorus ferrugineus (Olivier)(Coleoptera: Curculionidae) against Entomopathogenic Fungal Infections. *International Journal of Molecular Sciences*, *17*(9), 1518.

Kanost, M. R., Kawooya, J. K., Law, J. H., Ryan, R. O., Van Heusden, M. C., & Ziegler, R. (1990). Insect haemolymph proteins. *Advances in insect physiology*, *22*, 299-396.

Karlsson, C., Korayem, A. M., Scherfer, C., Loseva, O., Dushay, M. S., & Theopold, U. (2004). Proteomic analysis of the Drosophila larval hemolymph clot. *Journal of Biological Chemistry*, *279*(50), 52033-52041.

Kim, T., & Kim, Y. (2005). Overview of innate immunity in Drosophila. *Journal of biochemistry and molecular biology*, *38*(2), 121.

Lai, S. C., Chen, C. C., & Hou, R. F. (2002). Immunolocalization of prophenoloxidase in the process of wound healing in the mosquito *Armigeres subalbatus* (Diptera: Culicidae). *Journal of medical entomology*, *39*(2), 266-274.

Law, J. H. (2002). Insects, oxygen, and iron. *Biochemical and biophysical research communications*, *292*(5), 1191-1195.

Li, J., Fang, Y., Zhang, L., & Begna, D. (2011). Honeybee (Apis mellifera ligustica) drone embryo proteomes. *Journal of insect physiology*, *57*(3), 372-384.

Li, J., Wu, J., Rundassa, D. B., Song, F., Zheng, A., & Fang, Y. (2010). Differential protein expression in honeybee (Apis mellifera L.) larvae: underlying caste differentiation. *PLoS One*, *5*(10), e13455.

Liu, H., Jiravanichpaisal, P., Cerenius, L., Lee, B. L., Söderhäll, I., & Söderhäll, K. (2007). Phenoloxidase is an important component of the defense against *Aeromonas hydrophila* infection in a crustacean, *Pacifastacus leniusculus*. *Journal of Biological Chemistry*, *282*(46), 33593-33598.

Liu, L., Li, G., Sun, P., Lei, C., & Huang, Q. (2015). Experimental verification and molecular basis of active immunization against fungal pathogens in termites. *Scientific reports*, *5*.

Loseva, O., & Engström, Y. (2004). Analysis of signal-dependent changes in the proteome of Drosophila blood cells during an immune response. *Molecular & Cellular Proteomics*, *3*(8), 796-808.

Nesvizhskii, A. I., Keller, A., Kolker, E., & Aebersold, R. (2003). A statistical model for identifying proteins by tandem mass spectrometry. *Analytical chemistry*, *75*(17), 4646-4658.

Nichol, H., Law, J. H., & Winzerling, J. J. (2002). Iron metabolism in insects. *Annual review of entomology*, *47*(1), 535-559.

Randolt, K., Gimple, O., Geissendörfer, J., Reinders, J., Prusko, C., Mueller, M. J., ... & Beier, H. (2008). Immune-related proteins induced in the hemolymph after aseptic and septic injury differ in honey bee worker larvae and adults. *Archives of insect biochemistry and physiology*, *69*(4), 155-167.

Rodriguez-Andres, J., Rani, S., Varjak, M., Chase-Topping, M. E., Beck, M. H., Ferguson, M. C., ... & Fazakerley, J. K. (2012). Phenoloxidase activity acts as a mosquito innate immune response against infection with Semliki Forest virus. *PLoS Pathog*, *8*(11), e1002977.

Sandiford, S. L., Dong, Y., Pike, A., Blumberg, B. J., Bahia, A. C., & Dimopoulos, G. (2015). Cytoplasmic actin is an extracellular insect immune factor which is secreted upon immune challenge and mediates phagocytosis and direct killing of bacteria, and is a Plasmodium antagonist. *PLoS Pathog*, *11*(2), e1004631.

Scharlaken, B., De Graaf, D. C., Memmi, S., Devreese, B., Van Beeumen, J., & Jacobs, F. J. (2007). Differential protein expression in the honey bee head after a bacterial challenge. *Archives of insect biochemistry and physiology*, *65*(4), 223-237.

Schwanhäusser, B., Busse, D., Li, N., Dittmar, G., Schuchhardt, J., Wolf, J., ... & Selbach, M. (2011). Global quantification of mammalian gene expression control. *Nature*, *473*(7347), 337-342.

Sies, H. (1997). Oxidative stress: oxidants and antioxidants. *Experimental physiology*, *82*(2), 291-295.

Taft, A. S., Chen, C. C., Li, J., & Christensen, B. M. (2001). Molecular cloning of two prophenoloxidase genes from the mosquito *Aedes aegypti*. *Insect molecular biology*, *10*(1), 97-103.

Thompson, G. J., Crozier, Y. C., & Crozier, R. H. (2003). Isolation and characterization of a termite transferrin gene up-regulated on infection. *Insect molecular biology*, *12*(1), 1-7.

Thorne, K. J., Oliver, R. C., & Barrett, A. J. (1976). Lysis and killing of bacteria by lysosomal proteinases. *Infection and Immunity*, *14*(2), 555-563.

Vierstraete, E., Cerstiaens, A., Baggerman, G., Van den Bergh, G., De Loof, A., & Schoofs, L. (2003). Proteomics in *Drosophila melanogaster*: first 2D database of larval hemolymph proteins. *Biochemical and biophysical research communications*, *304*(4), 831-838.

Vierstraete, E., Verleyen, P., Baggerman, G., D'Hertog, W., Van den Bergh, G., Arckens, L., ... & Schoofs, L. (2004). A proteomic approach for the analysis of instantly released wound and immune proteins in *Drosophila melanogaster* hemolymph. *Proceedings of the National Academy of Sciences of the United States of America*, *101*(2), 470-475.

Wang, D., Kim, B. Y., Lee, K. S., Yoon, H. J., Cui, Z., Lu, W., ... & Jin, B. R. (2009). Molecular characterization of iron binding proteins, transferrin and ferritin heavy chain subunit, from the bumblebee *Bombus ignitus*. *Comparative Biochemistry and Physiology Part B: Biochemistry and Molecular Biology*, *152*(1), 20-27.

Wang, W. X., Wang, Y. P., Deng, X. J., Dang, X. L., Tian, J. H., Yi, H. Y., ... & Lai, R. (2009). Molecular and functional characterization of a c-type lysozyme from the Asian corn borer, Ostrinia furnacalis. *Journal of insect science*, *9*(17), 1-13.

Woltedji, D., Fang, Y., Han, B., Feng, M., Li, R., Lu, X., & Li, J. (2013). Proteome analysis of hemolymph changes during the larval to pupal development stages of honeybee workers (Apis mellifera ligustica). *Journal of proteome research*, *12*(11), 5189-5198.

Yu, K. H., Kim, K. N., Lee, J. H., Lee, H. S., Kim, S. H., Cho, K. Y., ... & Lee, I. H. (2002). Comparative study on characteristics of lysozymes from the hemolymph of three lepidopteran larvae, Galleria mellonella, Bombyx mori, Agrius convolvuli. *Developmental & Comparative Immunology*, *26*(8), 707-713.

Yun, E. Y., Kang, S. W., Hwang, J. S., Goo, T. W., Kim, S. H., Jin, B. R., ... & Kim, K. Y. (1999). Molecular cloning and characterization of a cDNA encoding a transferrin homolog from *Bombyx mori*. *Biological chemistry*, *380*(12), 1455-1459.

Yoshiga, T., Georgieva, T., Dunkov, B. C., Harizanova, N., Ralchev, K., & Law, J. H. (1999). *Drosophila melanogaster* transferrin. *European journal of biochemistry*, *260*(2), 414-420.

Zdybicka-Barabas, A., & Cytryńska, M. (2011). Involvement of apolipophorin III in antibacterial defense of *Galleria mellonella* larvae. *Comparative Biochemistry and Physiology Part B: Biochemistry and Molecular Biology*, *158*(1), 90-98.

Zeng, Y., Hu, X. P., & Suh, S. J. (2016). Characterization of Antibacterial Activities of Eastern Subterranean Termite, *Reticulitermes flavipes*, against Human Pathogens. *PloS one*, *11*(9), e0162249.

Zhang, Y., Dong, Z., Wang, D., Wu, Y., Song, Q., Gu, P., ... & Xia, Q. (2014). Proteomics of larval hemolymph in *Bombyx mori* reveals various nutrient-storage and immunity-related proteins. *Amino acids*, *46*(4), 1021-1031.

Zug, R., & Hammerstein, P. (2015). Wolbachia and the insect immune system: what reactive oxygen species can tell us about the mechanisms of Wolbachia–host interactions. *Frontiers in microbiology*, *6*, 1201.

Supplementary Data

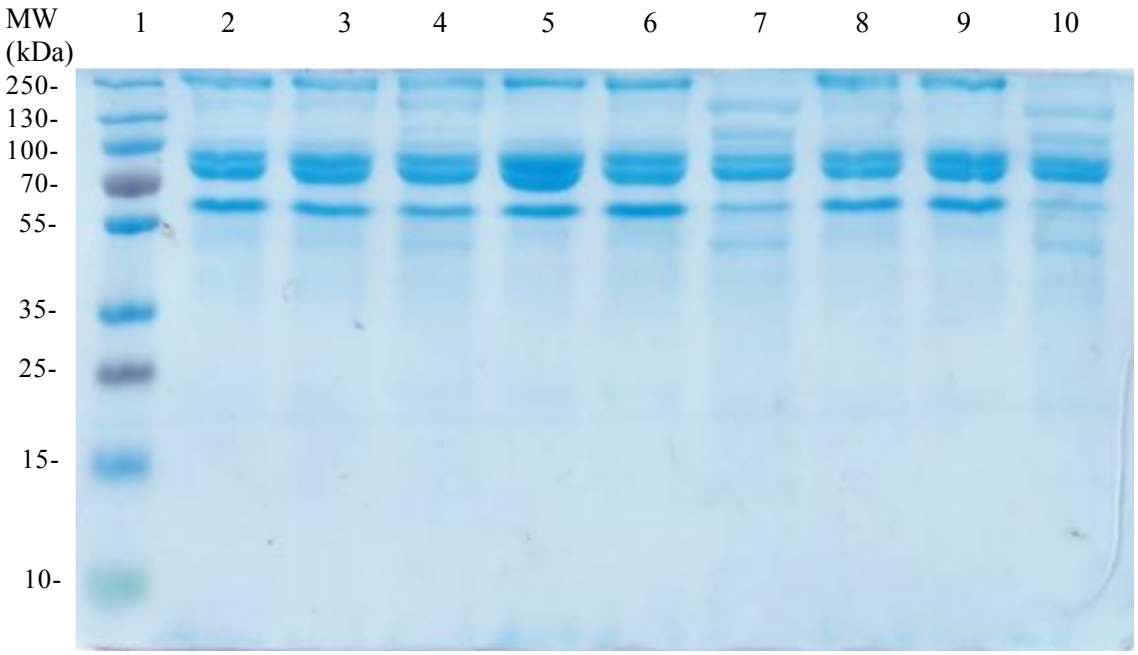

Supplementary Figure 4.1 8% SDS-PAGE analysis of hemolymph proteins. Lane 1: Protein Ladder (10–250 kDa); Lanes 2–4: The collection of hemolymph proteins from naïve, MRSA-challenged, and *P. aeruginosa*-challenged termites, respectively. Lanes 5-7: The second collection of hemolymph proteins from naïve, MRSA-challenged, and *P. aeruginosa*-challenged termites, respectively. Lanes 8-10: The third collection of hemolymph proteins from naïve, MRSA-challenged, and *P. aeruginosa*-challenged termites, respectively.

Supplementary Table 4.1 Identified proteins from hemolymph of naïve and MDR challenged *R. flavipes*.

Cluster	Protein	Accession Number	Molecular Weight (Da)	Identification Probability (%)	sequence coverage (%)
1	Actin	AGM32156.1	41,702.80	100.00	24.00
2	beta tubulin-3	AGM32401.1	24,144.70	100.00	28.60
3	Cluster of hypothetical protein L798_09047	KDR17045.1 [3]			
	hypothetical protein L798_09047	KDR17045.1	28,209.70	44.10	6.90
	Regucalcin [*Zootermopsis nevadensis*]	KDR12743.1			
	Regucalcin, partial [*Zootermopsis nevadensis*]	KDR17044.1			
4	Transferrin	AAQ62963.2	80,051.90	47.20	0.00
5	Calponin-likey domain containing protein	AGM32561.1	20,466.70	49.80	0.00
6	Cluster of endogenous cellulase	AAU20853.2 [11]			
	endogenous cellulase	AAU20853.2	48,676.70	100.00	42.90
	endo-beta-1,4-glucanase	AGP76416.1	48,857.10	63.40	5.36
	cellulase	AAK12339.1	48,794.10	29.40	0.00
	endoglucanase	AFD33365.1	49,090.80	48.10	6.70
	endo-beta-1,4-glucanase	ADB12483.1	49,036.70	33.70	0.00
	Chain A, the structure of endoglucanase from termite at pH 6.5.	gi|28373493|pdb|1KSD|A	47,802.80	8.40	2.31
	glycoside hydrolase family 9	AMH40362.1			
	glycoside hydrolase family 9	AMH40364.1			
	endo-beta-1,4-glucanase, partial	BAD66681.1	13,310.80	5.10	53.20
	glycoside hydrolase family 9	AMH40359.1			
	putative endo-beta-1,4-glucanase NtEG2, partial	BAD12011.1			
7	ferritin, heavy subunit	AGM32344.1	24,920.70	100.00	32.90

8	Cluster of Retinal dehydrogenase 2	KDR10336.1 [2]			
	Retinal dehydrogenase 2	KDR10336.1	52,505.00	100.00	24.60
	aldehyde dehydrogenase-like protein, partial	AGM32641.1	30,168.80	100.00	33.30
9	Papilin	KDR22055.1	259,145.20	100.00	4.42
10	Cluster of Plasma alpha-L-fucosidase	KDR21959.1 [7]			
	Plasma alpha-L-fucosidase	KDR21959.1	55,103.00	100.00	15.10
	PREDICTED: plasma alpha-L-fucosidase-like	XP_015122125.1	54,060.50	41.30	1.50
	Alpha-L-fucosidase	EZA56254.1			
	PREDICTED: plasma alpha-L-fucosidase-like	XP_015122125.1	54,060.50	41.30	1.50
	PREDICTED: alpha-L-fucosidase-like	XP_014273318.1			
	unknown	AEE62189.1			
11	Cluster of hypothetical protein L798_11509	KDR14754.1 [2]			
	hypothetical protein L798_11509	KDR14754.1	61,206.50	100.00	8.00
	PREDICTED: uncharacterized protein LOC107162408	XP_015364774.1			
12	Cluster of beta-glucosidase, partial	BAO85044.1 [4]			
	beta-glucosidase, partial	BAO85044.1	34,400.40	25.80	3.00
	beta-glucosidase, partial	AGM32287.1	32,982.60	44.70	3.12
	beta-glucosidase	ADD92156.1	54,269.80	19.10	1.91
	beta-glucosidase	AEW67361.1	54,821.10	54.10	1.89
13	Beta-ureidopropionase	KDR12152.1	44,048.10	100.00	7.22
14	hypothetical protein L798_00618, partial	KDR22779.1	125,889.00	99.40	1.17
15	Cluster of glutathione S-transferase	AFZ78680.1 [6]			
	glutathione S-transferase	AFZ78680.1	27,599.30	99.90	4.60
	Glutathione S-transferase omega-2	KDR22869.1	27,937.90	99.50	7.53
	PREDICTED: pyrimidodiazepine synthase-like	XP_015366984.1			
	PREDICTED: pyrimidodiazepine synthase-like	XP_014274047.1			
	PREDICTED: pyrimidodiazepine synthase-like	XP_014273825.1			

16	lipocalin / cytosolic fatty-acid binding protein	AGM32122.1	14,752.30	100.00	19.10
17	Cluster of Glycogen phosphorylase	EZA48982.1 [9]			
	Glycogen phosphorylase	EZA48982.1	97,169.30	92.90	3.08
	PREDICTED: glycogen phosphorylase	XP_014091031.1	97,412.10	16.60	1.42
	PREDICTED: glycogen phosphorylase	XP_014292615.1	97,236.20	43.70	1.42
	PREDICTED: glycogen phosphorylase isoform X1	XP_015375987.1 (+1)			
	glycogen phosphorylase	AFO54708.2	96,494.00	33.50	1.43
	muscle glycogen phosphorylase	NP_001116811.1	96,456.40	8.60	2.50
	PREDICTED: glycogen phosphorylase	XP_015120639.1			
	glycogen phosphorylase, partial	AGC97435.1			
18	Apolipophorin, partial	KDR18107.1	464,485.60	100.00	0.93
19	Cluster of sorbitol dehydrogenase, partial	AHZ00204.1 [6]			
	Sorbitol dehydrogenase	KDR24482.1	33,932.30	100.00	9.69
	PREDICTED: sorbitol dehydrogenase-like	XP_014289176.1			
	sorbitol dehydrogenase, partial	AHZ00204.1			
	sorbitol dehydrogenase	NP_001037592.1			
	PREDICTED: sorbitol dehydrogenase-like	XP_015371890.1			
	Sorbitol dehydrogenase	EZA47058.1			
20	Cluster of peptidyl-prolyl cis-trans isomerase	AGM32516.1 [3]			
	peptidyl-prolyl cis-trans isomerase	AGM32516.1	22,450.00	100.00	26.20
	PREDICTED: peptidyl-prolyl cis-trans isomerase	XP_014278363.1	17,964.20	27.30	9.09
	Peptidyl-prolyl cis-trans isomerase	KDR15281.1	22,269.20	7.70	4.37
21	Cluster of Multifunctional protein ADE2, partial	KDR09851.1 [6]			
	Multifunctional protein ADE2, partial	KDR09851.1	46,639.90	9.40	0.00
	Multifunctional protein ADE2	EZA56375.1			

	Chain D, Crystal Structure Of The Invertebrate Bi-functional Purine Biosynthesis Enzyme	gi|453056256|pdb|4JA0|D			
	unknown	AEE61839.1			
	PREDICTED: multifunctional protein ADE2	XP_014101019.1			
	PREDICTED: multifunctional protein ADE2	XP_014270656.1			
22	Cluster of Protein lethal(2)essential for life	KDR22815.1 [2]			
	Protein lethal(2)essential for life	KDR22815.1	24,347.10	100.00	14.40
	PREDICTED: heat shock protein Hsp-12.2	XP_014288127.1			
23	hypothetical protein L798_01615	KDR07960.1	74,182.40	45.30	0.00
24	Cluster of SCP-like extracellular domain containing protein 2	AGM32430.1 [2]			
	SCP-like extracellular domain containing protein 2	AGM32430.1	26,032.30	100.00	18.40
	Venom allergen 3	KDR14384.1			
25	putative chemosensory protein	BAU20278.1	16,438.50	99.90	16.80
26	putative phosphoserine aminotransferase	KDR19432.1	40,638.50	99.40	2.96
27	Cluster of uncharacterized protein	AGM32706.1 [2]			
	uncharacterized protein	AGM32706.1	18,969.00	100.00	16.30
	Cytosolic carboxypeptidase-like protein 5	KDR22169.1			
28	Protein yellow	KDR22429.1	48,684.60	100.00	4.24
29	PREDICTED: bifunctional purine biosynthesis protein PURH	XP_015365809.1	64,894.10	99.50	3.72
30	Cluster of hexamerin I	AAU20851.2 [24]			
	hemocyanin-like protein	AIO11839.1	81,874.00	100.00	15.00
	hexamerin I	AAU20851.2	87,664.40	100.00	68.60
	hexamerin II	AAU20852.2	86,895.50	100.00	57.40
	RecName: Full=Allergen Cr-PI	Q25641.1	81,176.50	100.00	6.57
	hypothetical protein L798_01880	KDR21644.1	91,079.50	99.90	13.60

	hexamarin-2, partial	ADX66726.1	50,098.20	59.10	28.60
	Hexamerin	EZA60531.1			
	allergen, partial	AAB63595.1	46,747.80	23.90	6.62
	VHDL receptor	AAR32136.1	89,796.40	60.30	1.20
	basic juvenile hormone sensitive hemolymph protein two	AAA27883.1 (+1)	89,693.90	11.40	1.20
	hexamerin 3, partial	CAM84198.1	66,674.40	10.20	0.00
	cyanoprotein alpha subunit precursor	BAA13323.1	80,049.10	12.20	0.00
	PREDICTED: arylphorin subunit alpha-like	XP_015112084.1			
	hypothetical protein L798_01877	KDR21642.1			
	hexamerine	AAT76805.1			
	cyanoprotein alpha subunit precursor	BAA13323.1			
	Arylphorin subunit alpha	EZA60532.1			
	unknown	AEE63239.1	85,738.00	81.10	1.24
	allergen, partial	AAB09632.1	75,514.00	12.90	5.39
	allergen, partial	AAB62731.1	56,190.00	5.50	5.53
	Chain D, Crystal Structure Of Antheraea Pernyi Arylphorin	gi|229597916|pdb|3GWJ|D	80,415.80	5.10	0.00
	unknown	AEE63608.1	85,029.70	6.10	1.26
	86 kDa early-staged encapsulation inducing protein	BAA81665.2	90,626.10	48.80	1.19
31	Cluster of Apolipophorin	KDR17854.1 [3]			
	Apolipophorin	KDR17854.1	378,583.70	100.00	11.90
	apolipophorin-like protein	AFZ78833.1	17,730.40	100.00	59.00
	Phosphatidylinositol 3-kinase regulatory subunit alpha	KDR18118.1			
32	Cluster of Transferrin	KDR19744.1 [5]			
	Transferrin	KDR19744.1	80,060.20	100.00	21.30

	transferrin	AAN03488.1	79,979.30	100.00	13.50
	PREDICTED: transferrin	XP_015109887.1	77,392.30	99.70	2.84
	Transferrin	EZA53240.1			
	transferrin	BAQ94504.1			
33	Cluster of Chain W, Molecular Models Of Averaged Rigor Crossbridges From Tomograms Of Insect Flight Muscle	gi|27066064|pdb|1O18|W [15]			
	Chain W, Molecular Models Of Averaged Rigor Crossbridges From Tomograms Of Insect Flight Muscle	gi|27066064|pdb|1O18|W (+1)	41,817.90	100.00	35.50
	Actin-5C	EZA56475.1	41,822.70	88.40	27.90
	PREDICTED: actin, clone 403-like	XP_014286815.1	41,803.80	94.90	16.80
	actin, partial	AMR43732.1	34,740.10	90.90	35.40
	PREDICTED: actin-5, muscle-specific	XP_014093464.1	41,769.70	73.80	29.50
	Actin, clone 403	KDR17904.1	41,854.80	99.90	43.60
	PREDICTED: actin-42A-like	XP_015369527.1	41,824.50	98.90	35.40
	unknown	AEE61657.1	41,777.80	99.60	37.00
	actin 5c, partial	ACO60321.1	30,679.30	60.00	44.20
	PREDICTED: actin, indirect flight muscle	XP_014087796.1	41,700.90	57.20	26.30
	putative beta-actin, partial	ADZ52965.1	21,374.20	80.80	42.90
	muscle-specific actin 3	AAQ24507.1	41,676.50	58.90	26.30
	PREDICTED: LOW QUALITY PROTEIN: actin-like	XP_015116371.1	31,369.00	31.90	43.50
	actin	AAA02814.1	41,777.80	12.90	43.90
34	Cluster of hypothetical protein L798_04756, partial	KDR20892.1 [20]			
	hypothetical protein L798_04756, partial	KDR20892.1	40,104.80	100.00	36.20
	arginine kinase 1	CAZ65719.1	39,990.30	100.00	29.60
	arginine kinase	ANJ04641.1	40,029.70	77.60	21.90

	arginine kinase, partial (mitochondrion)	ALS08437.1	25,837.50	99.90	26.20
	arginine kinase, partial (mitochondrion)	ALS08389.1	25,823.40	11.00	20.50
	arginine kinase	ADF31833.1	39,746.20	100.00	18.60
	arginine kinase 2	CAZ65717.1	41,911.70	17.70	8.87
	arginine kinase	NP_001037402.1	39,992.50	15.30	7.32
	PREDICTED: arginine kinase isoform X1	XP_015121223.1	41,648.70	18.20	9.12
	arginine kinase, partial (mitochondrion)	ALS08471.1	25,826.60	10.90	14.80
	Arginine kinase	EZA47168.1	41,625.30	14.00	12.00
	arginine kinase, partial (mitochondrion)	ALS08443.1	25,721.30	29.70	20.10
	arginine kinase, partial (mitochondrion)	ALS08481.1	25,724.30	14.50	14.80
	unknown	AEE62891.1	40,054.70	14.70	13.00
	arginine kinase, partial (mitochondrion)	ALS08439.1 (+1)	25,666.10	7.70	20.50
	arginine kinase, partial (mitochondrion)	ALS08358.1	25,741.30	36.00	14.80
	arginine kinase, partial (mitochondrion)	ALS08382.1	25,606.40	11.20	3.93
	arginine kinase 2, partial	CAZ65716.1	29,122.40	5.40	14.80
	arginine kinase, partial (mitochondrion)	ALS08393.1			
35	Cluster of catalase	AFV36369.1 [9]			
	catalase	NP_001036912.1	56,900.60	82.70	2.96
	catalase	AFV36369.1	57,571.80	100.00	27.60
	Catalase	KDR21530.1	57,880.60	71.90	14.20
	catalase	AFC98367.1	56,765.90	63.00	5.92
	Catalase	KDR07976.1			
	Catalase	EZA54346.1	57,918.10	8.70	0.00
	catalase	AFG31725.1	56,874.40	18.70	5.13
	catalase, partial	ABE28534.1	25,096.50	99.70	10.70
	PREDICTED: catalase	XP_015364010.1	56,941.10	10.80	11.10
36	Cluster of PREDICTED: tubulin beta-4B chain-like	XP_015122701.1 [19]			

	PREDICTED: tubulin beta-4B chain	XP_014290748.1	30,344.00	41.70	22.50
	PREDICTED: tubulin beta-1 chain-like isoform X1	XP_014275235.1 (+1)	50,250.70	24.30	27.00
	PREDICTED: tubulin beta chain-like isoform X1	XP_014294309.1 (+1)	51,091.40	11.10	8.81
	PREDICTED: tubulin beta chain-like	XP_015122755.1	50,139.60	35.80	15.40
	PREDICTED: tubulin beta-4B chain-like	XP_015122701.1	49,845.00	100.00	22.20
	PREDICTED: tubulin beta chain-like	XP_014286016.1	51,038.50	99.90	11.30
	PREDICTED: tubulin beta chain-like	XP_015118401.1	49,566.10	75.00	13.00
	Tubulin beta-3 chain	EZA57340.1 (+1)	51,113.40	67.60	13.20
	PREDICTED: tubulin beta chain-like	XP_015120506.1			
	PREDICTED: tubulin beta chain-like	XP_014278577.1	50,029.00	80.70	4.70
	PREDICTED: tubulin beta chain	XP_014090445.1	51,257.20	45.80	5.92
	PREDICTED: tubulin beta chain-like	XP_014271954.1	49,564.60	11.70	2.70
	beta-tubulin	NP_001036888.1	51,353.70	69.10	19.30
	putative beta-tubulin, partial	AGM32580.1	30,868.50	53.90	21.10
	PREDICTED: tubulin beta chain-like	XP_015372097.1	49,721.80	37.60	10.60
	beta-tubulin, partial	AIW65077.1	28,967.80	68.00	20.20
37	Cluster of alpha tubulin, partial	AGM32279.1 [13]			
	alpha tubulin, partial	AGM32279.1	33,342.00	100.00	14.60
	Tubulin alpha chain, testis-specific	KDR23449.1	50,109.30	99.80	10.00
	PREDICTED: tubulin alpha chain, testis-specific-like	XP_015376239.1	51,965.90	91.20	11.60
	Tubulin alpha-1 chain	KDR15366.1	50,010.60	99.90	24.40
	alpha-tubulin	NP_001036885.1	50,079.40	41.60	18.00
	Tubulin alpha-3 chain	EZA62520.1	49,966.00	47.60	7.19
	unknown	AEE61427.1	49,820.30	83.00	22.90
	Tubulin alpha-1C chain	KDR07532.1	48,675.40	13.70	7.62

	Tubulin alpha-3 chain	KDQ71495.1 (+1)	49,284.60	64.90	5.47
	Tubulin alpha-1 chain	KDR02444.1	52,463.10	46.80	13.60
	PREDICTED: tubulin alpha chain-like isoform X1	XP_015123831.1 (+1)	51,600.40	24.20	8.97
38	Cluster of phenoloxidase 2, partial	AHB39936.1 [8]			
	phenoloxidase 2, partial	AHB39936.1	79,529.40	100.00	7.78
	Phenoloxidase subunit A3	KDR18501.1	79,605.50	99.80	5.04
	hexamerin 2 precursor, partial	AGR40412.1	53,136.20	42.10	0.00
	hexamerin 4, partial	CAM84199.1	71,837.80	99.30	3.50
	hexamerin 1	CAM84196.1	82,524.40	83.60	2.42
	PREDICTED: phenoloxidase 2-like	XP_014277062.1			
	PREDICTED: phenoloxidase 2-like	XP_015378845.1			
	PREDICTED: phenoloxidase 2-like	XP_014276959.1			
39	Cluster of aldo-keto reductase	AFV36370.1 [7]			
	PREDICTED: aldose reductase-like	XP_014287922.1			
	aldo-keto reductase	AFV36370.1	37,900.20	100.00	43.30
	Aldo-keto reductase family 1 member B10	KDR07716.1	36,268.60	99.80	19.10
	hypothetical protein L798_00664, partial	KDR09443.1			
	unknown	AEE63226.1			
	PREDICTED: aldose reductase-like	XP_015121681.1			
	Aldo-keto reductase family 1 member B10	EZA59353.1	35,666.10	6.20	5.99
40	apolipophorin-III isoform 2	AFZ78835.1	21,771.80	100.00	14.80
41	Cluster of PREDICTED: heat shock 70 kDa protein cognate 2 isoform X1	XP_014089864.1 [41]			
	PREDICTED: heat shock 70 kDa protein cognate 2 isoform X1	XP_014089864.1	103,651.80	86.40	3.38
	Heat shock 70 kDa protein cognate 3	KDR23518.1	72,375.50	37.70	2.44
	heat shock protein 70	AHE77377.1	71,223.50	99.90	7.07
	chaperone dnaK	EZO35528.1			
	heat shock protein 70	AGE92595.1	69,823.30	99.20	4.57

Heat shock 70 kDa protein cognate 4	KDR23254.1	42,600.30	99.90	17.80
heat shock protein 70A	ACD63050.1	70,698.80	13.00	2.35
Heat shock protein 70 A1	KDR08926.1	69,455.50	52.50	1.74
PREDICTED: heat shock-related 70 kDa protein 2-like	XP_014274983.1	70,868.40	32.40	4.16
Heat shock 70 kDa protein cognate	EZA53141.1			
PREDICTED: heat shock-related 70 kDa protein 2-like	XP_014274983.1			
heat shock protein 70	ABL06948.1	70,251.20	9.60	0.00
PREDICTED: heat shock 70 kDa protein cognate 4 [	XP_015366002.1	72,389.30	6.90	2.41
PREDICTED: heat shock protein 70 B2-like	XP_015117241.1	69,161.00	52.30	2.54
heat shock protein 70	ADE05296.1 (+1)	71,244.70	54.70	8.74
PREDICTED: heat shock protein 68-like	XP_014272950.1	69,862.20	28.80	0.00
hsp70 family member, partial	AAO21473.1	71,410.80	41.10	1.53
heat shock protein 70, partial	AHE77387.1	70,192.80	26.70	4.37
heat shock protein 70	AGF34717.1			
CRE-HSP-3 protein	XP_003117830.1			
PREDICTED: heat shock protein 70 A1-like	XP_015372059.1			
heat shock inducible HSP70, partial	AGM39425.1	15,842.80	5.30	8.57
Heat shock 70 kDa protein cognate	EZA48451.1	70,241.50	48.90	4.21
PREDICTED: heat shock 70 kDa protein cognate 1	XP_014088467.1			
heat shock inducible HSP70, partial	AGM39425.1			
PREDICTED: major heat shock 70 kDa protein Ba-like isoform X1	XP_014293117.1	70,038.90	46.30	4.27
unknown	AEE62651.1	70,148.80	84.60	2.50
heat shock cognate 70 protein	ACO57618.1	70,917.50	73.80	2.03
inducible heat shock 70 kDa protein, partial	AAG42838.1			
heat shock protein 70	AGF34718.1	71,196.60	6.50	6.76

	PREDICTED: heat shock 70 kDa protein cognate 2-like	XP_014275032.1	68,312.40	66.70	2.57
	PREDICTED: heat shock protein 70-like	XP_014089050.1			
	PREDICTED: heat shock protein 68-like	XP_015373896.1			
	heat shock cognate 70 protein	ACA53150.1	71,284.60	12.00	7.02
	heat shock protein 70a	AHA36968.1	71,103.50	8.50	4.17
	PREDICTED: heat shock protein 70 B2-like	XP_015371967.1	68,377.50	13.10	4.33
	PREDICTED: major heat shock 70 kDa protein Ba-like	XP_014289183.1	70,089.90	13.30	4.27
	heat shock protein 70	AHE77386.1			
	inducible heat shock 70 kDa protein, partial	AAG01177.2			
	heat shock protein 70, partial	ACD63048.1			
42	PREDICTED: LOW QUALITY PROTEIN: uncharacterized protein LOC106621780, partial	XP_014096235.1	2,067,529.10	76.30	0.00
43	Cluster of gram-negative bacteria binding protein 1, partial	AEK64796.1 [3]	41,501.80	100.00	11.90
	gram-negative bacteria binding protein 1, partial	AEK64796.1	41,501.80	100.00	27.00
	gram negative bacteria binding protein 1	AAZ08487.1	42,588.40	11.60	11.60
	gram negative bacteria binding protein 1	AAZ08490.1			
44	Cluster of PREDICTED: laminin subunit beta-1	XP_010173980.1 [20]			
	PREDICTED: laminin subunit beta-1	XP_010173980.1			
	PREDICTED: laminin subunit beta-1, partial	XP_014427649.1			
	Laminin subunit beta-1, partial	KFQ37544.1 (+1)			
	Laminin subunit beta-1	EMP30347.1 (+1)	200,419.40	32.70	0.00
	PREDICTED: LOW QUALITY PROTEIN: laminin subunit beta-1	XP_005010332.1			
	Laminin subunit beta-1, partial	KFO88248.1 (+1)			
	PREDICTED: laminin subunit beta-1	XP_005292397.1	198,140.90	34.80	0.00

	PREDICTED: LOW QUALITY PROTEIN: laminin subunit beta-1	XP_009982860.1			
	PREDICTED: laminin subunit beta-1	XP_009634373.1			
	PREDICTED: laminin subunit beta-1	XP_005292397.1			
	PREDICTED: laminin subunit beta-1	XP_010720462.1			
	PREDICTED: laminin subunit beta-1	XP_005498160.1			
	Laminin subunit beta-1, partial	KGL97946.1 (+1)			
	PREDICTED: laminin subunit beta-1	XP_013801983.1			
	PREDICTED: laminin subunit beta-1	XP_011570080.1			
	PREDICTED: laminin subunit beta-1	XP_009664293.1			
45	Gelsolin, cytoplasmic, partial	KDR14655.1	74,144.10	100.00	3.93
46	PREDICTED: uncharacterized protein LOC106678290 isoform X3	XP_014272203.1	1,373,149.40	99.90	0.00
47	Cluster of putative fructose 1,6-bisphosphate aldolase	AAT01078.1 [9]			
	fructose 1,6-bisphosphate aldolase	NP_001091766.1			
	putative fructose 1,6-bisphosphate aldolase	AAU84937.1 (+1)			
	putative fructose 1,6-bisphosphate aldolase	AAT01078.1 (+1)	39,700.90	100.00	26.90
	unknown	AEE62864.1			
	PREDICTED: fructose-bisphosphate aldolase-like	XP_014088227.1	39,954.80	43.90	7.44
	PREDICTED: fructose-bisphosphate aldolase	XP_014085563.1	39,554.50	6.80	3.30
	Chain A, The Crystal Structure Of Fructose-1,6-Bisphosphate Aldolase From Drosophila Melanogaster At 2.5 Angstroms Resolution	gi|253722156|pdb|1FBA|A	39,027.90	6.10	5.26
48	Cluster of enolase] (AGM32397.1)	AGM32397.1 [10]	47,107.00	97.80	6.47
49	Cluster of Laminin subunit alpha-3, partial	KFO61539.1 [9]			
	Laminin subunit alpha-3, partial	KFO61539.1	360,634.60	50.00	0.00
	PREDICTED: laminin subunit alpha-3	XP_014167454.1			
	PREDICTED: laminin subunit alpha-3	XP_008926621.1			

	PREDICTED: laminin subunit alpha-3	XP_009665364.1			
	PREDICTED: laminin subunit alpha-3	XP_009088176.1			
	PREDICTED: laminin subunit alpha-3	XP_012427366.1			
	PREDICTED: laminin subunit alpha-3	XP_014108844.1			
	PREDICTED: laminin subunit alpha-3	XP_014125097.1			
	PREDICTED: laminin subunit alpha-3 isoform X1	XP_014426018.1			
50	Cluster of Transketolase	KDR18110.1 [7]			
	PREDICTED: transketolase-like	XP_014099875.1	71,136.40	50.40	3.36
	Transketolase	KDR18110.1	68,071.90	100.00	9.58
	PREDICTED: transketolase-like protein 2 isoform X1	XP_015111220.1 (+1)			
	PREDICTED: transketolase-like protein 2	XP_015373572.1	67,488.00	88.40	2.08
	transketolase	NP_001040158.1	67,385.30	14.00	2.09
	PREDICTED: transketolase-like protein 2	XP_014090115.1			
51	Cluster of elongation factor 1-alpha	AGO46411.1 [27]			
	elongation factor 1-alpha	AGO46411.1	50,630.70	80.20	2.60
	elongation factor 1-alpha, partial	ABW99004.1			
	elongation factor 1-alpha, partial	ABW98970.1			
	elongation factor 1-alpha (EF1-alpha) protein	AGM32604.1			
	elongation factor 1 alpha, partial	ACY74331.1	38,315.00	12.60	8.76
	elongation factor 1-alpha, partial	AHW84463.1	40,466.70	16.40	9.73
	elongation factor 1-alpha, partial	ABW99000.1 (+1)			
	elongation factor 1 alpha, partial	ACB71693.1			
	elongation factor 1-alpha, partial	ALS09030.1			
	elongation factor 1 alpha, partial	ACB87164.1	10,849.20	99.70	18.80
	elongation factor 1 alpha, partial	ACB71691.1 (+3)	17,485.80	55.50	19.10
	elongation factor 1 alpha, partial	ADM15740.1	25,271.90	12.50	9.36

	elongation factor 1 alpha, partial	ADM15729.1	25,370.00	45.10	13.20
	elongation factor 1 alpha, partial	ACB87167.1			
	elongation factor 1-alpha, partial	ADK90452.1			
	elongation factor 1 alpha, partial	AHH31040.1			
	elongation factor 1 alpha, partial	ACB87169.1			
	elongation factor 1-alpha, partial	ABW99030.1			
	elongation factor-1 alpha, partial	AAF89857.1	36,226.10	8.70	8.76
	elongation factor-1 alpha, partial	AAF89848.1			
	elongation factor 1 alpha, partial	ADM15835.1			
	elongation factor 1 alpha, partial	ADM15728.1	23,522.90	7.60	13.50
	elongation factor 1 alpha, partial	ADM15767.1			
52	PREDICTED: zinc finger protein 594-like	XP_014270891.1-DECOY	0	41.70	0.00
53	Cluster of putative odorant-binding protein	BAU20271.1 [4]			
	putative odorant-binding protein	BAU20271.1	22,371.00	100.00	21.60
	PREDICTED: protein D3	XP_014086915.1			
	PREDICTED: protein D3-like	XP_015368042.1			
	Phosphatidylethanolamine-binding protein 1	KDR14299.1			
54	Cluster of glutathione-S-transferase	AGO46413.1 [4]			
	glutathione-S-transferase	AGO46413.1	24,719.00	100.00	28.70
	glutathione s-transferase D2	AFJ75818.1			
	glutathione s-transferase D2	AFJ75802.1			
	Glutathione S-transferase 1-1	KDR11943.1			
55	Cluster of 14-3-3 protein zeta	KDR15025.1 [9]			
	14-3-3 protein zeta	KDR15025.1 (+1)	28,174.30	100.00	22.40
	14-3-3 epsilon, partial	BAI66121.1			
	14-3-3 protein epsilon	ANJ04668.1	29,189.90	6.60	0.00
	PREDICTED: 14-3-3 protein epsilon	XP_014279405.1	29,127.90	99.80	4.30

	PREDICTED: 14-3-3 protein zeta isoform X1	XP_015380501.1 (+1)	28,166.30	13.70	7.29
	PREDICTED: 14-3-3 protein epsilon	XP_015377637.1			
	PREDICTED: 14-3-3 protein zeta isoform X2	XP_014287713.1			
56	Cluster of heat shock protein 90	ABW87791.1 [15]			
	hsp90	AMA66329.1 (+1)	81,807.00	12.10	4.06
	heat shock protein 90	ABW87791.1	82,652.10	99.70	3.48
	Heat shock protein 83	KDR11182.1	83,425.20	99.80	5.37
	heat shock protein 90	AGF34719.1	83,206.80	5.20	1.94
	heat shock protein 82	AAB05639.1	82,157.20	8.50	1.94
	heat shock 90 kDa protein	AHB18587.1	82,089.90	21.70	1.95
	heat shock protein 90	ACO57617.1	82,162.60	89.60	5.45
	unknown	AEE61673.1	81,305.30	90.10	3.67
	heat shock protein 90	AHE77376.1	82,123.70	12.70	3.63
	heat shock protein 90, partial	ABF01016.1			
	PREDICTED: heat shock protein 83	XP_015111241.1	82,600.60	6.80	3.34
	Heat shock protein HSP 90-alpha	EZA50089.1			
	PREDICTED: heat shock protein 83	XP_014284945.1			
	PREDICTED: heat shock protein 83	XP_015371422.1			
57	ferritin-like precursor, partial	AGM32322.1	23,487.20	100.00	20.50
58	Ferritin subunit	KDR16113.1	24,804.80	100.00	7.34
59	Cluster of glyceraldehyde-3-phosphate dehydrogenase	AGO46412.1 [5]			
	glyceraldehyde-3-phosphate dehydrogenase	AGO46412.1	35,425.00	91.60	6.63
	Glyceraldehyde-3-phosphate dehydrogenase	KDR24072.1	35,583.80	45.20	6.63
	PREDICTED: glyceraldehyde-3-phosphate dehydrogenase 2	XP_014085420.1			
	PREDICTED: glyceraldehyde-3-phosphate dehydrogenase 2-like	XP_014094245.1			

	PREDICTED: glyceraldehyde-3-phosphate dehydrogenase 2	XP_014089453.1			
60	Cluster of PREDICTED: moesin/ezrin/radixin homolog 1 isoform X2	XP_014102416.1 [14]			
	PREDICTED: moesin/ezrin/radixin homolog 1 isoform X2	XP_014102416.1	73,808.70	99.50	1.44
	PREDICTED: moesin/ezrin/radixin homolog 1 isoform X1	XP_014276429.1 (+2)	68,861.10	10.50	0.00
	PREDICTED: moesin/ezrin/radixin homolog 1 isoform X1	XP_015377803.1 (+1)	67,746.80	19.80	1.75
	PREDICTED: moesin/ezrin/radixin homolog 1 isoform X1	XP_015127945.1 (+1)	68,073.90	70.70	3.30
	moesin ezrin radixin-like protein	KMQ97014.1	72,205.30	9.20	2.78
	PREDICTED: moesin/ezrin/radixin homolog 1 isoform X1	XP_011688748.1	67,970.40	7.80	1.57
	PREDICTED: moesin/ezrin/radixin homolog 1 isoform X2	XP_011882086.1 (+1)	68,899.50	6.20	1.54
	Chain A, Moesin From Spodoptera Frugiperda At 2.1 Angstroms Resolution	gi|122920502|pdb|2I1J|A			
61	Moesin/ezrin/radixin-like protein 1, partial RecName: Full=Titin; AltName: Full=D-Titin; AltName: Full=Kettin	KDR10362.1 Q9I7U4.3	2,066,054.90	79.80	0.00
62	Cluster of Myosin heavy chain, muscle, partial	KDR15411.1 [14]			
	Myosin heavy chain, muscle, partial	KDR15411.1			
	PREDICTED: myosin heavy chain, muscle isoform X26	XP_014282764.1 (+1)	225,167.30	23.50	0.00
	Myosin heavy chain, muscle	EZA50495.1	225,020.80	95.40	0.00
	PREDICTED: myosin heavy chain, muscle isoform X3	XP_015375209.1 (+3)	224,808.60	72.60	0.00

	PREDICTED: myosin heavy chain, muscle isoform X3	XP_014098305.1 (+2)	224,553.50	88.20	1.22
	PREDICTED: myosin heavy chain, muscle isoform X16	XP_015123925.1	222,749.10	82.80	1.23
	Myosin heavy chain, muscle	KDR06531.1			
	Chain C, The First X-ray Crystal Structure Of An Insect Muscle Myosin. Drosophila Melanogaster, Skeletal Muscle Myosin Ii, An Embryonic Isoform, Subfragment-1	gi|651207826|pdb|4QBD|C			
63	Putative cysteine proteinase	KDR17524.1	169,698.70	100.00	1.45
64	Cluster of Elongation factor 2	KDR09305.1 [5]			
	Elongation factor 2	KDR09305.1	94,604.90	78.50	2.01
	translation elongation factor 2 isoform 2	NP_001163865.1	94,785.50	25.80	2.01
	PREDICTED: translation elongation factor 2	XP_015379817.1	94,677.00	25.50	0.00
	Elongation factor, partial	EZA47862.1	99,329.00	44.10	1.13
	PREDICTED: translation elongation factor 2	XP_014276798.1	94,648.60	13.10	2.25
65	Hemocytin, partial	KDR23192.1	337,184.90	100.00	1.35
66	hypothetical protein	AGM32086.1	20,712.60	100.00	17.20
67	Cluster of Cu/Zn superoxide dismutase	AGM32998.1 [2]			
	Cu/Zn superoxide dismutase	AGM32998.1	15,876.30	99.90	22.10
	Superoxide dismutase [Cu-Zn]	KDR12362.1	15,878.30	84.50	22.10
68	Cluster of actin-depolymerizing factor 1	AGM32262.1 [2]			
	actin-depolymerizing factor 1	AGM32262.1	16,961.40	100.00	34.50
	PREDICTED: cofilin/actin-depolymerizing factor homolog	XP_014090201.1			
69	Cluster of Isocitrate dehydrogenase [NADP] cytoplasmic	KDR07905.1 [7]			
	isocitrate dehydrogenase	NP_001040134.1	46,178.20	42.50	0.00
	PREDICTED: isocitrate dehydrogenase [NADP] cytoplasmic	XP_015116437.1	52,403.00	11.80	2.13

	Isocitrate dehydrogenase [NADP] cytoplasmic	KDR07905.1	45,972.60	15.70	0.00
	Isocitrate dehydrogenase [NADP] cytoplasmic	EZA49618.1			
	PREDICTED: isocitrate dehydrogenase [NADP] cytoplasmic	XP_014284665.1	46,226.70	36.30	4.40
	PREDICTED: isocitrate dehydrogenase [NADP] cytoplasmic	XP_015376628.1			
	PREDICTED: isocitrate dehydrogenase [NADP] cytoplasmic	XP_014284665.1			
70	putative defense protein	AFZ78849.1	20,774.30	100.00	12.10
71	Cluster of thymosin beta-4 family protei	AGM32065.1 [2]			
	thymosin beta-4 family protein	AGM32065.1	14,661.00	100.00	30.00
	hypothetical protein L798_14751	KDR22896.1	22,959.00	6.90	10.90
72	Angiotensin-converting enzyme, partial	KDR23166.1	124,542.00	100.00	2.35
73	Cluster of PREDICTED: vesicle-fusing ATPase 1-like	XP_015373753.1 [11]			
	PREDICTED: vesicle-fusing ATPase 1-like	XP_015373753.1			
	PREDICTED: transitional endoplasmic reticulum ATPase TER94	XP_015365471.1			
	unnamed protein product, partial	CAV33750.1			
	PREDICTED: transitional endoplasmic reticulum ATPase TER94	XP_015365471.1	89,300.30	8.20	0.00
	PREDICTED: transitional endoplasmic reticulum ATPase TER94 isoform X1	XP_014103656.1 (+1)	95,268.70	19.20	0.00
	PREDICTED: vesicle-fusing ATPase 1	XP_014094393.1			
	Transitional endoplasmic reticulum ATPase TER94	KDR08983.1	89,326.20	7.40	1.62
	transitional endoplasmic reticulum ATPase TER94	NP_001037003.1	89,155.40	12.50	2.73
	PREDICTED: vesicle-fusing ATPase 1-like	XP_015115308.1			
	unknown	AEE61431.1			
74	Selenium-binding protein 1-A	KDR09028.1	58,866.30	100.00	5.94

75	malate dehydrogenase, partial	AGM32510.1	32,910.10	45.20	0.00
76	Cluster of peroxiredoxin-like protein	AFZ78682.1 [2]			
	peroxiredoxin-like protein	AFZ78682.1	19,540.30	100.00	9.29
	Peroxiredoxin-5, mitochondrial	KDR23852.1			
77	Cluster of BGGZ	AMY26906.1 [2]			
	BGGZ	AMY26906.1	56,447.20	39.00	0.00
	beta-glucosidase	ADK12988.1	56,602.40	100.00	10.10
78	Cluster of Synaptic vesicle membrane protein VAT-1-like protein-like, partial	KDR16462.1 [4]			
	Synaptic vesicle membrane protein VAT-1-like protein-like, partial	KDR16462.1	53,431.30	100.00	1.88
	vesicle amine transport protein	NP_001093281.1			
	Synaptic vesicle membrane protein VAT-1-like protein-like protein, partial	EZA60962.1			
	PREDICTED: synaptic vesicle membrane protein VAT-1 homolog-like	XP_015372517.1			
79	Cluster of Filamin-B	EZA55995.1 [5]			
	Filamin-B	EZA55995.1	273,249.90	9.40	0.00
	PREDICTED: filamin-A isoform X1	XP_015127256.1	243,216.50	15.60	0.00
	filamin C, partial	AHY99902.1			
80	PREDICTED: laminin subunit alpha-1	XP_014086161.1	447,679.20	83.80	0.00
81	PREDICTED: twitchin isoform X1	XP_015366994.1 (+9)	988,324.10	91.00	0.00
82	Cluster of unknown	AEE63566.1 [2]			
	unknown	AEE63566.1	39,748.70	99.90	9.89
	PREDICTED: glycerol-3-phosphate dehydrogenase [NAD(+)], cytoplasmic-like	XP_015124812.1			
83	Calmodulin	KDR17262.1	21,604.50	100.00	15.90
84	Cluster of Phosphoglycerate kinase	KDR15993.1 [6]			
	Phosphoglycerate kinase	KDR15993.1	44,839.70	100.00	16.80

	Phosphoglycerate kinase	EZA59046.1	54,561.60	39.90	2.98
	PREDICTED: phosphoglycerate kinase isoform X1	XP_014287903.1 (+1)			
	PREDICTED: LOW QUALITY PROTEIN: probable phosphoglycerate kinase, partial	XP_015379155.1			
	unknown	AEE63606.1			
85	alpha-tubulin 2	AGM32992.1	28,777.80	97.80	16.30
86	Cluster of PREDICTED: V-type proton ATPase catalytic subunit A isoform 2	XP_014100281.1 [8]			
	PREDICTED: V-type proton ATPase catalytic subunit A isoform 2	XP_014100281.1			
	vacuolar-type H+-ATPase	AGO46410.1	68,380.20	9.20	2.44
	PREDICTED: V-type proton ATPase catalytic subunit A isoform 1	XP_014096916.1			
	V-type proton ATPase catalytic subunit A	KDR22470.1			
	V-type proton ATPase catalytic subunit A	EZA47674.1			
	PREDICTED: V-type proton ATPase catalytic subunit A	XP_015374087.1			
	PREDICTED: V-type proton ATPase catalytic subunit A	XP_014272529.1			
	PREDICTED: V-type proton ATPase catalytic subunit A isoform 2-like, partial	XP_014101601.1			
87	PREDICTED: pericentrin-like	XP_014278058.1	414,528.90	90.10	0.00
88	Cluster of PREDICTED: bifunctional purine biosynthesis protein PURH	XP_014098367.1 [2]			
	PREDICTED: bifunctional purine biosynthesis protein PURH	XP_014098367.1	63,719.00	27.70	2.88
	Bifunctional purine biosynthesis protein PURH	KDR19778.1	64,044.50	79.30	2.87
89	Cluster of Pyruvate kinase	KDR19430.1 [7]			
	PREDICTED: pyruvate kinase-like	XP_015118194.1	57,461.40	26.40	0.00
	Pyruvate kinase	KDR19430.1	63,510.70	85.40	0.00

	PREDICTED: pyruvate kinase-like isoform X1	XP_015364930.1 (+1)			
	unknown	AEE62869.1			
	PREDICTED: pyruvate kinase-like isoform X1	XP_014098110.1			
	pyruvate kinase, partial	AHZ00177.1			
90	PREDICTED: protein vreteno-like isoform X1	XP_014085370.1	87,549.80	6.50	0.00
91	Teneurin-3	KDR07188.1	318,043.90	85.00	0.00
92	Cluster of cellulase	AGT15839.1 [2]			
	cellulase	AGT15839.1	47,461.20	46.00	3.42
	cellulase	AGT15840.1	48,774.20	24.50	3.35
93	putative vitellogenin protein, partial	BAU20285.1	158,866.60	100.00	4.41
94	Cluster of ribosomal protein S27A	AAL62473.1 [4]			
	ribosomal protein S27A	AAL62473.1	17,973.50	99.90	21.80
	Ubiquitin	KDR08584.1	25,926.90	58.70	7.86
	Ubiquitin	KDR13616.1	17,201.70	9.20	11.80
	Ubiquitin	KDR23619.1			
95	putative epidermal growth factor receptor, partial	CAC35008.1	159,585.80	7.30	0.00
96	Dynein beta chain, ciliary, partial	KDR11876.1	510,758.20	71.80	0.00
97	PREDICTED: gram-negative bacteria-binding protein 1 isoform X1	XP_014094525.1-DECOY	0	60.90	0.00
98	Cluster of Prostaglandin reductase 1	KDR24385.1 [2]			
	Prostaglandin reductase 1	KDR24385.1	37,154.10	100.00	5.93
	PREDICTED: prostaglandin reductase 1-like	XP_015379832.1			
99	Cluster of Ribose-phosphate pyrophosphokinase	KDR10178.1 [5]			
	Ribose-phosphate pyrophosphokinase 2, partial	KDR10178.1	40,817.50	85.00	9.12
	PREDICTED: ribose-phosphate pyrophosphokinase 1	XP_014096108.1	38,515.60	72.80	7.58
	Ribose-phosphate pyrophosphokinase	EZA48694.1	40,153.40	12.00	0.00
	PREDICTED: ribose-phosphate pyrophosphokinase 1 isoform X1	XP_015121691.1	42,151.40	7.00	0.00

	unknown	AEE62916.1			
100	Cluster of PREDICTED: microtubule-associated protein 1A isoform X1	XP_012622048.1 [3]			
	PREDICTED: microtubule-associated protein 1A isoform X1	XP_012622048.1 (+1)	323,052.30	100.00	0.95
	PREDICTED: LOW QUALITY PROTEIN: microtubule-associated protein 1A	XP_006201777.2			
101	Hemocyte protein-glutamine gamma-glutamyltransferase	KDR22723.1	80,640.20	100.00	5.31
102	antioxidant enzyme (heavy metal associated)	AGM32333.1	7,967.00	100.00	29.70
103	PREDICTED: uncharacterized protein LOC107173889	XP_015380104.1	192,354.60	22.60	0.00
104	Cluster of PREDICTED: histone H4-like	XP_004934019.2 [5]			
	PREDICTED: histone H4-like	XP_004934019.2 (+3)	11,381.80	99.50	7.52
	PREDICTED: histone H4-like	XP_015377639.1			
105	PREDICTED: ankyrin-3-like isoform X5	XP_015374146.1	184,990.60	75.80	0.00
106	Cluster of PREDICTED: ATP synthase subunit alpha, mitochondrial	XP_015124302.1 [6]			
	PREDICTED: ATP synthase subunit alpha	XP_015124302.1	59,317.50	46.40	1.82
	unknown	AEE62575.1			
	mitochondrial ATP synthase alpha subunit	ANJ04654.1			
	PREDICTED: ATP synthase subunit alpha	XP_014292528.1	59,751.20	35.90	1.82
	F0F1 ATP synthase subunit alpha	AID76763.1 (+1)	55,394.20	15.40	0.00
107	Cluster of PREDICTED: alpha,alpha-trehalose-phosphate synthase [UDP-forming]-like isoform X1	XP_015365044.1 [5]			
	PREDICTED: alpha,alpha-trehalose-phosphate synthase [UDP-forming]-like isoform X1	XP_015365044.1			
	PREDICTED: alpha,alpha-trehalose-phosphate synthase [UDP-forming] isoform X1	XP_014279588.1 (+1)			

	trehalose-6-phosphate synthase, partial	AEW67358.1			
	Alpha,alpha-trehalose-phosphate synthase [UDP-forming] A	KDR19655.1	93,810.20	12.70	4.12
108	Synaptojanin-1	KDR22712.1	106,289.80	35.60	0.00
109	polyubiquitin	AFZ78850.1	26,096.00	99.50	6.52
110	Glutamine synthetase 2 cytoplasmic	KDR18484.1	41,182.90	99.50	5.43
111	PREDICTED: uncharacterized protein LOC107161460	XP_015363363.1	105,266.80	100.00	1.56
112	hypothetical protein X777_07181	EZA53003.1	203,519.30	100.00	0.00
113	PREDICTED: microtubule-actin cross-linking factor 1 isoform X1	XP_014294731.1-DECOY (+5)	0	5.70	0.00
114	Cluster of PREDICTED: aldehyde dehydrogenase X, mitochondrial	XP_015110396.1 [6]			
	PREDICTED: aldehyde dehydrogenase X, mitochondrial	XP_015110396.1	52,435.40	12.20	0.00
	mitochondrial aldehyde dehydrogenase	NP_001040198.1			
	PREDICTED: aldehyde dehydrogenase, cytosolic 1-like isoform X1	XP_015110397.1 (+2)			
	Retinal dehydrogenase	EZA52207.1	53,224.60	29.90	4.71
115	thioredoxin-like protein	AFZ78678.1	11,772.60	100.00	26.70
116	PREDICTED: gamma-aminobutyric acid receptor alpha-like	XP_014286667.1	57,579.80	49.60	0.00
117	Voltage-dependent calcium channel subunit alpha-2/delta-3	EZA57148.1	285,937.10	55.20	0.00
118	Cluster of Phospholipid hydroperoxide glutathione peroxidase, mitochondrial	KDR22003.1 [2]			
	Phospholipid hydroperoxide glutathione peroxidase, mitochondrial	KDR22003.1	21,837.70	99.50	5.64
	unknown	AEE61713.1			
119	Cluster of hypothetical protein L798_03098, partial	KDR07317.1 [4]			
	hypothetical protein L798_03098, partial	KDR07317.1	31,491.10	99.50	5.05

	PREDICTED: malate dehydrogenase, mitochondrial	XP_014088743.1			
	PREDICTED: malate dehydrogenase, mitochondrial-like	XP_014096270.1			
	unknown	AEE63021.1			
120	cysteine peptidase C12 containing ubiquitin carboxy-terminal hydrolase	AGM32543.1	25,265.70	100.00	10.60
121	Neurotrypsin	KDR22858.1	196,157.50	100.00	1.23
122	PREDICTED: microtubule-associated protein 1A	XP_008141282.1	324,691.20	81.90	0.00
123	RNA recognition motif (RRM), partial	AGM32678.1	33,044.50	100.00	9.18
124	Cluster of PREDICTED: tropomyosin isoform X6	XP_015110423.1 [4]			
	PREDICTED: tropomyosin isoform X6	XP_015110423.1 (+2)			
	PREDICTED: tropomyosin-1, isoforms 9A/A/B isoform X12	XP_014273426.1	29,498.70	25.10	5.16
125	Cluster of C-1-tetrahydrofolate synthase, cytoplasmic	KDR19573.1 [4]			
	C-1-tetrahydrofolate synthase, cytoplasmic	KDR19573.1	100,912.10	6.90	0.00
	PREDICTED: C-1-tetrahydrofolate synthase, cytoplasmic	XP_014289250.1	102,705.00	7.50	1.04
	PREDICTED: C-1-tetrahydrofolate synthase, cytoplasmic isoform X1	XP_015111335.1 (+1)			
126	Cluster of Malate dehydrogenase, cytoplasmic, partial	KDR14372.1 [2]			
	Malate dehydrogenase, cytoplasmic, partial	KDR14372.1	32,849.50	50.50	0.00
	PREDICTED: malate dehydrogenase, cytoplasmic	XP_015375910.1			
127	Cluster of aldo-keto reductase 1 (AMJ21949.2)	AMJ21949.2 [3]			
	aldo-keto reductase 1	AMJ21949.2	37,724.00	99.50	4.49
	PREDICTED: alcohol dehydrogenase [NADP(+)] B-like	XP_014291627.1			

	PREDICTED: 1,5-anhydro-D-fructose reductase-like	XP_014292195.1			
128	putative Restnal dehydrogenase	AGM32911.1	16,597.30	100.00	36.40
129	Leucyl-tRNA synthetase, cytoplasmic	EZA54369.1	134,800.00	32.70	0.00
130	PREDICTED: keratin, type II cytoskeletal 1	XP_001381422.1	59,912.50	100.00	2.15
131	PREDICTED: filamin-A isoform X1	XP_015373051.1	204,893.50	100.00	2.10
132	Disks large-like protein	EZA57168.1	214,703.50	99.90	0.00
133	PREDICTED: heat shock protein 75 kDa, mitochondrial	XP_014089245.1	80,280.60	87.60	1.98
134	Cluster of Translationally-controlled tumor protein-like protein	EZA58324.1 [3]			
	Translationally-controlled tumor protein-like protein	EZA58324.1	19,862.20	44.90	0.00
	translationally controlled tumor protein	AHA86297.1			
	translationally-controlled tumor protein	AEI69350.1			
135	Teneurin-3	EZA50796.1	385,175.10	70.90	0.00
136	hypothetical protein L798_13352	KDR23662.1	55,166.10	100.00	3.11
137	PREDICTED: 5'-3' exoribonuclease 1	XP_014290344.1	178,535.70	82.70	0.00
138	Prostatic acid phosphatase	KDR11063.1	46,360.40	100.00	5.16
139	PREDICTED: fumarate hydratase, mitochondrial-like isoform X1	XP_014090185.1-DECOY (+1)	0	82.00	0.00
140	Cluster of Peroxiredoxin-6	KDR10377.1 [4]			
	Peroxiredoxin-6	KDR10377.1	24,761.10	99.90	10.50
	PREDICTED: peroxiredoxin-6-like isoform X1	XP_014274633.1 (+2)			
141	hypothetical protein Z043_111338	KPP69873.1	98,420.40	6.00	0.00
142	C-type lysozyme-2	AFZ78837.1	14,173.10	100.00	7.52
143	enolase	AGM32398.1	26,432.80	10.40	0.00
144	gram negative bacteria binding protein 1	AAZ08492.1	42,701.10	9.20	0.00
145	Cluster of inorganic pyrophosphatase, partial	AGM32607.1 [2]			

	inorganic pyrophosphatase, partial	AGM32607.1	34,448.50	10.60	0.00
	Inorganic pyrophosphatase	KDR14150.1			
146	Cluster of Voltage-dependent anion-selective channel protein 2	KDR18209.1 [2]			
	voltage-dependent anion-selective channel-like protein, partial	AGM32824.1	28,037.30	70.20	5.47
	Voltage-dependent anion-selective channel protein 2	KDR18209.1			
147	PAB-dependent poly(A)-specific ribonuclease subunit 2	KDR16171.1	147,806.00	100.00	3.28
148	Lysosomal aspartic protease	KDR23365.1	41,530.10	100.00	5.50
149	basic juvenile hormone sensitive hemolymph protein one	AAA27882.1	88,237.70	99.40	1.07
150	PREDICTED: uncharacterized protein LOC106681208 isoform X1	XP_014276894.1-DECOY (+1)	0	70.80	0.00
151	PREDICTED: oocyte zinc finger protein XlCOF19-like	XP_015369676.1-DECOY	0	67.40	0.00
152	Laminin subunit gamma-1, partial	EMP34462.1 (+1)	171,449.80	97.20	0.00
153	Cluster of transgelin	NP_001040372.1 [3]			
	transgelin	NP_001040372.1	20,891.00	28.50	6.91
	calponin-likey domain containing protein	AGM32416.1			
	PREDICTED: myophilin	XP_014279675.1			
154	PREDICTED: disks large homolog 5 isoform X1	XP_014279584.1 (+1)	182,726.10	45.50	0.00
155	Cluster of Lambda-crystallin-like protein	KDR11934.1 [2]			
	Lambda-crystallin-like protein	KDR11934.1	35,477.80	99.40	3.81
	PREDICTED: lambda-crystallin homolog	XP_015365806.1			
156	Cluster of PREDICTED: coiled-coil domain-containing protein 6	XP_013370224.1 [2]			
	PREDICTED: coiled-coil domain-containing protein 6	XP_013370224.1	63,832.50	99.90	7.18

	hypothetical protein cypCar_00023883	KTG00872.1			
157	Cluster of Beta-glucuronidase	KDR08779.1 [2]			
	Beta-glucuronidase	KDR08779.1	72,541.80	94.50	3.32
	PREDICTED: beta-glucuronidase	XP_012550948.1	76,315.40	10.90	3.16
158	Cluster of cytochrome c -like protein	AGM32375.1 [2]			
	cytochrome c-like protein	AGM32375.1	11,909.90	100.00	31.50
	unknown	AEE62389.1			
159	Cluster of hypothetical protein, partial	BAD89151.1 [4]			
	hypothetical protein, partial	BAD89151.1	8,808.40	99.80	42.40
	PREDICTED: larval cuticle protein A2B-like	XP_014279384.1			
	cuticle protein, putative	BAN20305.1	19,899.80	99.80	14.80
	Larval cuticle protein A3A	KDR13561.1	15,942.00	99.80	23.70
160	Calcyphosin-like protein	KDR20276.1	23,905.00	99.40	6.57
161	Protein disulfide-isomerase	KDR21216.1	55,806.40	100.00	5.24
162	PREDICTED: snRNA-activating protein complex subunit 3	XP_014094877.1	48,013.50	51.80	0.00
163	cathepsin L-like protein	AGM32335.1	37,383.10	96.40	5.37
164	PREDICTED: uncharacterized protein LOC106692969	XP_014294751.1-DECOY	0	98.40	0.00
165	Cluster of unknown	AEE63607.1 [3]			
	unknown	AEE63607.1	45,701.30	73.50	1.96
	PREDICTED: probable aspartate aminotransferase, cytoplasmic	XP_015127719.1			
	PREDICTED: probable aspartate aminotransferase, cytoplasmic	XP_014280105.1			
166	Profilin	KDR15557.1	13,770.40	99.30	11.90
167	Fructose-bisphosphate aldolase	EZA60106.1	39,744.00	61.10	3.28
168	PREDICTED: laminin subunit alpha-3	XP_013359753.1-DECOY	0	7.70	0.00
169	Eukaryotic translation initiation factor 4 gamma 3	KDR07102.1	72,667.90	12.80	0.00

170	PREDICTED: fatty acid synthase-like	XP_015113026.1	266,958.00	65.70	0.00
171	PREDICTED: ecto-ADP-ribosyltransferase 5-like isoform X2	XP_006032147.1	34,169.40	35.20	0.00
172	fructose-1,6-bisphosphate aldolase, partial	AGM32655.1	32,784.60	100.00	9.70
173	Beta-galactosidase	KDR22879.1	74,496.10	97.70	1.50
174	Beta-glucuronidase	KDR08780.1	75,503.40	99.90	4.08
175	PREDICTED: locomotion-related protein Hikaru genki, partial	XP_014093554.1	104,105.30	100.00	6.94
176	heat shock protein 75 kDa, mitochondrial-like	NP_001266361.1	78,964.00	60.10	2.02
177	Retinal dehydrogenase 1	KDR10337.1	56,775.90	12.40	1.54
178	PREDICTED: filamin-A-like	XP_004923608.2	90,054.90	33.30	1.55
179	DE-cadherin	EZA51390.1-DECOY	0	14.80	0.00
180	heat shock protein 90	ACD63052.1	81,676.60	34.40	3.08
181	PREDICTED: LOW QUALITY PROTEIN: transferrin	XP_014094629.1	72,423.50	29.10	2.80
182	Chain T, Complex of Leech-Derived Tryptase Inhibitor With Porcine Trypsin	gi|3212563|pdb|1LDT|T	23,000.00	99.78	27.33

Supplementary Table 4.2 Hemolymph proteins shared by naïve and MRSA-challenged *R. flavipes*.

Identified Proteins	Accession Number
aldo-keto reductase 1	AMJ21949.2
ribosomal protein S27A	AAL62473.1
VHDL receptor	AAR32136.1
uncharacterized protein	AGM32706.1
14-3-3 protein epsilon	ANJ04668.1
unknown	AEE63607.1
calponin-likey domain containing protein	AGM32416.1
heat shock protein 70, partial	AHE77387.1
unknown	AEE63239.1
arginine kinase, partial (mitochondrion)	ALS08443.1
arginine kinase, partial (mitochondrion)	ALS08389.1
beta-glucosidase	AEW67361.1
ferritin-like precursor, partial	AGM32322.1
unknown	AEE62891.1
unknown	AEE62651.1
catalase, partial	ABE28534.1
arginine kinase, partial (mitochondrion)	ALS08439.1
unknown	AEE62916.1
glycoside hydrolase family 9	AMH40362.1
heat shock protein 70	AGF34718.1
elongation factor 1 alpha, partial	ACB71693.1
elongation factor 1 alpha, partial	ACB71691.1
elongation factor 1 alpha, partial	ADM15740.1
elongation factor 1 alpha, partial	ADM15729.1
heat shock protein 70	AHE77386.1
beta-glucosidase	ADD92156.1

inorganic pyrophosphatase, partial	AGM32607.1
unknown	AEE62864.1
enolase	ACZ68117.1
putative enolase, partial	AJK30675.1
endo-beta-1,4-glucanase, partial	BAD66681.1
hexamerin 4, partial	CAM84199.1
arginine kinase 2, partial	CAZ65716.1
hexamerin 1	CAM84196.1
Tubulin alpha-3 chain	EZA62520.1
Arginine kinase	EZA47168.1
Heat shock 70 kDa protein cognate	EZA48451.1
Ribose-phosphate pyrophosphokinase	EZA48694.1
Translationally-controlled tumor protein-like protein	EZA58324.1
Filamin-B	EZA55995.1
Teneurin-3	EZA50796.1
Laminin subunit beta-1	EMP30347.1
Heat shock 70 kDa protein cognate	EZA53141.1
Chain C, The First X-ray Crystal Structure Of An Insect Muscle Myosin. Drosophila Melanogaster, Skeletal Muscle Myosin Ii, An Embryonic Isoform, Subfragment-1	gi|651207826|pdb|4QBD|C
Chain D, Crystal Structure Of The Invertebrate Bi-functional Purine Biosynthesis Enzyme Paics At 2.8 A Resolution	gi|453056256|pdb|4JA0|D
Transitional endoplasmic reticulum ATPase TER94	KDR08983.1
Ubiquitin	KDR13616.1
Superoxide dismutase [Cu-Zn]	KDR12362.1
hypothetical protein L798_03098, partial	KDR07317.1
Neurotrypsin	KDR22858.1
Hemocyte protein-glutamine gamma-glutamyltransferase	KDR22723.1
Ubiquitin	KDR23619.1
Teneurin-3	KDR07188.1

Regucalcin	KDR12743.1
Ubiquitin	KDR08584.1
Ribose-phosphate pyrophosphokinase 2, partial	KDR10178.1
Selenium-binding protein 1-A	KDR09028.1
Glutamine synthetase 2 cytoplasmic	KDR18484.1
hypothetical protein L798_13352	KDR23662.1
Glutathione S-transferase omega-2	KDR22869.1
Profilin	KDR15557.1
Beta-galactosidase	KDR22879.1
transitional endoplasmic reticulum ATPase TER94	NP_001037003.1
fructose 1,6-bisphosphate aldolase	NP_001091766.1
vesicle amine transport protein	NP_001093281.1
muscle glycogen phosphorylase	NP_001116811.1
PREDICTED: enolase	XP_015117515.1
PREDICTED: plasma alpha-L-fucosidase-like	XP_015122125.1
PREDICTED: sorbitol dehydrogenase-like	XP_015371890.1
PREDICTED: phenoloxidase 2-like	XP_015378845.1
PREDICTED: microtubule-associated protein 1A isoform X1	XP_012622048.1
PREDICTED: filamin-A isoform X1	XP_015127256.1
PREDICTED: heat shock protein Hsp-12.2	XP_014288127.1
PREDICTED: aldose reductase-like	XP_014287922.1
PREDICTED: transitional endoplasmic reticulum ATPase TER94	XP_015365471.1
PREDICTED: laminin subunit beta-1	XP_005292397.1
PREDICTED: fructose-bisphosphate aldolase-like	XP_014088227.1
PREDICTED: ribose-phosphate pyrophosphokinase	XP_014096108.1
PREDICTED: transitional endoplasmic reticulum ATPase TER94-like	XP_014294276.1
PREDICTED: 1,5-anhydro-D-fructose reductase-like	XP_014292195.1
PREDICTED: heat shock 70 kDa protein cognate 2-like	XP_014275032.1

PREDICTED: catalase	XP_015364010.1
PREDICTED: 14-3-3 protein epsilon	XP_014279405.1
PREDICTED: enolase	XP_014089074.1
PREDICTED: ribose-phosphate pyrophosphokinase 1 isoform X1	XP_015121691.1
PREDICTED: alpha-L-fucosidase isoform X1	XP_015367656.1
PREDICTED: alcohol dehydrogenase [NADP(+)] B-like	XP_014291627.1

Supplementary Table 4.3 Hemolymph proteins shared by naïve and *P. aeruginosa*-challenged *R. flavipes*.

Identified Proteins	Accession Number
heat shock 90 kDa protein	AHB18587.1
glycogen phosphorylase	AFO54708.2
hsp90	AMA66329.1
heat shock cognate 70 protein	ACA53150.1
cathepsin L-like protein	AGM32335.1
heat shock protein 70	ABL06948.1
elongation factor 1-alpha, partial	ABW98970.1
unknown	AEE61713.1
Alpha-L-fucosidase	EZA56254.1
Catalase	EZA54346.1
Retinal dehydrogenase	EZA52207.1
Chain A, The Crystal Structure Of Fructose-1,6-Bisphosphate Aldolase From Drosophila Melanogaster At 2.5 Angstroms Resolution	gi|253722156|pdb|1FBA|A
Peroxiredoxin-6	KDR10377.1
hypothetical protein L798_00618, partial	KDR22779.1
Apolipophorin, partial	KDR18107.1
Phosphoglycerate kinase	KDR15993.1
Laminin subunit beta-1, partial	KGL97946.1
Phosphatidylethanolamine-binding protein 1	KDR14299.1
Laminin subunit beta-1, partial	KFO88248.1
hypothetical protein cypCar_00023883	KTG00872.1
Tubulin alpha-1 chain	KDR02444.1
V-type proton ATPase catalytic subunit A	KDR22470.1
Lambda-crystallin-like protein	KDR11934.1
isocitrate dehydrogenase	NP_001040134.1
PREDICTED: isocitrate dehydrogenase [NADP] cytoplasmic	XP_015116437.1

PREDICTED: coiled-coil domain-containing protein 6	XP_013370224.1
PREDICTED: glycerol-3-phosphate dehydrogenase [NAD(+)], cytoplasmic-like	XP_015124812.1
PREDICTED: isocitrate dehydrogenase [NADP] cytoplasmic isoform X1	XP_014096133.1
PREDICTED: uncharacterized protein LOC107161460	XP_015363363.1
PREDICTED: V-type proton ATPase catalytic subunit A isoform 2	XP_014100281.1
PREDICTED: phenoloxidase 2-like	XP_014276959.1
PREDICTED: LOW QUALITY PROTEIN: microtubule-associated protein 1A	XP_006201777.2
PREDICTED: V-type proton ATPase catalytic subunit A isoform 1	XP_014096916.1
PREDICTED: 14-3-3 protein epsilon	XP_015377637.1
PREDICTED: laminin subunit beta-1	XP_005498160.1
PREDICTED: LOW QUALITY PROTEIN: probable phosphoglycerate kinase, partial	XP_015379155.1
PREDICTED: protein D3-like	XP_015368042.1
PREDICTED: glycogen phosphorylase	XP_015120639.1
PREDICTED: peroxiredoxin-6-like isoform X1	XP_014274633.1
PREDICTED: isocitrate dehydrogenase [NADP] cytoplasmic	XP_014284665.1
PREDICTED: isocitrate dehydrogenase [NADP] cytoplasmic	XP_015376628.1

Supplementary Table 4.4 Hemolymph proteins shared by MRSA-challenged and *P. aeruginosa*-challenged *R. flavipes*.

Identified Proteins	Accession Number
PAB-dependent poly(A)-specific ribonuclease subunit 2	KDR16171.1
catalase	NP_001036912.1
hexamerin 3, partial	CAM84198.1
heat shock protein 75 kDa, mitochondrial-like	NP_001266361.1
PREDICTED: tubulin beta chain-like	XP_015120506.1
Peroxiredoxin-5, mitochondrial	KDR23852.1
Regucalcin, partial	KDR17044.1
heat shock cognate 70 protein	ACO57618.1
arginine kinase, partial (mitochondrion)	ALS08382.1
hypothetical protein L798_00664, partial	KDR09443.1
elongation factor 1-alpha, partial	ADK90452.1
Venom allergen 3	KDR14384.1
Synaptic vesicle membrane protein VAT-1-like protein-like protein, partial	EZA60962.1
PREDICTED: heat shock protein 83	XP_015371422.1
PREDICTED: laminin subunit beta-1	XP_013801983.1
glutathione s-transferase D2	AFJ75802.1
Hexamerin	EZA60531.1
unnamed protein product, partial	CAV33750.1
transferrin	AAQ62963.2
Malate dehydrogenase, cytoplasmic, partial	KDR14372.1
PREDICTED: vesicle-fusing ATPase 1-like	XP_015373753.1
PREDICTED: laminin subunit alpha-3 isoform X1	XP_014426018.1
Transferrin	EZA53240.1
Heat shock protein 70 A1	KDR08926.1
PREDICTED: laminin subunit beta-1	XP_009634373.1
PREDICTED: histone H4-like	XP_015377639.1

Supplementary Table 4.5 Identified unique hemolymph proteins in naïve *R. flavipes*.

Identified Proteins	Accession Numbers
voltage-dependent anion-selective channel-like protein, partial	AGM32824.1
unknown	AEE63021.1
unknown	AEE61839.1
unknown	AEE62848.1
unknown	AEE63606.1
unknown	AEE61431.1
unknown	AEE63226.1
unknown	AEE62869.1
glutathione s-transferase D2	AFJ75818.1
glutathione s-transferase D2	AFJ75802.1
heat shock protein 70, partial	ACD63048.1
heat shock protein 90, partial	ABF01016.1
inducible heat shock 70 kDa protein, partial	AAG42838.1
gram negative bacteria binding protein 1	AAZ08490.1
C-type lysozyme-2	AFZ78837.1
elongation factor 1 alpha, partial	ADM15835.1
elongation factor-1 alpha, partial	AAF89848.1
SCP-like extracellular domain containing protein 2	AGM32430.1
hexamerin 2 precursor, partial	AGR40412.1
cellulase	AAK12339.1
trehalose-6-phosphate synthase, partial	AEW67358.1
enolase, partial	AHY99874.1
putative fructose 1,6-bisphosphate aldolase	AAU84937.1
endo-beta-1,4-glucanase	ADB12483.1
putative epidermal growth factor receptor, partial	CAC35008.1
Multifunctional protein ADE2	EZA56375.1
Isocitrate dehydrogenase [NADP] cytoplasmic	EZA49618.1
chaperone dnaK	EZO35528.1
V-type proton ATPase catalytic subunit A	EZA47674.1
Protein yellow	KDR22429.1
Beta-glucuronidase	KDR08779.1
Beta-glucuronidase	KDR08780.1
PREDICTED: translation elongation factor 2	XP_014276798.1
Alpha,alpha-trehalose-phosphate synthase [UDP-forming] A	KDR19655.1
Cytosolic carboxypeptidase-like protein 5, partial	KDR22169.1
Multifunctional protein ADE2, partial	KDR09851.1
Phosphatidylethanolamine-binding protein 1	KDR14299.1

mitochondrial aldehyde dehydrogenase	NP_001040198.1
PREDICTED: malate dehydrogenase, cytoplasmic	XP_015375910.1
PREDICTED: uncharacterized protein LOC107162408	XP_015364774.1
PREDICTED: heat shock 70 kDa protein cognate 3	XP_015112461.1
PREDICTED: lambda-crystallin homolog	XP_015365806.1
PREDICTED: beta-glucuronidase	XP_012550948.1
PREDICTED: 14-3-3 protein epsilon	XP_015377637.1
PREDICTED: alpha,alpha-trehalose-phosphate synthase [UDP-forming]-like isoform X1	XP_015365044.1
PREDICTED: phenoloxidase 2-like	XP_014277062.1
PREDICTED: aldehyde dehydrogenase X, mitochondrial	XP_015110396.1
PREDICTED: malate dehydrogenase, mitochondrial-like	XP_014096270.1
PREDICTED: aldehyde dehydrogenase, cytosolic 1-like isoform X1	XP_015110397.1
PREDICTED: glycogen phosphorylase isoform X1	XP_015375987.1
PREDICTED: alpha,alpha-trehalose-phosphate synthase [UDP-forming] isoform X1	XP_014279588.1
PREDICTED: microtubule-associated protein 1A	XP_008141282.1
hypothetical protein L798_01615	KDR07960.1
PREDICTED: bifunctional purine biosynthesis protein PURH	XP_015365809.1
PREDICTED: pyruvate kinase-like	XP_015118194.1
PREDICTED: pyruvate kinase-like isoform X1	XP_015364930.1
PREDICTED: cofilin/actin-depolymerizing factor homolog	XP_014090201.1
PREDICTED: malate dehydrogenase, mitochondrial	XP_014088743.1

Supplementary Table 4.6 Identified unique hemolymph proteins in MRSA-challenged *R. flavipes*.

Identified Proteins	Accession Number
heat shock protein 70	AGF34717.1
heat shock protein 90	ACD63052.1
heat shock inducible HSP70, partial	AGM39425.1
elongation factor 1 alpha, partial	ACB87164.1
elongation factor 1 alpha, partial	AHH31040.1
elongation factor 1-alpha, partial	ABW99004.1
glycoside hydrolase family 9	AMH40359.1
glycoside hydrolase family 9	AMH40364.1
arginine kinase, partial (mitochondrion)	ALS08358.1
filamin C, partial	AHY99902.1
mitochondrial ATP synthase alpha subunit	ANJ04654.1
translationally controlled tumor protein	AHA86297.1
F0F1 ATP synthase subunit alpha	AID76763.1
unknown	AEE62575.1
unknown	AEE62389.1
cuticle protein, putative	BAN20305.1
86 kDa early-staged encapsulation inducing protein	BAA81665.2
hypothetical protein, partial	BAD89151.1
14-3-3epsilon, partial	BAI66121.1
Voltage-dependent calcium channel subunit alpha-2/delta-3	EZA57148.1
Leucyl-tRNA synthetase, cytoplasmic	EZA54369.1
Disks large-like protein	EZA57168.1
Laminin subunit gamma-1, partial	EMP34462.1
Myosin heavy chain, muscle	EZA50495.1
Heat shock 70 kDa protein cognate 4	KDR23254.1
Laminin subunit alpha-3, partial	KFO61539.1
hypothetical protein Z043_111338	KPP69873.1
moesin ezrin radixin-like protein	KMQ97014.1
Myosin heavy chain, muscle	KDR06531.1
Larval cuticle protein A3A	KDR13561.1
transgelin	NP_001040372.1
RecName: Full=Titin; AltName: Full=D-Titin; AltName: Full=Kettin	Q9I7U4.3
PREDICTED: twitchin isoform X1	XP_015366994.1
PREDICTED: laminin subunit alpha-1	XP_014086161.1
PREDICTED: pericentrin-like	XP_014278058.1
PREDICTED: protein vreteno-like isoform X1	XP_014085370.1

PREDICTED: ankyrin-3-like isoform X5	XP_015374146.1
PREDICTED: uncharacterized protein LOC106678290 isoform X3	XP_014272203.1
PREDICTED: ATP synthase subunit alpha, mitochondrial	XP_014292528.1
PREDICTED: heat shock protein 70-like	XP_014089050.1
PREDICTED: myosin heavy chain, muscle isoform X16	XP_015123925.1
CRE-HSP-3 protein	XP_003117830.1
PREDICTED: heat shock protein 70 A1-like	XP_015372059.1
PREDICTED: transitional endoplasmic reticulum ATPase TER94 isoform X1	XP_014103656.1
PREDICTED: enolase isoform X1	XP_014288071.1
PREDICTED: myosin heavy chain, muscle isoform X3	XP_015375209.1
PREDICTED: laminin subunit alpha-3	XP_014108844.1
PREDICTED: myosin heavy chain, muscle isoform X3	XP_014098305.1
PREDICTED: fatty acid synthase-like	XP_015113026.1
PREDICTED: disks large homolog 5 isoform X1	XP_014279584.1
PREDICTED: myosin heavy chain, muscle isoform X26	XP_014282764.1
PREDICTED: laminin subunit beta-1, partial	XP_014427649.1
PREDICTED: prostaglandin reductase 1-like	XP_015379832.1
PREDICTED: protein D3	XP_014086915.1
PREDICTED: heat shock protein 68-like	XP_015373896.1
PREDICTED: aldose reductase-like	XP_015121681.1

Supplementary Table 4.7 Identified unique hemolymph proteins in *P. aeruginosa*-challenged *R. flavipes*.

Identified Proteins	Accession Number
elongation factor-1 alpha, partial	AAF89857.1
elongation factor 1 alpha, partial	ADM15728.1
elongation factor 1-alpha (EF1-alpha) protein	AGM32604.1
elongation factor 1-alpha, partial	ABW99030.1
fructose-1,6-bisphosphate aldolase, partial	AGM32655.1
heat shock protein 70a	AHA36968.1
arginine kinase, partial (mitochondrion)	ALS08393.1
enolase	AGM32398.1
basic juvenile hormone sensitive hemolymph protein one	AAA27882.1
gram negative bacteria binding protein 1	AAZ08492.1
sorbitol dehydrogenase, partial	AHZ00204.1
putative endo-beta-1,4-glucanase NtEG2, partial	BAD12011.1
transferrin	BAQ94504.1
cyanoprotein beta subunit precursor	BAA13324.1
cyanoprotein alpha subunit precursor	BAA13323.1
hypothetical protein X777_07181	EZA53003.1
Arylphorin subunit alpha	EZA60532.1
Sorbitol dehydrogenase	EZA47058.1
Aldo-keto reductase family 1 member B10	EZA59353.1
Heat shock protein HSP 90-alpha	EZA50089.1
Chain A, Moesin From Spodoptera Frugiperda At 2.1 Angstroms Resolution	gi|122920502|pdb|2I1J|A
Chain D, Crystal Structure of Antheraea Pernyi Arylphorin	gi|229597916|pdb|3GWJ|D
PREDICTED: heat shock 70 kDa protein cognate 1	XP_014088467.1
PREDICTED: heat shock protein 70 B2-like	XP_015371967.1
PREDICTED: heat shock protein 83	XP_014284945.1
PREDICTED: heat shock protein 68-like	XP_014272950.1
PREDICTED: major heat shock 70 kDa protein Ba-like	XP_014289183.1
Myosin heavy chain, muscle, partial	KDR15411.1
Dynein beta chain, ciliary, partial	KDR11876.1
Synaptojanin-1	KDR22712.1
hypothetical protein L798_14751	KDR22896.1
Eukaryotic translation initiation factor 4 gamma 3	KDR07102.1
Lysosomal aspartic protease	KDR23365.1
sorbitol dehydrogenase	NP_001037592.1
PREDICTED: transferrin	XP_015109887.1

PREDICTED: tubulin alpha chain-like isoform X1	XP_015123831.1
PREDICTED: multifunctional protein ADE2	XP_014101019.1
PREDICTED: LOW QUALITY PROTEIN: laminin subunit beta-1	XP_009982860.1
PREDICTED: phosphoglycerate kinase isoform X1	XP_014287903.1
PREDICTED: 5'-3' exoribonuclease 1	XP_014290344.1
PREDICTED: ecto-ADP-ribosyltransferase 5-like isoform X2	XP_006032147.1
PREDICTED: sorbitol dehydrogenase-like	XP_014289176.1
PREDICTED: laminin subunit alpha-3	XP_009665364.1
PREDICTED: laminin subunit beta-1	XP_009664293.1
PREDICTED: laminin subunit beta-1	XP_009461238.1
PREDICTED: arylphorin subunit alpha-like	XP_015112084.1
PREDICTED: LOW QUALITY PROTEIN: uncharacterized protein LOC106621780, partial	XP_014096235.1
PREDICTED: gamma-aminobutyric acid receptor alpha-like	XP_014286667.1
PREDICTED: snRNA-activating protein complex subunit 3	XP_014094877.1
PREDICTED: LOW QUALITY PROTEIN: laminin subunit beta-1	XP_005010332.1

Chapter Five

Research Summary and Future Perspectives

5.1 Research summary

My doctoral research projects were mainly focused on investigation and characterization of antibacterial proteins from the eastern subterranean termites, *Reticulitermes flavipes* in response to multidrug resistant bacteria, *Pseudomonas aeruginosa* and methicillin-resistant *Staphylococcus aerues* (MRSA). I collected field termites and reared them in the lab to standardize these organisms. By evaluating antibacterial activities of crude extract of unsterilized *R. flavipes* workders against a common soil entomopathogenic bacterium *Bacillus subtilis* using inhibition zone assay, and compared the sample with heat-treated crude extract as well as a positive control Ampicillin. I found that unsterilized termites constitutively present proteinaceous antibacterial compound(s) against *B. subtilis*. Furthermore, to determine the size range of uncharacterized antibacterial compound(s), I size-fractionated crude extracts into five fractions. Interestingly, different levels of antibacterial activity were observed in all five fractions (>300, 90-180, 30-90, 10-20, and <10 kDa) at the same concentration, indicating the existence of multiple active compounds in the crude extract and the active compounds may originate from cuticular bacteria (data were shown in appendix), gut microbes, and termite immune system. Based on the findings, I concentrated my research on surface-sterilized termites in order to exclude the possibility of cuticular bacteria generated antimicrobial compounds.

To evaluate the spectrum of antibacterial activity of whole body crude extract from surface-sterilized *R. flavipes*, a panel of bacteria (8 in total) including three MDR, four non-MDR human pathogens, and *B. subtilis* were selected for investigating their susceptibility on crude extract of standardized *R. flavipes* (considered as naïve termites). Through inhibition zone assay, I demonstrated that crude extract of naïve termites had a broad-spectrum activity against the non-MDR bacteria (two strains of *E. coli*, *S. aureus*, *Streptococcus pyogenes*, and *Samonlella* Typhimirum) but not the three MDR pathogens (*P. aeruginosa*, MRSA, and *Acinetobacter baumannii*). In addition, the antimicrobial activity changed dramatically when the termites were fed with either heat-killed *P. aeruginosa* or MRSA, particularly induced activity against the inducers but not *A. baumannii*. To clarify the origin of antibacterial compounds was related to termite immune response, I collected hemolymph and separated guts to determine their antagonistic activity. I then demonstrated that hemolymph, not the hindgut, was the primary source of antibiotic activity.

In the effort to continue characterizing antibacterial proteins against *P. aeruginosa* and MRSA, I investigated alterations in hemolymph protein profiles of *P. aeruginosa* and MRSA-challenged termites. The protein profiles were determined through two proteomic approaches via two-dimensional gel electrophoretic analyses and nano-liquid-chromatography-MS/MS analysis. Two-dimensional gel electrophoretic analyses of 493 hemolymph protein spots indicated that a total of 38 and 65 proteins were differentially expressed at least 2.5-fold upon being fed with *P. aeruginosa* and MRSA, respectively. Mass spectrometry (MS) analysis of hemolymph identified a total of 578 proteins. Upon further analysis of MS data, we observed 136 and 82 proteins that appeared to be differentially expressed at least 2.5-fold in response to *P. aeruginosa* and MRSA-challenge, respectively. I then found many of these differentially expressed hemolymph proteins

(actins, tublins, transferrin, dehydrogenases, peroxiredoxin, catalase and etc.) were involved in immune-related processes including iron metabolism, antioxidant-related response**,** general stress response, and immune effectors. Particularly, beta-glucuronidae, c-type lysozyme, actin, lysosomal aspartic protease, and phenoloxidase might be considered as immune effectors with antibacterial activity. These results from my dissertation research clearly provided an insight on protein compositional changes in defending bacterial challenge, and suggested regulation of humoral as well as cellular immunity in *R. flavipes* were primed by oral ingestion with MDRs.

5.2 Future studies

Based on the findings demonstrated in my doctoroal researches, I will seek two directions to continue investigation of termite immune response upon MDR infections for future research. First, I will determine the antibacterial activity of aforementioned immune effectors (beta-glucuronidae, c-type lysozyme, actin, lysosomal aspartic protease, and phenoloxidase) through amplification their genes and subcloned into a N-terminal 6x His-tag plasmid vector, pQEe-TriSystem (Qiagen; Valencia, CA). After molecules are expressed and purified, I will test their activity on the same panel of bacteria. Further researches on gene regulation of the confirmed antibacterial molecues could be carried on to broad our knowledge on termite innate immune response. Second, I would like to use RNAseq technology to measure the levels of R. flavipes transcripts in a very high-throughput and quantitative manner upon P. aeruginosa and MRSA infections. In detail, RNAseq will result sequence reads, and I will assemble them de novo to produce a genome-scale transcription map that consists of the transcriptional structure. In the meantime, this teccnology can provide us highly accurate database with a large dynamic range of quantifying expression levels. Through the data, we may discover genes of interest which relate to the differentially expressed proteins we detected through LC-MS/MS, and the relationship between the mRNA level and the expressed protein level is useful for the full understanding of

gene expression control. In addition, we may discover novel transcripts involved in insect immune responses that were not detected through proteomic analysis. These potential results might become the foundations of future downstream researches. Combing the results from LC-MS/MS and RNAseq of *R. flavipes* challenged with *P. aeruginosa* and MRSA, we will attain a better and more complete picture of immune changes of *R. flavipes* in response to external stimuli.

Appendix

External antibacterial activities of subterranean termite *Reticulitermes flavipes* against human pathogens reveal a potential for natural products discovery

Abstract

Given the long coevolutionary history between insects and their symbionts, some of the microorganisms have been proven for providing protections on insects beyond the role of affecting the animal's nutrition, development, and metabolism. In this study, inhibition zone assays were used to select the cultivable cuticular bacteria from eastern subterranean termite *Reticulitermes flavipes* with antagonistic effects on several human bacterial pathogens as well as an entomopathogenic bacterium *Bacillus subtilis*. Three bacterial families including Bacillaceae, Enterobacteriaceae, and Moraxellaceae isolated from termite cuticles appeared promising with respect to inhibition of *B. subtilis* and two common human pathogens *Staphylococcus aureus* and *Streptococcus pyogenes*. These isolates were identified by 16S rRNA sequencing as the Gram-positive *B. cereus* and the Gram-negative *Enterobacter asburiae*, *Citrobacter farmeri* as well as *Acinetobacter bereziniae***.** Different level of antibacterial activities of the identified isolates inhibiting the growth of the susceptible Gram-positive strains indicated a reliable protection for the insect against pathogenic microorganisms in the complex natural environment as well as may aid in devising new strategies for the utilization of antibiotic combination therapies in human medicine against increasingly resistant bacteria.

Introduction

Social insects, like other solitary insects, possess a series of defensive strategies to counter the spread of diseases between colony members when they live in confined and densely populated colonies (Rosengaus et al. 2007). Within a colony, individual insect fight off pathogens through antiseptic behaviors such as grooming, undertaking, and hygienic behavior (Cremer et al. 2007) but also to avoid bacteria, fungi, viruses, and nematodes by immunological reactions such as secretion of humoral mediators and activation of cellular defenses (Rosengaus et al. 2007). Interestingly, given the long coevolutionary history between insects and their symbionts, recent studies have demonstrated that several bacterial symbionts could protect the host against pathogens and parasites (Kaltenpoth et al. 2005, Mattoso et al. 2012, Brownlie and Johnson 2009, Oliver et al. 2003, Scott et al. 2008) beyond the role of affecting the animal's nutrition, development, and metabolism (Grenham et al. 2011). The protection can be mediated through competitive exclusion of pathogenic organisms, interaction with the host's immune system to enhance resistance against pathogenic infestation, or the production of chemicals that harm and/or deter antagonists (Koehler et al. 2013).

Interestingly, termites, like other social insects including ants, honeybees, and wasps (Mattoso et al. 2012, Alippi and Reynaldi 2006, Kroiss et al. 2010, Menasria et al. 2015) also employ chemical defenses against pathogens through the production of antibiotics by symbionts associated with their cuticle (Wang and Henderson 2013), gut (Rosengaus et al. 2014), and nest environment (Chouvenc et al. 2013, Padilla et al. 2015). For example, Wang and Henderson (2013) discovered that cuticular bacteria (*Lysinibacillus sphaericus*, *Serratia marcescens*, *Cedecea davisae*, and *Pseudomonas aeruginosa*) carried by *C. formosanus* are antagonistic against the entomopathogenic bacteria *Bacillus thruingiensis* subspecies *israelensis* and *B.*

thruingiensis subspecies *thuringiensis*. The normal hindgut flora of the Australian subterranean termites *Nasutitermes exitiosus* and the spirochaetes and/or protozoa in the milk termite *Coptotermes lacteus* influenced the entry and residency of foreign bacteria (Veivers et al. 1982). A recent study presented evidence that protozoa and/or associated bacteria colonizing the hindgut of *Zootermopsis angusticollis* express β-(1, 3)-glucanase activities against the entomopathogenic fungus *Metarhizium anisopliae* (Rosengaus et al. 2014). Other studies demonstrated that Actinobacteria (*Streptomyces* spp.) isolated from termite nests express antifungal activities against *M. anisopliae* (Chouvenc et al. 2013) as well as the antiviral activity against bovine viral diarrhea virus (BVDV) (Padilla et al 2015). However, there is no study reveal the possibility of cuticular bacteria associated with the eastern subterranean termites *Reticulitermes flavipes* express inhibitory activities against infectious human pathogens for natural antibiotic products discovery. In this study, we aim to answer the following question that do cuticular bacteria associated with *R. flavipes* inhibit the growth of infectious human pathogens?

Materials and Methods

Termite collection and preparation of cuticular wash

Reticulitermes flavipes were freshly collected on the Auburn University campus in the February of 2014 as described in Hu and Appel (2004). For cuticular wash (100 termites/treatment), every 10 termites were transferred into 1.5 ml centrifuge tube containing 18 µl 0.1% Tween 20 (Hamilton et al. 2011). About 16 µl of cuticular wash was extracted after gently agitated the tube for 10 s. For control group, 100 termites were cold immobilized and surface sterilized with 70% ethanol alcohol. After allowing ethanol alcohol to evaporate for 30 sec, cuticular wash solutions were prepared as described above. Cuticular washes from non-sterilized termites and surface-sterilized termites were used for antibacterial assays.

Bacteria preparation and inhibition zone assays

In order to screen cultivable bacteria that might provide a degree of protection for termites as well as a potential prospect for novel antibiotic agent, eight bacteria were selected to characterize the antibacterial activity of termite cuticular washes. Of the eight organisms, four are Gram-negative bacteria (*Pseudomonas aeruginosa* PAO1*, Acinetobacter baumannii* AYE*, Escherichia coli* O157:H7 CDC B1409-C1, and *Salmonella enterica* Typhimurium LT2), and the other four are Gram-positive bacteria (*Staphylococcus aureus*, Methicillin-resistant *S. aureus* (MRSA), *Streptococcus pyogenes,* and *Bacillus subtilis*). Among these bacteria, seven are human pathogens except *B. subtilis* being an entomopathogenic organism. Some of the microbial species are infectious to immune-compromised human beings, and have acquired drug resistance to commonly used antibiotics (Levy and Marshall 2004). For every antibacterial assay, each bacterium was freshly grown in Lysogeny Broth (LB) at 37°C with shaking at ~220 rpm to early-mid log-phase (OD_{600} = 0.3 ± 0.05) and diluted to ~2.5×10^7 CFU/ml. The antibacterial profile screening of termite cuticular washes was accomplished by a modified inhibition zone assay (Zeng et al. 2014). 10 µl of cuticular washes of non-sterilized termites and surface sterilized termites were added on bacterial lawn, using 1 µl Ampicillin as positive control and 10 µl 0.1% Tween 20 as negative control, respectively. Diameters of inhibition zones were measured after 12 h incubation. Three independent experiments were carried out with two replicates for each test. The ANOVA and Tukey's method (PROC GLM; $\alpha = 0.05$; SAS 9.2) were used to determine all possible pairwise differences among different treatments.

Selection of cuticular bacteria with antagonistic activities against susceptible microbial species

Cuticular wash solution from non-sterilized termite workers was diluted using sterilized distilled water ($1:10^7$). Every 100 µl diluted solution were spread on LB plate evenly, and incubate in 37 ^oC for 12 h. Single colonies were selected and cultured in 2 ml LB broth, and 20 µl overnight culture were regrown in 2 ml fresh LB to achieve early-mid log-phase. 10 µl of these bacterial cultures (approximately containing $3x10^7$ CFUs/ml) were tested on LB soft agar plate containing susceptible bacteria (*B. subtilis*, *S. aureus*, and *S. pyogenes*) using modified inhibition zone assay (Zeng et al. 2014). Antibacterial assay on susceptible bacteria were repeated three times with 3 replicates (N=9). Bacteria confirmed with antagonistic activities were cultured in fresh LB broth and stored in skim milk at -80 ^oC.

Identification of cuticular antagonistic bacteria

Bacteria that were exhibiting antagonistic activity were cultured overnight in 2 ml LB broth. 200 µl of each bacterial solution were centrifuged at 13, 200 rmp for 3 min, and washed in 200 µl sterilized MQ water twice, respectively. The resulting pellet was re-suspended in 200 µl MQ water as template for polymerase chain reaction (PCR). A pair of universal bacterial 16S rRNA gene primers (forward primer (SS421): 5'-AGAGTTTGATCMTGGCTCAG-3', and reverse primer (SS427): 5'-TACGGYTACCTTGTTACGACTT-3') was used to amplify of 16S rRNA gene fragments. PCR was performed in a 100 µl volume of Megatron (Ependorf) as follows: initial denaturation at 95^oC for 4 min; 30 cycles of (94 ^oC for 30 sec, 53 ^oC for 50 sec, 72 ^oC for 1.5 min), and a final extension at 72 ^oC for 10 min using tag enzymes. The resulted PCR products were sent to Laragene Sequencing & Genotyping (Culver City, CA) for sequencing using primers SS421, SS427, Y1 (5'-ATTAGCTAGTTGGTGAGG-3'), and Y2 (5'-

TAAGTCGGATTAGCTAGTTG-3'). Obtained sequences were aligned and compared with the GenBank database through BLAST (http://blast.ncbi.nlm.nih.gov/Blast.cgi?PAGE_TYPE=BlastSearch&BLAST_SPEC=MicrobialGenomes).

Phylogenetic analysis

To assess the phylogenetic relationships of the cuticular bacteria related to *R. flavipes*, a data set was built containing the most similar sequences retrieved from the GenBank, and the sequences of closely related species from each taxa were added as out groups to root the phylogenetic trees. The phylogenetic analysis was performed with nucleotide sequences using a molecular evolutionary genetic analysis (MEGA7), after multiple alignments of the data by CLUSTAL W. The tree was constructed using the neighbor-joining algorithm.

Results

Antibacterial activities of termite cuticular wash solutions

To determine if the cuticular microbes played a role in external defense of termites, the cuticular washes were tested on bacterial lawns through inhibition zone assay. Our results demonstrated that cuticular washes from surface sterilized or non-sterilized termites displayed discrepancy on inhibiting bacterial cell growth. The cuticular washes of non-sterilized termites inhibited the growth of three bacteria, showing the greatest activity on *B. subtilis*, and followed by *S. aureus* and *S. pyogenes* (Table 1), while other bacteria including the three MDRs were not affected. The cuticular wash solution from surface sterilized termites and the negative control (0.1% Tween 20 solution) had no activity at all. These results suggest that the termite-derived cuticular washes are sufficient to inhibit bacterial cell viability.

Antibacterial activities of cuticular bacteria

Given the confirmation of the inhibition function of the cuticular washes from non-

sterilized termites, we further isolated 18 single colonies from incubation of diluted cuticular washes on LB plates. These colonies were cultured and tested on susceptible bacteria (*B. subtilis*, *S. aureus*, and *S. pyogenes*) for their antagonistic effects. Interestingly, 4 of 18 bacteria (designated as S1, S2, S3, and S4) affected bacterial cell viability (Figure 1). S1 inhibited the growth of two bacteria, producing a larger clear zone on *B. subtilis* than *S. aureus*, but had no effect on *S. pyogenes* (Appendix Figure 1A). S2 produced a smaller zone on *B. subtilis* when compared to S1 (Appendix Figure 1B). S3 showed stronger inhibiting activity on *S. aureus* (Appendix Figure 1C) than S1. S4 is the only bacterium showing antagonistic activity on *S. pyogenes* (Appendix Figure 1D) among the four cuticular bacteria.

Identification of the antagonistic bacterial strains

The 16S rRNA gene sequence BLAST analysis revealed high identity with *B. cereus* for strain S1, *Enterobacter asburiae* for strain S2, *Citrobacter farmeri* for strain S3, and *Acinetobacter bereziniae* for strain S4 (Appendix Figure 2), and the identities were confirmed by standard bacteriological procedures including production of catalase, coagulase, respiratory type and by the antagonistic effect from *B. cereus* (ATCC BAA-1005), *Enterobacter asburiae* (ATCC 35955), and *Citrobacter farmeri* (ATCC 51634) purchased from ATCC.

Discussion

Previously documented antibacterial activities of termites are usually originated from the insect hemolymph and organs (Lamberty et al. 2001; Zeng et al. 2016; Matsuura et al. 2007). In termites, although a few cuticular bacterial strains carried by *C. formosanus* demonstrated a degree of protection against entomopathogenic bacteria *B. thruingiensis* subspecies *israelensis* and *B. thruingiensis* subspecies *thuringiensis* (Wang and Henderson 2013), there is no study revealing the possibility that bacteria isolated from termites could be a potential use in natural antibiotic-like product discovery. In the current study, we assessed the antagonistic effects of

cultivable cuticular bacteria isolated from a structural pest, the eastern subterranean termite *R. flavipes* against eight bacteria. We observed several cuticular bacteria displaying antagonistic effects against a common soil entomopathogenic bacterium *B. subtilis* and two common human pathogens *S. aureus* and *S. pyogenes*. The antagonistic bacteria belong to families including Bacillaceae, Enterobacteriaceae, and Moraxellaceae. After phylogenetic analysis and biochemical verification, these antagonistic bacteria are the Gram-positive *B. cereus* and the Gram-negative *E. asburiae*, *C. farmeri*, and *A. bereziniae***.** Although we did not sample bacteria from *R. flavipes*' nest, the results suggest that representatives of these bacterial families may be commonly present in the termite nest environments they live in because all four bacteria were reported being found in soil and water environment.

Insects have evolved a wide range of mechanisms to defend themselves against antagonists. In addition to the insect immune system, several types of symbiosis play significant roles in protecting the host. One of these strategies involves the utilization of antimicrobial compounds provided by symbiotic bacteria to protect the host or its nutritional resources from pathogens and parasites (Indiragandhi et al. 2007, Dillon and Dillon 2004, Genta et al. 2006). Interestingly, many of the mutualistic microorganisms involved in insect defensive mechanisms belong to the bacterial phylum Actinobacteria (Seipke et al. 2012) due to their capacity to produce a wide variety of secondary metabolites with antimicrobial properties (Kroiss et al. 2010, Watve et al., 2001). This is evidenced by studies that cuticular bacteria identified from various insect species were the antibiotic-producing Actinomycetes which provide a degree of protection against entomopathogenic fungi and bacteria (Currie et al. 1999, Mattoso et al. 2012, Poulsen et al. 2011). However, according to our results, we did not isolate and identify any *Streptomyces* spp. with antagonistic effects against the tested bacteria. It is well known that many symbiotic

microbes are extremely difficult to culture in isolation, and even when these microbes can grow in culture, they are often extremely fastidious, requiring a specific combination of growth conditions and nutrients normally provisioned by the host to meet their physiological needs (Staudacher et al. 2016). Therefore, metagenomics is recommended for future study to investigate the bacterial community carried on termite cuticle to reveal the possibility that the antibacterial activity observed in this study is related to the uncultivated cultures.

Bacillus cereus has been documented as normal microorganisms associated with social insects such as honeybees and termites (Alippi et al. 2000, Alippi and Reynaldi 2006, König 2006). This organism plays roles in the digestion of polysaccharides and aromatic compounds (König 2006) as well as the production of bacteriocins or antifungal compounds against bacteria and fungi (Alippi et al. 2000, Alippi and Reynaldi 2006). Previous study reported cerein, an antibacterial protein purified from *B. cereus* was effective specifically against other *B. cereus* strains but not to *B. subtilis* and *S. aureus* which we examined in our study (Naclerio et al. 1993). Thus, it is likely that possibly new antibiotic-like product(s) rather than cerein is (are) responsible for the inhibition of the susceptible bacteria. *E. asburiae* and *C. farmeri* were also reported as bacterial symbionts inhabiting in the Formasan subterranean termites *Coptotermes formosanus* (Adams and Boopathy 2005, Tikhe et al. 2015). Interestingly, our results suggest that these two bacteria isolated from cuticles of *R. flavipes* are antagonistic to *B. subtilis* or *S. aureus*. This is supported by a recent study demonstrated that diverse antimicrobial lipopeptides purified from several strains of *C. farmeri* and *Enterobacter* spp. displaying antibacterial activity against several Gram-positive bacteria including *S. aureus* (Mandal et al. 2013). To our knowledge, this is the first report that *A. bereziniae* being reported relate with a termite species

with antibacterial activity against *S. pyogenes*, although it was characterized from the gut of house flies *Musca domestica* (Gupta et al. 2011).

Most interestingly, our antibacterial assay demonstrates that different level of antibacterial activities of the identified Gram-positive (*B. cereus*) and Gram-negative bacteria (*E. asburiae, C. farmeri, and A. bereziniae*) inhibiting the growth of the susceptible Gram-positive bacteria which indicate that at least one antibacterial compound was involved in antagonistic effects. In addition, it is likely that the antibiotic production by the termite symbionts may serve as a reliable protection for the termite against pathogenic microorganisms in the subterranean nest. The termite-symbiosis provides one of the examples of antibiotics serving as an efficient defense in the natural environment and may aid in devising new strategies for the utilization of antibiotic combination therapies in human medicine against increasingly resistant bacteria. Thus, further studies such as methanol extraction and GC-MS analysis are needed for characterizing the antibacterial compounds produced by these termite-related strains.

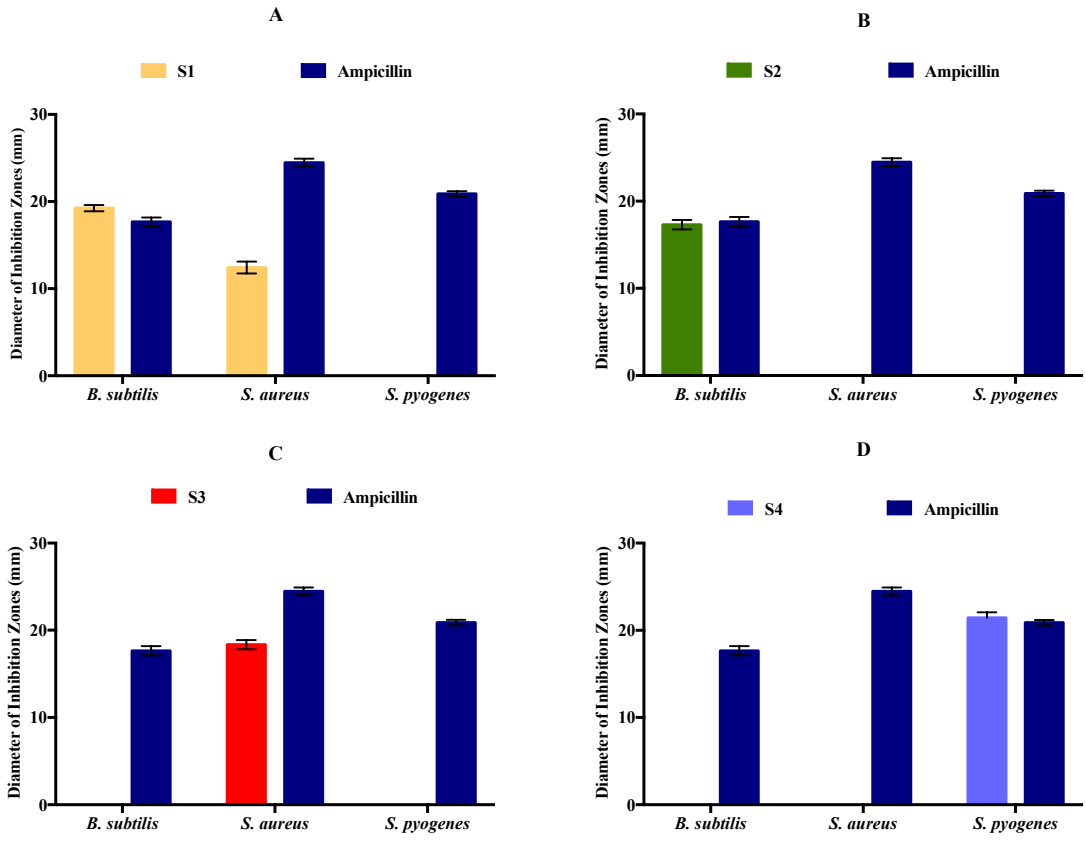

Appendix Figure 1 Antibacterial activities of cuticular bacteria (A) S1, (B) S2, (C) S3, and (D) S4 from non-sterilized termites in comparison with Ampicillin (25 µg), as measured by inhibition zone diameter (mm) (N=9) after 24 h incubation at 37°C.

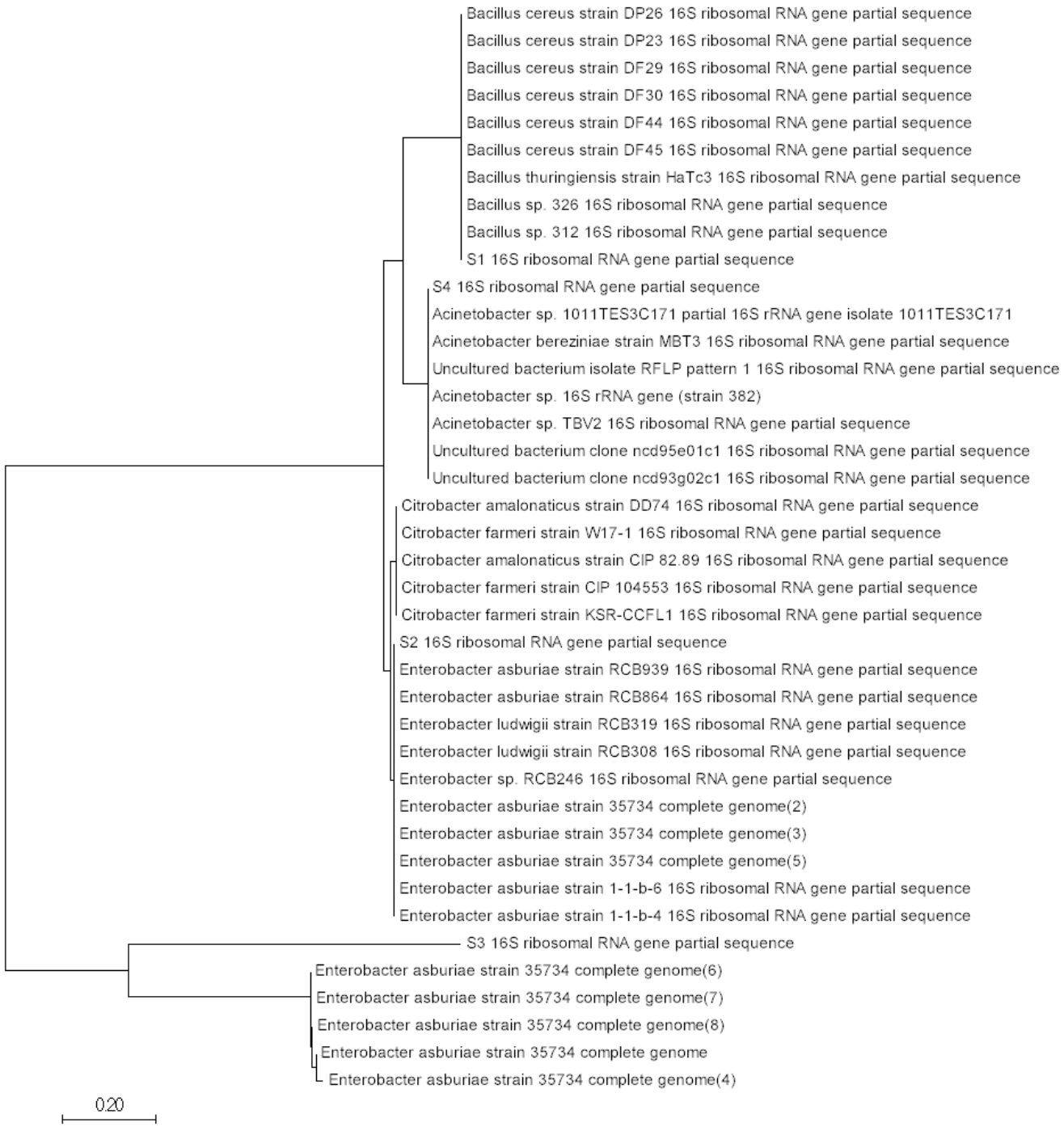

Appendix Figure 2 Neighbour-joining phylogenetic tree of 16S rRNA gene sequences of the four termite cuticular strains showing the relationship with the most similar sequences retrieved from the GenBank. The tree is drawn to scale, with branch lenths in the same units as

those of the evolutionary distances used to infer the phylogenetic tree.

Appendix Table 1. Antibacterial activities of termite cuticular wash solutions in comparison with Ampicillin and 0.1% Tween 20, as measured by the diameter (mm; mean ± SE) of inhibition zone (N = 9) after 24 h incubation at 37°C.

Bacteria			Cuticular washes from non-sterilized termites	Cuticular washes from surface sterilized termites	Ampicillin (25 μg)	0.1% Tween 20
Entomopathogen		*B. subtilis*	24.57 ± 0.80[a]	0	19.86 ± 0.75[b]	0
Infectious	Non-MDR	*S. aureus*	18.89 ± 0.74[b]	0	23.23 ± 0.80[a]	0
		S. pyogenes	15.24 ± 0.56[b]	0	18.27 ± 0.68[a]	0
		E. coli O157:H7	0	0	10.38 ± 0.52	0
		S. Typhimurium	0	0	15.39 ± 0.66	0
	MDR	MRSA	0	0	0	0
		P. aeruginosa	0	0	0	0
		A. baumannii	0	0	0	0

References

Adams, L., & Boopathy, R. (2005). Isolation and characterization of enteric bacteria from the hindgut of Formosan termite. *Bioresource technology*, *96*(14), 1592-1598.

Alippi, A. M., Perelló, A. E., Sisterna, M. N., Greco, N. M., & Cordo, C. A. (2000). Potential of Spore-forming bacteria as biocontrol agents of wheat foliar diseases under laboratory and greenhouse conditions/Das Potential der sporenbildenden Bakterien bei der biologischen Bekämpfung von Blattkrankheiten der Weizenpflanzen under Labor-und Gewächshausbedingungen. *Zeitschrift für Pflanzenkrankheiten und Pflanzenschutz/Journal of Plant Diseases and Protection*, 155-169.

Alippi, A. M., & Reynaldi, F. J. (2006). Inhibition of the growth of *Paenibacillus* larvae, the causal agent of American foulbrood of honeybees, by selected strains of aerobic spore-forming bacteria isolated from apiarian sources. *Journal of invertebrate pathology*, *91*(3), 141-146.

Brownlie, J. C., & Johnson, K. N. (2009). Symbiont-mediated protection in insect hosts. *Trends in microbiology*, *17*(8), 348-354.

Chouvenc, T., Efstathion, C. A., Elliott, M. L., & Su, N. Y. (2013). Extended disease resistance emerging from the faecal nest of a subterranean termite. *Proceedings of the Royal Society of London B: Biological Sciences*, *280*(1770), 20131885.

Cremer, S., Armitage, S. A., & Schmid-Hempel, P. (2007). Social immunity. *Current biology*, *17*(16), R693-R702.

Currie, C. R., Scott, J. A., Summerbell, R. C., & Malloch, D. (1999). Fungus-growing ants use antibiotic-producing bacteria to control garden parasites. *Nature*, *398*(6729), 701-704.

Dillon, R. J., & Dillon, V. M. (2004). The gut bacteria of insects: nonpathogenic interactions. *Annual Reviews in Entomology*, *49*(1), 71-92.

Genta, F. A., Dillon, R. J., Terra, W. R., & Ferreira, C. (2006). Potential role for gut microbiota in cell wall digestion and glucoside detoxification in *Tenebrio molitor* larvae. *Journal of insect physiology*, *52*(6), 593-601.

Grenham, S., Clarke, G., Cryan, J. F., & Dinan, T. G. (2011). Brain–gut–microbe communication in health and disease. *Frontiers in physiology*, *2*, 94.

Gupta, A. K., Nayduch, D., Verma, P., Shah, B., Ghate, H. V., Patole, M. S., & Shouche, Y. S. (2012). Phylogenetic characterization of bacteria in the gut of house flies (*Musca domestica* L.). *FEMS microbiology ecology*, *79*(3), 581-593.

Hamilton, C., Lay, F., & Bulmer, M. S. (2011). Subterranean termite prophylactic secretions and external antifungal defenses. *Journal of insect physiology*, *57*(9), 1259-1266.

Hu, X. P., & Appel, A. G. (2004). Seasonal variation of critical thermal limits and temperature tolerance in Formosan and eastern subterranean termites (Isoptera: Rhinotermitidae). *Environmental Entomology*, *33*(2), 197-205.

Indiragandhi, P., Anandham, R., Madhaiyan, M., Poonguzhali, S., Kim, G. H., Saravanan, V. S., & Sa, T. (2007). Cultivable bacteria associated with larval gut of prothiofos-resistant, prothiofos-susceptible and field-caught populations of diamondback moth, *Plutella xylostella* and their potential for, antagonism towards entomopathogenic fungi and host insect nutrition. *Journal of applied microbiology*, *103*(6), 2664-2675.

Kaltenpoth, M., Göttler, W., Herzner, G., & Strohm, E. (2005). Symbiotic bacteria protect wasp larvae from fungal infestation. *Current Biology*, *15*(5), 475-479.

Koehler, S., Doubský, J., & Kaltenpoth, M. (2013). Dynamics of symbiont-mediated antibiotic production reveal efficient long-term protection for beewolf offspring. *Frontiers in zoology*, *10*(1), 1.

König, H. (2006). Bacillus species in the intestine of termites and other soil invertebrates. *Journal of Applied Microbiology*, *101*(3), 620-627.

Kroiss, J., Kaltenpoth, M., Schneider, B., Schwinger, M. G., Hertweck, C., Maddula, R. K., ... & Svatoš, A. (2010). Symbiotic streptomycetes provide antibiotic combination prophylaxis for wasp offspring. *Nature Chemical Biology*, *6*(4), 261-263.

Lamberty, M., Zachary, D., Lanot, R., Bordereau, C., Robert, A., Hoffmann, J. A., & Bulet, P. (2001). Insect immunity constitutive expression of a cysteine-rich antifungal and a linear antibacterial peptide in a termite insect. *Journal of Biological Chemistry*, *276*(6), 4085-4092.

Levy, S. B., & Marshall, B. (2004). Antibacterial resistance worldwide: causes, challenges and responses. *Nature medicine*, *10*, S122-S129.

Mandal, S. M., Sharma, S., Pinnaka, A. K., Kumari, A., & Korpole, S. (2013). Isolation and characterization of diverse antimicrobial lipopeptides produced by Citrobacter and Enterobacter. *BMC microbiology*, *13*(1), 1.

Matsuura, K., Tamura, T., Kobayashi, N., Yashiro, T., & Tatsumi, S. (2007). The antibacterial protein lysozyme identified as the termite egg recognition pheromone. *PLoS One*, *2*(8), e813.

Mattoso, T. C., Moreira, D. D., & Samuels, R. I. (2012). Symbiotic bacteria on the cuticle of the leaf-cutting ant *Acromyrmex subterraneus subterraneus* protect workers from attack by entomopathogenic fungi. *Biology letters*, *8*(3), 461-464.

Menasria, T., Samir, T. I. N. E., Mahcene, D., Benammar, L., Megri, R., Boukoucha, M., &

Debabza, M. (2015). External bacterial flora and antimicrobial susceptibility patterns of *Staphylococcus* spp. and *Pseudomonas* spp. isolated from two household Cockroaches, *Blattella germanica* and *Blatta orientalis*. *Biomedical and Environmental Sciences*, *28*(4), 316-320.

Naclerio, G., Ricca, E., Sacco, M., & De Felice, M. (1993). Antimicrobial activity of a newly identified bacteriocin of Bacillus cereus. *Applied and Environmental Microbiology*, *59*(12), 4313-4316.

Oliver, K. M., Russell, J. A., Moran, N. A., & Hunter, M. S. (2003). Facultative bacterial symbionts in aphids confer resistance to parasitic wasps. *Proceedings of the National Academy of Sciences*, *100*(4), 1803-1807.

Padilla, M. A., Rodrigues, R. A. F., Bastos, J. C. S., Martini, M. C., Barnabé, A. C. D. S., Kohn, L. K., ... & Arns, C. W. (2015). Actinobacteria from termite mounds show antiviral activity against bovine viral diarrhea virus, a surrogate model for hepatitis C virus. *Evidence-Based Complementary and Alternative Medicine*, *2015*.

Poulsen, M., Oh, D. C., Clardy, J., & Currie, C. R. (2011). Chemical analyses of wasp-associated Streptomyces bacteria reveal a prolific potential for natural products discovery. *PLoS One*, *6*(2), e16763.

Rosengaus, R. B., Cornelisse, T., Guschanski, K., & Traniello, J. F. (2007). Inducible immune proteins in the dampwood termite *Zootermopsis angusticollis*. *Naturwissenschaften*, *94*(1), 25-33.

Rosengaus, R. B., Schultheis, K. F., Yalonetskaya, A., Bulmer, M. S., DuComb, W. S., Benson, R. W., ... & Godoy-Carter, V. (2014). Symbiont-derived β-1, 3-glucanases in a social insect:

mutualism beyond nutrition. *Frontiers in microbiology*, *5*, 607.

Scott, J. J., Oh, D. C., Yuceer, M. C., Klepzig, K. D., Clardy, J., & Currie, C. R. (2008). Bacterial protection of beetle-fungus mutualism. *Science*, *322*(5898), 63-63.

Seipke, R. F., Barke, J., Ruiz-Gonzalez, M. X., Orivel, J., Douglas, W. Y., & Hutchings, M. I. (2012). Fungus-growing Allomerus ants are associated with antibiotic-producing actinobacteria. *Antonie Van Leeuwenhoek*, *101*(2), 443-447.

Staudacher, H., Kaltenpoth, M., Breeuwer, J. A., Menken, S. B., Heckel, D. G., & Groot, A. T. (2016). Variability of bacterial communities in the moth *Heliothis virescens* indicates transient association with the host. *PloS one*, *11*(5), e0154514.

Tikhe, C. V., Sethi, A., Delatte, J., & Husseneder, C. (2016). Isolation and assessment of gut bacteria from the Formosan subterranean termite, *Coptotermes formosanus* (Isoptera: Rhinotermitidae), for paratransgenesis research and application. *Insect science*.

Veivers, P. C., O'Brien, R. W., & Slaytor, M. (1982). Role of bacteria in maintaining the redox potential in the hindgut of termites and preventing entry of foreign bacteria. *Journal of Insect Physiology*, *28*(11), 947-951.

Wang, C., & Henderson, G. (2013). Evidence of Formosan subterranean termite group size and associated bacteria in the suppression of entomopathogenic bacteria, *Bacillus thuringiensis* subspecies *israelensis* and *thuringiensis*. *Annals of the Entomological Society of America*, *106*(4), 454-462.

Watve, M. G., Tickoo, R., Jog, M. M., & Bhole, B. D. (2001). How many antibiotics are produced by the genus Streptomyces? *Archives of microbiology*, *176*(5), 386-390.

Zeng, Y., Hu, X. P., Yu, X. Q., & Suh, S. J. Multiple antibacterial activities of proteinaceous

compounds in crude extract from the eastern subterranean termite, *Reticulitermes flavipes* Kollar (Blattodea: Isoptera: Rhinotermitidae). *Adv Res*, 2(8), 455-461.

Supplementary Data

Appendix Table 1 Bacterial sequences of 16s rRNA

Bacterial name	16S rRNA sequence
Bacillus cereus	AGGGTGATCGGCCACACTGGGACTGAGACACGGCCCAGACTCCTACGGGAGGCAGCAG TAGGGAATCTTCCGCAATGGACGAAAGTCTGACGGAGCAACGCCGCGTGAGTGATGAA GGCTTTCGGGTCGTAAAACTCTGTTGTTAGGGAAGAACAAGTGCTAGTTGAATAAGCTG GCACCTTGACGGTACCTAACCAGAAAGCCACGGCTAACTACGTGCCAGCAGCCGCGGT AATACGTAGGTGGCAAGCGTTATCCGGAATTATTGGGCGTAAAGCGCGCGCAGGTGGT TTCTTAAGTCTGATGTGAAAGCCCACGGCTCAACCGTGGAGGGTCATTGGAAACTGGG AGACTTGAGTGCAGAAGAGGAAAGTGGAATTCCATGTGTAGCGGTGAAATGCGTAGAG ATATGGAGGAACACCAGTGGCGAAGGCGACTTTCTGGTCTGTAACTGACACTGAGGCG CGAAAGCGTGGGGAGCAAACAGGATTAGATACCCTGGTAGTCCACGCCGTAAACGATG AGTGCTAAGTGTTAGAGGGTTTCCGCCCTTTAGTGCTGAAGTTAACGCATTAAGCACTC CGCCTGGGGAGTACGGCCGCAAGGCTGAAACTCAAAGGAATTGACGGGGGCCCGCACA AGCGGTGGAGCATGTGGTTTAATTCGAAGCAACGCGAAGAACCTTACCAGGTCTTGAC ATCCTCTGAAAACCCTAGAGATAGGGCTTCTCCTTCGGGAGCAGAGTGACAGGTGGTG CATGGTTGTCGTCAGCTCGTGTCGTGAGATGTTGGGTTAAGTCCCGCAACGAGCGCAAC CCTTGATCTTAGTTGCCATCATTAAGTTGGGCACTCT
Enterobacter asburiae	GAGCTTGCTCCCGGGTGACGAGCGGCGGACGGGTGAGTAATGTCTGGGAAACTGCCTG ATGGAGGGGGATAACTACTGGAAACGGTAGCTAATACCGCATAACGTCGCAAGACCAA AGAGGGGGACCTTCGGGCCTCTTGCCATCAGATGTGCCCAGATGGGATTAGCTAGTAG GTGGGGTAACGGCTCACCTAGGCGACGATCCCTAGCTGGTCTGAGAGGATGACCAGCC ACACTGGAACTGAGACACGGTCCAGACTCCTACGGGAGGCAGCAGTGGGGAATATTGC ACAATGGGCGCAAGCCTGATGCAGCCATGCCGCGTGTATGAAGAAGGCCTTCGGGTTG TAAAGTACTTTCAGCGGGGAGGAAGGTGTTGAGGTTAATAACCTCAGCAATTGACGTT ACCCGCAGAAGAAGCACCGGCTAACTCCGTGCCAGCAGCCGCGGTAATACGGAGGGTG CAAGCGTTAATCGGAATTACTGGGCGTAAAGCGCACGCAGGCGGTCTGTCAAGTCGGA TGTGAAATCCCCGGGCTCAACCTGGGAACTGCATTCGAAACTGGCAGGCTAGAGTCTTG TAGAGGGGGGTAGAATTCCAGGTGTAGCGGTGAAATGCGTAGAGATCTGGAGGAATAC CGGTGGCGAAGGCGGCCCCCTGGACAAAGACTGACGCTCAGGTGCGAAAGCGTGGGG AGCAAACAGGATTAGATACCCTGGTAGTCCACGCCGTAAACGATGTCGACTTGGAGGT

	TGTGCCCTTGAGGCGTGGCTTCCGGAGCTAACGCGTTAAGTCGACCGCCTGGGGAGTAC GGCCGCAAGGTTAAAACTCAAATGAATTTGACGGGGGCCCGCACAAGCGGTGGAGCAT GTGGTTTAATTTCGATGCAACGCGAAG
Citrobacter farmeri	CGCCTCCCGAAGGTTAAGCTACCTACTTCTTTTGCAACCCACTCCCATGGTGTGACGGG CGGTGTGTACAAGGCCCGGGAACGTATTCACCGTGGCATTCTGATCCACGATTACTAGC GATTCCGACTTCATGGAGTCGAGTTGCAGACTCCAATCCGGACTACGACATACTTTATG AGGTCCGCTTGCTCTCGCGAGGTCGCTTCTCTTTGTATATGCCATTGTAGCACGTGTGTA GCCCTGGTCGTAAGGGCCATGATGACTTGACGTCATCCCCACCTTCCTCCAGTTTATCA CTGGCAGTCTCCTTTGAGTTCCCGGCCGGACCGCTGGCAACAAAGGATAAGGGTTGCGC TCGTTGCGGGACTTAACCCAACATTTCACAACACGAGCTGACGACAGCCATGCAGCAC CTGTCTCACAGTTCCCGAAGGCACCNANNCATCTCTGCNAAGTTCTGTGGATGTCAAGA CCAGGTAAGGTTCTTCGCGTTGCATCGAATTAAACCACATGCTCCACCGCTTGTGCGGG CCCCCGTCAATTCATTTGAGTTTTAACCTTGCGGCCGTACTCCCCAGGCGGTCTATTTAA CGCGTTAGCTCCGGAAGCCACGCCTCAAGGGCACAACCTCCAAATAGACATCGTTTAC GGCGTGGACTACCAGGGTATCTAATCCTGTTTGCTCCCCACGCTTTCGCACCTGAGCGT CAGTCTTCGTCCAGGGGGCCGCCTTCGCCACCGGTATTCCTCCAGATCTCTACGCATTTC ACCGCTACACCTGG
Acinetobacter bereziniae	TGATCCGCCACACTGGGACTGAGACACGGCCCAGACTCCTACGGGAGGCAGCAGTGGG GAATATTGGACAATGGGCGCAAGCCTGATCCAGCCATGCCGCGTGTGTGAAGAAGGCC TTTTGGTTGTAAAGCACTTTAAGCGAGGAGGAGGCTCTCTTAGTTAATACCTAAGATGA GTGGACGTTACTCGCAGAATAAGCACCGGCTAACTCTGTGCCAGCAGCCGCGGTAATA CAGAGGGTGCGAGCGTTAATCGGATTTACTGGGCGTAAAGCGTGCGTAGGCGGCTTTTT AAGTCGGATGTGAAATCCCCGAGCTTAACTTGGGAATTGCATTCGATACTGGGAAGCTA GAGTATGGGAGAGGATGGTAGAATTCCAGGTGTAGCGGTGAAATGCGTAGAGATCTGG AGGAATACCGATGGCGAAGGCAGCCATCTGGCCTAATACTGACGCTGAGGTACGAAAG CATGGGGAGCAAACAGGATTAGATACCCTGGTAGTCCATGCCGTAAACGATGTCTACT AGCCGTTGGGGCCTTTGAGGCTTTAGTGGCGCAGCTAACGCGATAAGTAGACCGCCTG GGGAGTACGGTCGCAAGACTAAAACTCAAATGAATTGACGGGGGCCCGCACAAGCGGT GGAGCATGTGGTTTAATTCGATGCAACGCGAAGAACCTTACCTGGCCTTGACATACTAG AAACTTTCCAGAGATGGATTGGTGCCTTCGGGAATCTAGATACAGGTGCTGCATGGCTG TCGTCAGCTCGTGTCGTGAGATGTTGGGTTAAGTCCCGCAACGAGCGCAACCCTTTTCC TTACTTGCCAGCATTTCGGATGGGAACTTTAAGGATACTGCCAGTGACAAACTGG